RESEARCH & DEVELOPMENT

The Effect of Contaminated Soil and Groundwater on Subsurface Utilities, Surface Water and Drainage

Payam Hosseini
Sultan Alhomair
Zahra Faeli
Mohammed Gabr
Detlef Knappe
Mohammad Pour-Ghaz

Department of Civil, Construction, and Environmental Engineering
North Carolina State University

DRAFT

NCDOT Project #2017-08

Dec 2019

The Effect of Contaminated Soil and Groundwater on Subsurface Utilities, Surface Water and Drainage

FINAL REPORT - DRAFT

Prepared by:

Payam Hosseini

Sultan Alhomair

Zahra Faeli

Mohammed Gabr

Detlef Knappe

Mohammad Pour-Ghaz

A report on research sponsored by:

THE NORTH CAROLINA DEPARTMENT OF TRANSPORTATION

Dec 2019

1. Report No.	2. Government Accession No. *…leave blank…*	3. Recipient's Catalog No. *…leave blank…*
4. Title and Subtitle The Effect of Contaminated Soil and Groundwater on Subsurface Utilities, Surface Water and Drainage		5. Report Date July 31st 2019 6. Performing Organization Code *...leave blank…*
7. Author(s) Payam Hosseini; Sultan Alhomair; Zahra Faeli; Mohammed Gabr; Detlef Knappe; Mohammad Pour-Ghaz		8. Performing Organization Report No. *...leave blank…*
9. Performing Organization Name and Address NORTH CAROLINA STATE UNIVERSITY Department of Civil, Construction, and Environmental Engineering Campus Box 7908, Raleigh, NC 27695-7908		10. Work Unit No. (TRAIS) *...leave blank…* 11. Contract or Grant No. *...leave blank…*
12. Sponsoring Agency Name and Address North Carolina Department of Transportation Research and Development Unit 104 Fayetteville Street Raleigh, North Carolina 27601		13. Type of Report and Period Covered Final Report August 1st 2016 - July 31st 2019 14. Sponsoring Agency Code NCDOT Project #2017-08
Supplementary Notes: *...leave blank…*		

16. Abstract

Information in this report documents the results from experimental and modeling studies to quantify the effect of subsurface contaminants on installed subsurface utilities (pipelines) commonly employed by the North Carolina Departments of Transportation. The focus of the study was on quantifying and modeling the effect of benzene and tetrachloroethylene (PCE) on the durability of PVC and concrete pipes as well as neoprene (polychloroprene), nitrile (acrylonitrile butadiene rubber or Buna-N), and Grade A Viton® (fluoroelastomer rubber or FKM) gaskets. In addition, migration of contaminates through utility installation areas was investigated using several saturated and unsaturated flow scenarios to provide a better understanding of the alternation of the contaminant transport regime with the installation of pipes in contaminated subsurface media. Modeling also included the effect of several mitigation measures on the migration of contaminants into concrete pipes with an assumed level of damage, and therefore quality, of concrete and gaskets. Benzene and PCE are selected as contaminants in the study because of their prevalence within the Right of Way in North Carolina and also represent petroleum-based and dry-cleaning solvent contaminant categories. The experimental results were used to develop a degradation model for the tested materials with proposed approach to account for the effect of contaminant concentration on the degradation rate. The experimental results also included data on the effect of benzene and PCE on the compressive strength of concrete material. Experimental measurements of the rate of absorption and vapor diffusion of benzene and PCE through concrete used for pipe manufacturing are reported. The effect Xypex® as a waterproofing agent on the rate of absorption and vapor diffusion is measured and reported. The results from computational simulations were used to evaluate the transport of benzene in saturated and unsaturated subsurface media within the pipeline trench over an extended period of time (10-20 years.) The computational simulations included contaminant transport from a continuous source and transient sources; the efficiency of mitigation strategies and plumb migration prevention on contaminant transport were also evaluated. Modeling results provided the breakthrough of benzene concentration and mass as a function of time for the various analyses scenarios considered herein.

17. Key Words Degradation modeling; PVC, Neoprene, Nitrile, Viton®, gasket, benzene, PCE, concrete pipe, mass transport, diffusion, saturated flow, unsaturated flow, contamination	18. Distribution Statement *...leave blank…*		
19. Security Classif. (of this report) Unclassified	20. Security Classif. (of this page) Unclassified	21. No. of Pages 154	22. Price *...leave blank…*

Form DOT F 1700.7 (8-72) **Reproduction of completed page authorized**

DISCLAIMER

The contents of this report reflect the views of the author(s) and not necessarily the views of the University. The author(s) are responsible for the facts and the accuracy of the data presented herein. The contents do not necessarily reflect the official views or policies of either the North Carolina Department of Transportation or the Federal Highway Administration at the time of publication. This report does not constitute a standard, specification, or regulation.

ACKNOWLEDGMENTS

The authors would like to acknowledge the support of the North Carolina Department of Transportation Office of Research and Development. The authors thank the project's steering committee members for their valuable technical input, including providing site data and facilitating site visit, throughout the project period, especially those of Mr. Cyrus Parker. The technical support provided by NC State Constructed Facilities Laboratory (CFL) staff, Mr. Jerry Atkinson and Mr. Johnathan McEntire, is greatly acknowledged.

EXECUTIVE SUMMARY

This report documents the results from the experimental and computational studies that were performed to quantify the effect of subsurface contaminants on installed subsurface utilities (pipelines) commonly employed by the North Carolina Departments of Transportation. The focus of the study was on quantifying and modeling the effect of benzene and tetrachloroethylene (PCE) on the durability of PVC and concrete pipes as well as neoprene (polychloroprene - CR), nitrile (acrylonitrile butadiene rubber or Buna-N), and Grade A Viton® (fluoroelastomer rubber or FKM) gaskets. In addition, migration of contaminates through subsurface utility installation areas, using several saturated and unsaturated flow scenarios, are performed to provide a better understanding of the alternation of the contaminant transport regime with the installation of pipes in contaminated subsurface media. Modeling included the effect of installed mitigation measures on the migration of contaminants into concrete pipes with different quality of concrete and gaskets. Benzene and PCE are selected as contaminants in the study because of their prevalence adjacent to transportation corridors; they also represent petroleum-based and dry-cleaning solvent categories. The experimental results of degradation of mechanical properties of gaskets have been used to develop a degradation model for the tested materials. Modifications to the model are proposed to account for the effect of concentration on the durability of the material. Also reported herein, are the experimental results showing the effect of benzene and PCE on the compressive strength of concrete material. Experimental measurements of the rate of absorption and vapor diffusion of benzene and PCE through concrete, used for pipe manufacturing, are also reported. The effect of Xypex® as a waterproofing agent on the rate of absorption and vapor diffusion is measured and reported. Modeling effort included computational simulations to evaluate the transport of benzene in saturated and unsaturated subsurface pipeline trench corridors over an extended period of time (10-20 years). The computational simulations included contaminant transport from continuous sources and transient sources; the efficiency of three different mitigation strategies in reducing the rate of contaminant transport was also evaluated. Modeling results provided the breakthrough of benzene concentrations as a function of time for the various analyses scenarios considered herein.

Experimental results indicate that benzene is more detrimental than PCE in terms of degradation of the tensile strength of PVC and rubber gasket materials. Among rubber gaskets, Viton® performed the best, followed by nitrile and then neoprene when exposed to benzene and PCE aqueous solutions at their solubility limits (i.e. 1790 mg/L and 206 mg/L, respectively). Severe swelling was observed for neoprene and nitrile samples when exposed to benzene solution at an elevated temperature of 140 ºF (accelerated condition). The experimental results of degradation of tensile strength is used to develop a degradation model for these materials. Modifications to the model are proposed to account for the effect of concentrations below saturation levels on the degradation rate.

Also reported herein are the experimental results showing the effect of benzene and PCE on the compressive strength of concrete materials. Results indicated that benzene and/or PCE did not affect the compressive strength of concrete in statistically significant manner. Experimental measurements of the rate of absorption and vapor diffusion of benzene and PCE through concrete used for pipe manufacturing were performed. The effectiveness of Xypex® as a waterproofing agent on the rate of absorption and vapor diffusion is measured and reported. The presence of PCE did not affect the rate of water absorption in concrete. In addition, the application of Xypex® did not reduce the sorption rate of concrete pipe materials.

The measured diffusion coefficient of PCE vapor through the concrete pipe was found to be one order of magnitude lower than that of benzene vapor. Xypex® admixture reduced the diffusion coefficient of benzene vapor by 24%.

Results from modeling the subsurface domain, assuming saturated conditions, indicated that the permeated benzene concentrations through the subsurface concrete pipe are highly dependent on the saturated hydraulic conductivity of the native soil. When the native soil is sandy clay (k_{soil} = 10^{-5} cm/s), no benzene concentration is predicted within the pipe with assumed damaged gaskets after 20 years. Therefore, a damaged gasket, as defined in this report, should not be a concern when the native soils have relatively low hydraulic conductivity ($k \leq 10^{-5}$ cm/s). The highest potential of benzene concentration breakthrough the pipe, and mass of benzene flowing out of the pipe, was computed when a damaged pipe, rather than a damaged gasket, was assumed in the analyses. This was due to the larger surface area of the pipe through which benzene breakthrough occurs. Therefore, and depending on the extent of the damage to the pipe, such damage can prove to be more critical for the potential occurrence of contamination breakthrough compared to the damage to the gaskets.

Results from benzene transport scenarios through unsaturated subsurface profile and pipe trench corridor were obtained through numerical modeling. The release of NAPL of benzene was assumed to occur 6ft (1.85 m) below the ground surface. Two scenarios of depth to groundwater were utilized in the analyses; groundwater level located at 7 ft (~2.1m), and 10 ft (~3m) below ground surface, respectively (1.25m and 0.35m from pipe invert). In both of these scenarios, the source of contamination is assume to be unaffected by the location of the groundwater. The results from the analyses indicated that the release of benzene, as NAPL-phase, leads to mass breakthrough the pipe in both gas and aqueous phases; this occurs while the NAPL-phase benzene is limited to the area around the initial source of contamination. Given the assumptions made during modeling, the results indicated that the groundwater table level has a significant impact on the diffusion of benzene in gas phase. Larger concentrations and mass ingress through the pipe were predicted for the lower water level scenario. This is due to the larger unsaturated thickness of soil domain and the greater availability of air voids for the mass exchange to take place. An additional scenario was analyzed where the water level rises and causes the NAPL to migrate toward the pipe. A benzene saturation of 1% was applied above groundwater table, located at

1.25m and 0.35m from pipe invert. As such, the NAPL migrated toward the pipe as the water table level raised. Results from these analyses indicated higher concentration and mass transfer into the pipe as the water table raised. The thickness of NAPL phase benzene at the contamination source just affects the concentrations inside the pipe by 13% and shows less effect compared to the location of the groundwater table.

Results from the simulations of different extent of damage in gasket and pipe materials indicated that severely damaged gaskets caused benzene to permeate into the pipe in higher concentrations by more than two orders of magnitude versus undamaged gaskets within 2 years after the release. Results also indicated that approximately 60% increase in concentrations and mass transferred into the pipe can occur due to damaged pipe. The effect of volatilization to the atmosphere and adsorption to the soil on transport mitigation in cases of unsaturated soil was significant.

Results from assessing the efficacy of mitigation measures were obtained from the model with a simulation time of 20 years. The results indicated that the use of a flowable fill method is a long-term engineering control with the potential of reducing the concentration and the mass of benzene breaking through the pipe by as much as 99.9 %. In the case of clay barrier installation, the concentration of benzene is reduced by 22 % for 20 years of simulation time, and the mass of benzene is decreased by 30 % for the same period. Therefore, the clay barrier could be an effective method to protect the trench and subsurface pipe for a specific time. Results from simulating the installation of anti-seep collar indicated a decreased concentrations of benzene breaking through the pipe by 60% for the 20 years and decreased the mass of benzene flowing out of the pipe by 44 % for the same period. The natural hydraulic gradient of the site affects the level of contamination breaking through the pipe such that lower gradients, leads to a smaller mass of contamination through the pipe. Thus, the existing Hydrogeology of the site and the properties of the subsurface pipe need to be ascertained during the design and modeling phase and then ensured during the construction phase.

Results obtained in this study are summarized in the Tables below.

Table S1. Comparative performance of gasket materials exposed to contaminated water.

Exposure media	Highest strength	Lowest strength
Pure water	Viton®	Neoprene
Aqueous solution of PCE	Viton®	Neoprene
Aqueous solution of benzene	Viton®	Neoprene

Table S2. The effect of exposure to contaminations on properties of concrete

Material	Description	Exposure media	Properties	Result
Mortar	Same mix design as concrete pipe	Aqueous solution of PCE and benzene and pure water	Compressive strength	No changes detected after one year
Concrete	Obtained from concrete pipe	Aqueous solution of PCE and pure water	Unsaturated sorption	No changes detected
Mortar	Without Xypex®	Aqueous solution of PCE and pure water	Unsaturated sorption	No changes detected
	With Xypex®	Aqueous solution of PCE and pure water	Unsaturated sorption	No changes detected
Concrete	Obtained from concrete pipe	Saturated vapors of benzene and PCE	Vapor diffusion	$D_{Benzene}$ = 2.88×10^{-12} m^2/s D_{PCE} = 0.24×10^{-12} m^2/s
Mortar	Without Xypex®	Saturated vapor of benzene	Vapor diffusion	24% reduction of benzene diffusion coefficient by using Xypex®
	With Xypex®			

Table S3. Benzene breakthrough the subsurface concrete pipe for the damage to gaskets and pipe with different native soil types

Native soils	Benzene concentration	
	Damaged pipe conditions	Damaged gasket conditions
Sandy clay soils ($k_{soil}=10^{-5}$ cm/s)	Benzene below 5 µg/l	No benzene detected
Sandy soils ($k_{soil}=10^{-3}$ cm/s)	Benzene reached 5 µg/l	Benzene below 5 µg/l

Table S4. Efficacy of mitigation measures

Mitigation methods	Result	
	Concentration of benzene	Mass of benzene
Flowable fill	99.9% reduction	99.9% reduction
Clay barrier	22% reduction	30% reduction
Anti-seep collar	60% reduction	44% reduction

Table S5. Benzene breakthrough the subsurface concrete pipe in case of unsaturated subsurface profile

Analysis factors	Description	Result			
		Concentration of benzene		Mass of benzene	
		Aqueous phase	Gas phase	Aqueous phase	Gas phase
water table level from pipe invert	0.35m (1.15ft) / Benzene source in unsaturated zone and horizontal distance from pipe	94% reduction in case of raised water table compared to lower level of wt	94% reduction in case of raised water table compared to lower level of wt	90% reduction in case of raised wt compared to lower level of wt	90% reduction in case of raised water table compared to lower level of wt
	1.25m (4.1ft)/ Benzene source in unsaturated zone and horizontal distance from pipe				
	0.35m (1.15ft)/ benzene source floating on water table at pipe location	35.5% increase in case of raised water table compared to lower level of wt	35.5% increase in case of raised water table compared to lower level of wt	-	-
	1.25m (4.1ft)/benzene source floating on water table at pipe location				
Pipe material quality	High quality (w/c=0.4-0.45)	77% reduction compared to med quality	77% reduction compared to med quality	65% reduction compared to med quality	65% reduction compared to med quality
	Med quality (w/c=0.45-0.5)	Base case	Base case	Base case	Base case
	Low quality (w/c=0.55-0.6)	65% increase compared to med quality	65% increase compared to med quality	114% increase compared to med quality	114% increase compared to med quality

Analysis factors	Description	Result			
		Concentration of benzene		Mass of benzene	
		Aqueous phase	Gas phase	Aqueous phase	Gas phase
Gasket material quality	Damaged gasket	More than two orders of magnitude increase in damaged gasket	More than two orders of magnitude increase in damaged gasket	More than two orders of magnitude increase in damaged gasket	More than two orders of magnitude increase in damaged gasket
	Undamaged gasket				
NAPL thickness	0.6m (2ft)	13% decrease by reducing NAPL thickness	13% decrease by reducing NAPL thickness	20% decrease by reducing NAPL thickness	20% decrease by reducing NAPL thickness
	0.3m (1ft)				
Native soil material	Sandy clay ($k=6.24\times10^{-5}$ cm/s)	Increase by a factor of 6 with higher k	Increase by a factor of 6 with higher k	-	-
	Sand ($k=2\times10^{-3}$ cm/s)				
Mitigation method	With anti-seep collar	97% reduction with anti-seep collar	97% reduction with anti-seep collar	96% reduction with anti-seep collar	96% reduction with anti-seep collar
	Without anti-seep collar				
Volatilization to the atmosphere	Water table at 1.25m (4.1ft)	98% of total mass lost to the atmosphere			
Adsorption to the soil	Water table at 1.25m (4.1ft)/ organic carbon fraction of 0.1%	4% -34% of remained mass in domain adsorbed to the soil in first to the last year			

TABLE OF CONTENTS

1. Introduction

A large number of subsurface utilities and drainage pipes are installed by the North Carolina Department of Transportation (NCDOT) every year. In many instances these subsurface structures are installed in profiles with known contamination and therefore appropriate materials and construction methods need to be adopted. However, in some cases the contamination type or extent is not known; these include for example spills near existing drainage system. Among potential contaminants, benzene and tetrachloroethylene (PCE) from petroleum hydrocarbons and dry-cleaning solvents, respectively, are known to be the most prevalent (Holsen et al., 1991a; EPA, 2002; Koo, 2012). These contaminants may adversely affect the service life and long-term performance of subsurface utilities and drainage infrastructure. This is especially the case where plastic pipes and rubber gaskets are used since these materials can rapidly deteriorate in the presence of these contaminants. Among materials used in subsurface utilities are PVC and concrete pipes as well as rubber gaskets with neoprene (polychloroprene - CR), nitrile (Acrylonitrile butadiene rubber or Buna-N), and Viton® (fluoroelastomer rubber or FKM) being the most common.

In addition to the potential of material degradation, the installation of subsurface utilities may create a conduit for the accelerated migration of contaminants, resulting in environmental implications. The effect of utility installations on contaminated groundwater plumes have received little to no attention in literature. Furthermore, other related issues including ingress by diffusion of contaminants into concrete utilities and their transport in water and drainage systems need to be studied. Furthermore, the diffusion coefficient benzene and PCE in concrete have not been previously reported in the literature.

Therefore, the objectives of testing and analyses work conducted in this project include:

1. Quantify the effect of benzene and PCE on the durability of PVC, neoprene, nitrile, and Grade A Viton®;
2. Develop a degradation model that can be used to predict the degradation of these materials exposed to benzene and PCE;
3. Quantify the effect of common contaminants on the compressive strength of concrete used in production of concrete pipes;
4. Quantify the rate of vapor diffusion (vapor diffusion coefficient) of benzene and PCE through concrete that is used in concrete pipe manufacturing;
5. Model migration of contaminates through utility installation subsurface areas using saturated and unsaturated flow scenarios to provide a better understanding of the alternation of the contaminant transport regime with the installation of subsurface pipes in contaminated soil or groundwater media; and,

6. Model the effect of several contaminant transport mitigation measures on the breakthrough of contaminants into concrete pipes considering several scenarios regarding the quality of the concrete and gaskets.

2. Research Approach

Each of the objectives mentioned above have been addressed through a systematic study. A brief description of the approaches used to achieve the six stated objectives is summarized herein.

Objective 1: Quantify the effect of benzene and PCE on the durability of PVC, neoprene, nitrile, and Grade A Viton®

Dog-bone shaped specimens were prepared from a green PVC pressure pipe segment. All specimens were cut from an 8-inch diameter pipe conforming to ANSI/AWWA C900 with a dimension ratio (DR) of 18 (which is equivalent to the pressure class of 235 psi.) Since the pipe wall thickness was 0.55", Type III ASTM D638 specimens were used following the standard specification. Rubber gasket specimens were cut from commercially available rubber sheets (i.e., CR, NBR, and FKM) using a press die with the dimensions specified for Type C dumbbell specimens according to ASTM D412. The thickness of sheets was 0.125" and the specimens were 4.5-inch long.

Accelerated aging was achieved by conditioning the specimens in aqueous solutions with 1790 mg/L benzene or 206 mg/L PCE (i.e., at their solubility limits) at three different temperatures of 68 ºF (ambient temperature), 104 ºF, and 140 ºF. Specimens were placed in packer bottles and conditioned; specimens were tested after 1 week, 6 weeks, 3 months, and 7 months. In addition to exposure to benzene and PCE, a set of control specimens were exposed to water at all three temperatures. Note that the reason for using benzene and PCE at their solubility limits is to consider the highest contamination level of benzene and PCE that can exist in groundwater contaminated with petroleum or dry-cleaning agents.

Aqueous solutions of benzene and PCE (1790 mg/L and 206 mg/L, respectively) were prepared by adding mass that is 10-20 times more than their solubility level of the corresponding chemicals to maintain the saturation level during the aging. Bottles were monitored to check the availability of contaminants (benzene or PCE) every 14 days and more chemicals were added, if needed, to maintain the saturation level. In preparing benzene- or PCE- aqueous solutions, deionized water and American Chemical Society (ACS) analytical grade of benzene and PCE were utilized to avoid the existence of other chemicals and substances which may affect the impact of the chemicals of interest. After preparing headspace-free bottles and sealing them using a commercial chemical- and heat-resistant sealant, the bottles were then put in water tanks with controlled temperatures (104 ºF and 140 ºF) until the specified testing times.

At each testing time, the specimens were removed from the bottles and then placed in a laboratory oven set at 104 °F to dry. Depending on the specimen type and aging duration, drying took up to 48 hours. Specimens were considered "dry" when less than 0.1% change in the weight of specimen within an hour was measured.

Mechanical properties of the aged and unaged PVC and rubber gasket specimens were measured according to ASTM D638 and ASTM D412, respectively. The loading rate for all specimens was set at 2 in/min (50 mm/min).

Objective 2: Develop a degradation model that can be used to predict the degradation of these materials exposed to benzene and PCE.

To develop the degradation models, Williams-Landel-Ferry (WLF) technique was adopted to achieve a specific relationship for the property loss/gain as a function of time. WLF model utilizes time-temperature superposition master curve where these are built by combining the results of mechanical test at some specific ages and temperatures; the WLF equation is shown as (1):

$$\log(a_T) = \frac{c_1\,(T-T_o)}{c_2+(T-T_o)} \quad (1)$$

where a_T is the shift factor of the curve of the measured tensile strength at each specific temperature (T) over time, T_o is the reference temperature (taken as fixed at 68 °F in this study), and c_1 and c_2 are two coefficients dependent upon the material type.

All data measured at temperatures higher than the reference temperature (T_o) over time, were shifted in time. The master curve at the reference temperature was then constructed by fitting a curve to all data including shifted (at temperatures other than reference) and reference temperature data. Using the obtained master curve, one can predict how long it will take to reach a specified strength loss (property degradation) limit which in turn can be translated into the service life of the material aging naturally under the exposure media.

It should be noted that in developing the model, the tensile strength of aged specimens for each material of interest was normalized to their unaged tensile strength mentioned. The normalized tensile strength (T_N) at each age and temperature was then used for modeling purposes. Moreover, to find the shift factors for each aging temperature, root-mean-square error or RSME function (2) was minimized to obtain the best fit.

$$RSME = \sqrt{\frac{\sum_{i=1}^{n}(P_i-T_N)^2}{n}} \quad (2)$$

where P_i is the predicted data based on the degradation function (exponential here) and shifted time, and n is the number of data collected for each specific material at all aging temperatures and durations.

Objective 3: Quantify the effect of common contaminants on the compressive strength of concrete used in production of concrete pipes

Compressive strength of mortar with the same mix proportions to that of concrete pipe was measured to assess the effect of water contamination on the mechanical properties of concrete pipe. The tensile strength testing was carried out in accordance with ASTM C109 on five replicates. Deionized (clean) water was used as a control exposure medium and an aqueous solution of benzene and PCE at their solubility limit, dissolved in deionized water, was prepared as the contaminated water exposure medium. Compressive testing on mortar specimens was performed after 6 and 12 months of exposure to clean and contaminated water.

Objective 4: Quantify the rate of vapor diffusion (vapor diffusion coefficient) of benzene and PCE through concrete that is used in concrete pipe manufacturing

To evaluate the sorption rates of unsaturated (dry) concrete pipe when exposed to contaminated water, sorptivity test was performed according to ASTM C1585. Control exposure media of deionized water and aqueous PCE solution at its solubility limit i.e., 206 mg/L were prepared to resemble uncontaminated and contaminated water medias, respectively. Mortar specimens were cast with and without Xypex® admixture in order to examine the effect of waterproofing admixture on the sorption rates of concrete pipe materials. The exposure media were pure water and PCE aqueous solution similar to those adopted for testing concrete pipe specimens.

Diffusion of contaminants in vapor phase through concrete pipe can affect the quality of water transported by the pipeline system. The movement of organic contaminants through concrete pipe occurs due to the difference between the concentration of organic molecules inside and outside of concrete pipe wall. Accordingly, to measure the diffusion coefficient of benzene and PCE vapors through concrete pipe specimens, an in-house diffusion cell was developed and employed. Sampling was performed within three weeks after the contact of organic vapor to the concrete specimen. Samples were taken from the downstream bottle resembling the water inside the pipe. After measuring the diffused mass of contaminant of interest, Fick's second law was used to calculate the diffusion coefficient.

After performing diffusion testing on concrete pipe specimens, and since benzene showed a higher diffusion coefficient, mortar specimens were prepared with the same mix proportions as the pipe concrete material used in this study to quantify the diffusion coefficient of benzene vapor through piping material. Testing was conducted with and without incorporation of Xypex®.

Objective 5: Model migration of contaminates through utility installation subsurface areas using saturated and unsaturated flow scenarios to provide a better understanding of the alternation of the contaminant transport regime with the installation of subsurface pipes in contaminated soil or groundwater media

Work in this was focused on assessing the effect of a continuous source of contamination on concrete pipe installed in an initially uncontaminated site. In this case, benzene in soil and groundwater was used as representative species of contamination given its prevalence in projects conducted by NCDOT. The analyses were conducted using Visual MODFLOW Flex software combining MODFLOW-2005 with MT3DMS engines. The simulated analyses scenarios included assumed intact and damaged conditions for pipe and gaskets. The damage level was simulated through varying the hydraulic conductivity (k) parameter used in the numerical analyses for the pipe and gasket materials. The site conditions were selected based on the average range of hydrologic parameters representative of regions in the coastal area of North Carolina.

In parallel, to study the impact of benzene leakage into nearby subsurface drainage concrete pipe located in the unsaturated zone, a numerical model was developed using T2VOC module of "Transport Of Unsaturated Groundwater and Heat (TOUGH)" and Petrasim2018 Graphic User Interface codes. This code was used for simulating the coupled transport of water, vapor, non-condensible gas, and heat in porous and fractured media, and was developed at the Lawrence Berkeley National Laboratory. To aid with the modeling scenarios, a site in North Carolina was used to develop the study parameters and the analysis domain.

The model domain is estimated based on the extent of plume, pipe joints distance, boundaries, and monitoring well locations. In situ groundwater gradients is applied to the model. Volatilization to the atmosphere is included and is modeled through a layer at the ground surface with specific boundary conditions. The advection, diffusion and adsorption parameters of the site soils with benzene contamination are applied in the analyses. Three different conditions of concrete pipe materials were compared based on various unsaturated transport properties of concrete. Two scenarios of damaged/undamaged conditions were considered for gaskets. The groundwater table is raised during the analyses to assess the effect of depth to groundwater table on contaminant distribution among the aqueous and gas phases and the corresponding transport mechanism. The effect of source geometry and size on benzene propagation is evaluated through different thickness of benzene in NAPL phase at the source. The breakthrough concentrations inside the pipe in gas and aqueous phases and also mass ingress into the pipe have been evaluated with the effect of an atmosphere layer considered in the analyses.

Objective 6: Model the effect of several contaminant transport mitigation measures on the breakthrough of contaminants into concrete pipes considering several scenarios regarding the quality of the concrete and gaskets

To study the effect of several mitigation measures, the benzene concentration and the mass being transported through the subsurface pipe installed at a contaminated site were modeled. The efficacy of two hardening practices and plumb migration prevention were assessed for the case of saturated flow. A site in Jacksonville, North Carolina, where data were available on gasoline leakage generated from underground storage tanks at a gas station was used for developing the analyses parameters. The potential mitigation measures of installing flowable fill around the pipe, using clay barrier to line the pipe trench, and installing a series of anti-seep collars were modeled assuming saturated flow conditions as worst-case scenario. Furthermore, the case of anti-seep collar was also modeled assuming unsaturated conditions since this is a method commonly used by NCDOT for mitigation of benzene transport.

3. Experimental Methods

Materials utilized and methods adopted in the experimental and numerical parts of the project are discussed in detail in Appendix B.

4. Results and Discussion

4.1. Degradation of Tensile Strength of PVC and Gasket Materials

Figure 1, Figure 2, and Figure 3 show the results of loss in tensile strength of materials exposed to water (control environment). When exposed to water, the maximum tensile strength loss for neoprene was about 31% which occurred at 140 ^{o}F after 13 weeks. Also, after 30 weeks of aging, there is 22% and 28% reduction in the tensile strength for neoprene specimens exposed to deionized water at 68 ^{o}F and 104 ^{o}F, respectively.

For nitrile specimens exposed to water (Figure 1, Figure 2, and Figure 3), the maximum reduction in tensile strength was about 16% observed at 140 ^{o}F after 13 weeks. This value is approximately half of that obtained for neoprene specimens with the same exposure time and age.

For Viton® specimens, and as shown in Figure 1, Figure 2, and Figure 3, 10 to 15% reduction in tensile strength with exposure to water is observed but this reduction is independent of exposure duration and to some extent independent of temperature. This indicates that the effect of water on durability of Viton® specimen is significantly smaller as compared to other gasket materials tested. According to data in Figure 1, Figure 2, and Figure 3, considering the values for tensile strength and its variations, it can be concluded that the influence of temperature is almost insignificant for Viton® specimens being aged in water at the three test temperatures of 68, 104, and 140 ^{o}F.

As shown in Figure 1, Figure 2, and Figure 3, the results for PVC specimens indicate that the drop in the tensile strength is negligible as compared to gasket materials. It is noted herein that the PVC

specimens were significantly thicker than gasket specimens and this difference between the performance of PVC and gaskets are expected. After 13 weeks of exposure at 140 ºF, the strength loss was 7%. Even after 30 weeks of exposure, the strength loss was still 7-8%.

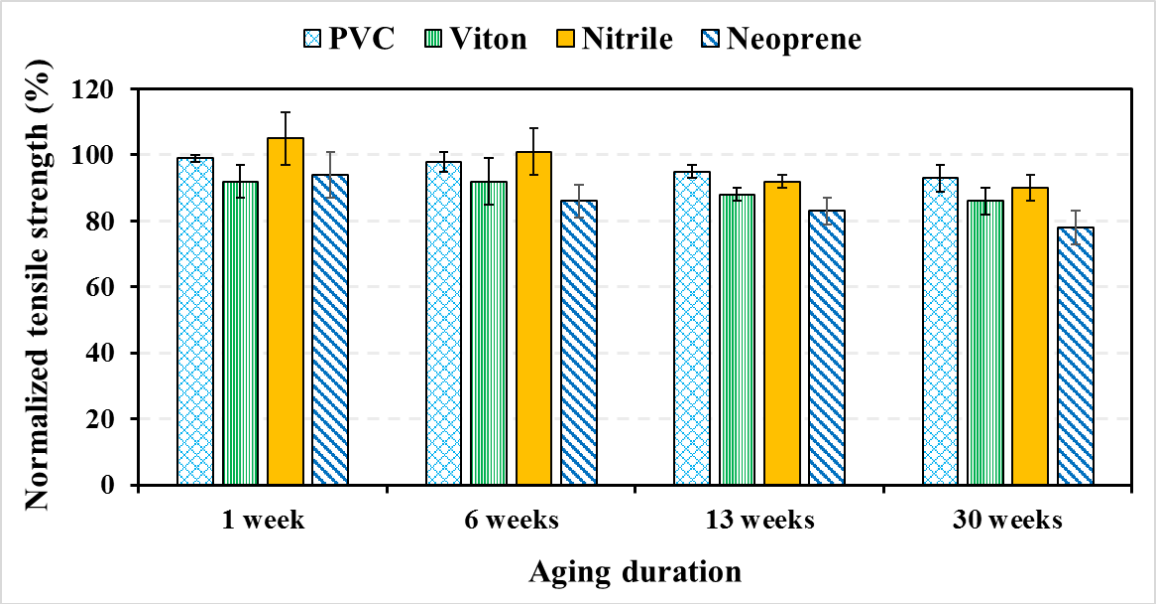

Figure 1: Tensile strength of PVC and rubber specimens exposed to deionized water at an aging temperature of 68 ºF.

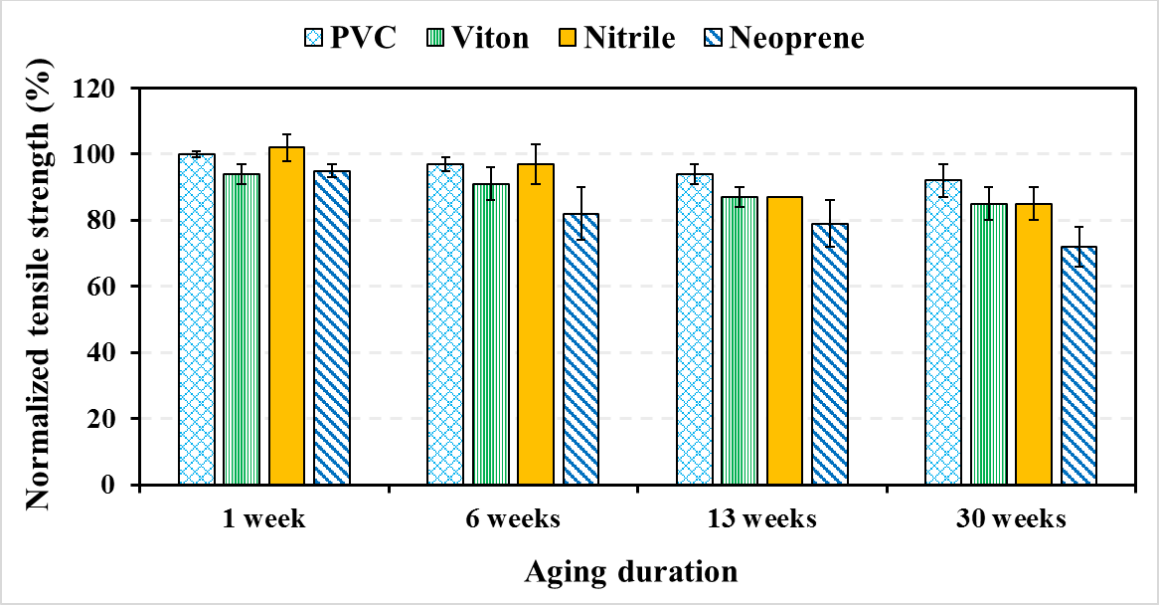

Figure 2: Tensile strength of PVC and rubber specimens exposed to deionized water at an aging temperature of 104 ºF.

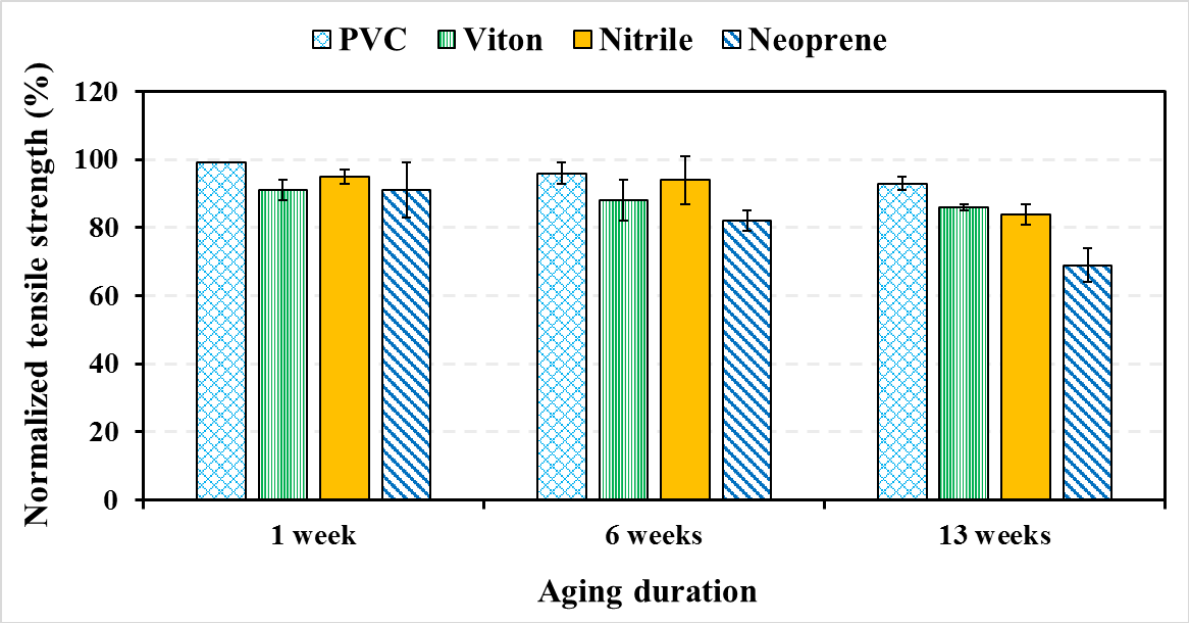

Figure 3: Tensile strength of PVC and rubber specimens exposed to deionized water at an aging temperature of 140 ºF.

Highlights: When exposed to water (in the absence of any contaminants) the order in which gasket materials retained higher tensile strength is: Viton®, nitrile, and neoprene.

The observed 10-15% reduction in tensile strength of Viton® was independent of exposure duration and temperature indicating that this reduction is potentially the maximum reduction expected in the absence of contaminants.

Figure 4, Figure 5, and Figure 6 show the results of reduction in tensile strength of PVC and gasket materials when exposed to PCE at three different temperatures. When exposed to aqueous solution of PCE at its solubility limit i.e., 206 mg/L, tensile strength of neoprene reduces dramatically with increasing the exposure time and/or temperature: the maximum drop was 54% obtained at 140 ºF after 13 weeks. According to data in Figure 4 and Figure 5, the tensile strength of neoprene specimens dramatically dropped to 65% and 58% of the strength of unaged specimens once they were exposed to PCE aqueous solution at 68 ºF and 104 ºF, respectively, for 30 weeks.

Based on data in Figure 4, Figure 5, and Figure 6, the largest drop in tensile strength of nitrile is 38% measured for the specimens aged at 140 ºF after 13 weeks. The tensile strength of nitrile specimens decreased 29% and 38% with 30-week exposure to PCE aqueous solution at 68 ºF and 104 ºF, respectively.

The results for Viton® exposed to PCE indicated that the largest strength loss was 29% which occurred at 140 ºF after 13 weeks. The results also indicated that the maximum tensile strength loss was about 28% for Viton® specimens when exposed to PCE solution at 104 ºF observed after 30 weeks of exposure.

Among all data obtained by performing tension testing on PVC specimens exposed to various media, the highest reduction in PVC tensile strength (22%) was detected at the exposure age of 25 weeks at 140 ºF (which is the longest exposure time and the highest aging temperature). This means the reduction in tensile strength of PVC is highly temperature dependent. As a matter of comparison, the decrease in tensile strength of PVC specimens were 13% and 17% once the exposure temperatures were 68 ºF and 104 ºF, respectively, after 30 weeks of exposure to PCE solution.

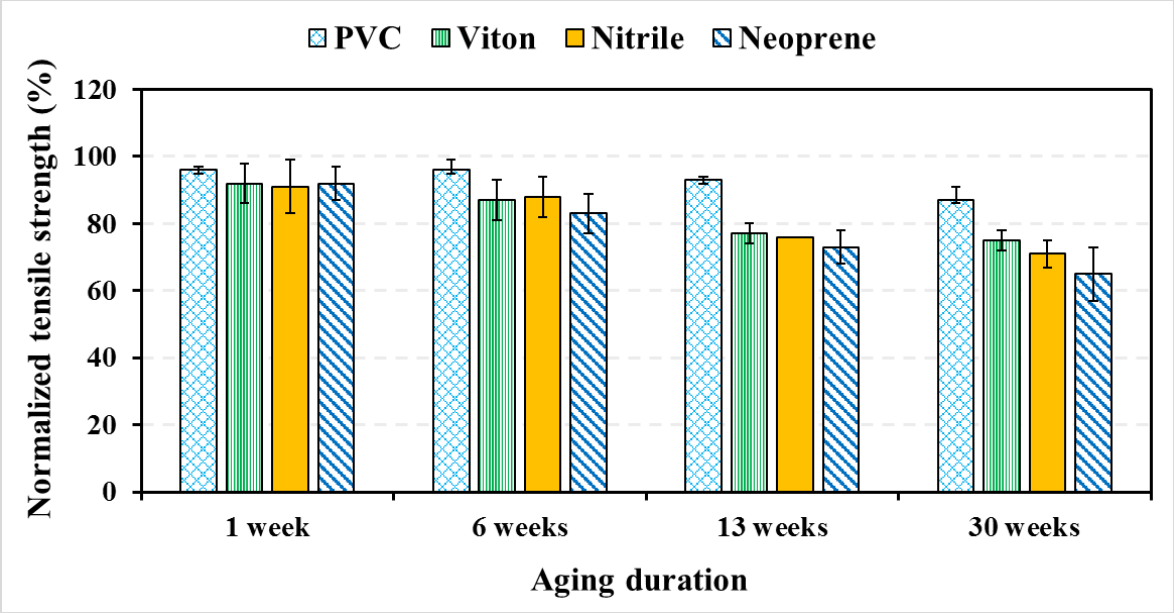

Figure 4: Tensile strength of PVC and rubber specimens exposed to PCE aqueous solution at an aging temperature of 68 ºF.

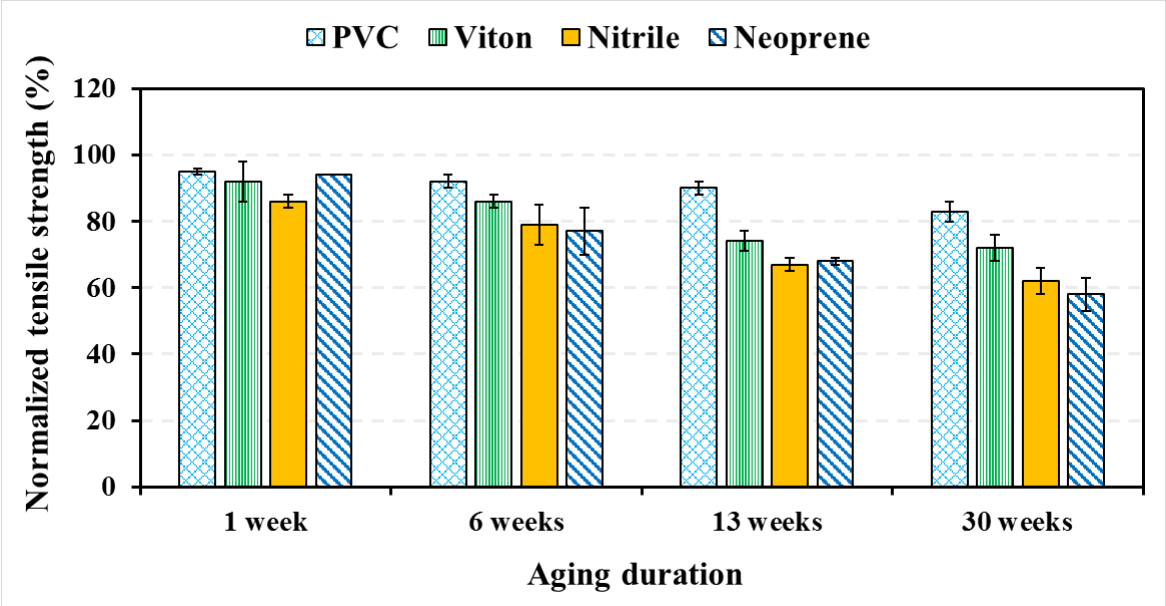

Figure 5: Tensile strength of PVC and rubber specimens exposed to PCE aqueous solution at an aging temperature of 104 °F.

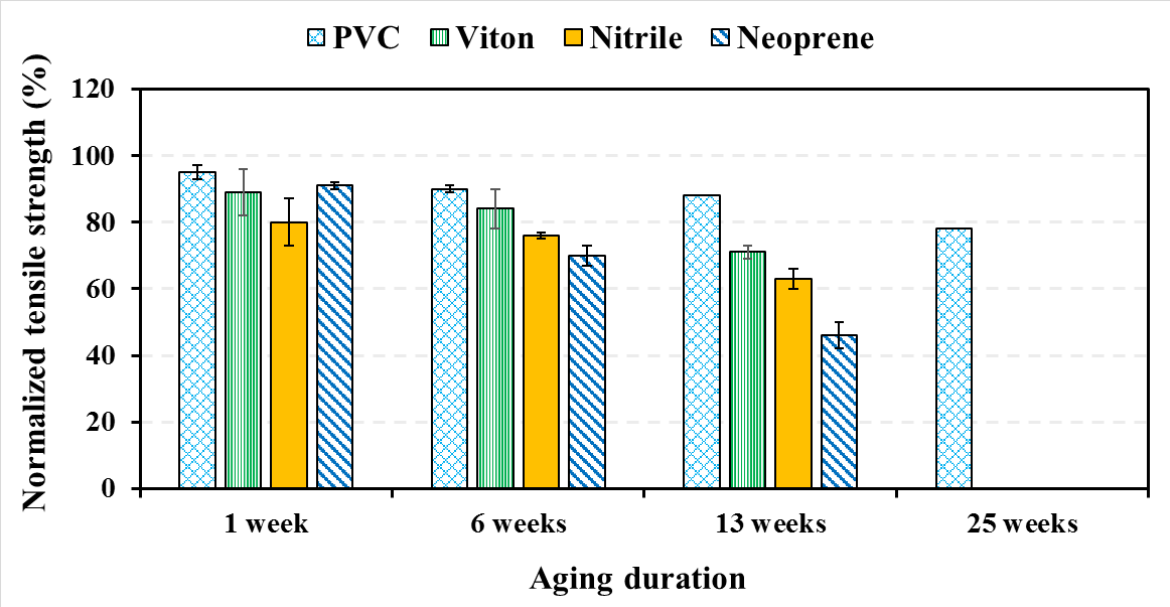

Figure 6: Tensile strength of PVC and rubber specimens exposed to PCE aqueous solution at an aging temperature of 140 °F.

Highlights: When exposed to PCE aqueous solution at its solubility limit (i.e., 206 mg/L), the gasket materials retained higher tensile strength in the following order: Viton®, nitrile, and neoprene. The degradation in strength was more pronounced when the exposure duration and/or aging temperature were elevated.

The decrease in PVC resistance to tensile strength degradation once exposed to PCE aqueous solution was intensified at higher temperatures.

Figure 7, Figure 8, and Figure 9 show the tensile strength loss of materials exposed to benzene aqueous solution at its solubility limit (i.e., 1790 mg/L) at different temperatures. It is noted that very rapid degradation of the neoprene specimens was observed, shown by swollen specimens (Figure 10). As a result, performing tensile test was not possible for the neoprene specimens being exposed to benzene at 140 ºF.

In Figure 7, Figure 8, and Figure 9, the maximum measured strength loss for neoprene was 64% which occurred at 104 ºF after 30 weeks. Moreover, neoprene specimens' tensile strength degradation at 68 ºF is 50% after 30 weeks of exposure. This means neoprene specimens became weak tensile strength-wise when exposed to benzene aqueous solutions. As can been seen in Figure 7, Figure 8, and Figure 9, similar to neoprene specimens, the issue of extensive swelling was observed for nitrile specimens exposed to benzene at 140 ºF. After 13 weeks of exposure at 140 ºF, the specimens are almost entirely degraded which did not allow us to conduct tensile strength testing. Additionally, there was a significant drop in mechanical strength of nitrile specimens aged in benzene aqueous solution for 30 weeks as observed in the case of neoprene. The maximum strength loss is 51% caused at 104 ºF.

Based on Figure 7, Figure 8, and Figure 9 which show the results for Viton® exposed to benzene, the maximum tensile strength drop of 50% was obtained for the specimens being aged at 140 ºF after 13 weeks of exposure. It should be noted that Viton® was the only material that could be tested after 13 weeks of exposure to benzene at 140 ºF. According to data shown in Figure 7, Figure 8, and Figure 9, and as shown for other gasket materials (i.e., neoprene and nitrile), benzene can dramatically impact the tensile strength of rubber gaskets. Exposure to the benzene aqueous solution at its solubility limit (i.e. 1790 mg/L) led to a decline of the tensile strength of Viton® specimens by about 38% and 46% aged at 68 ºF and 104 ºF, respectively, for 7 months.

According to data shown in Figure 7, Figure 8, and Figure 9, the highest drop in tensile strength of PVC specimens after 13 weeks of exposure was measured for specimens aged at 140 ºF (61%). Note that because of the softening of the specimen ends when exposed to benzene, the tension test could not be performed on the original specimen due to loss of contact pressure at grips. Therefore, the specimens were cut at their both ends, and the mid-section of the PVC specimens were then tested. While this introduced some error, which is manifested in having large standard division, we believe that the significantly lower strength is indeed mainly due to exposure to benzene. Among all the PVC specimens tested, the highest drop in tensile strength (79%) was obtained for

specimens aged at 104 ºF after 30 weeks. It should be noted that softening induced into in the specimens aged for 30 weeks is the most important reason for the relatively large strength loss observed. Note that the decrease in tensile strength of PVC specimens exposed to benzene solution was higher than that of Viton® specimens at elevated temperatures of 104 ºF and 140 ºF. This means PVC specimens were more susceptible to degradation than Viton® specimens once exposed to benzene solutions.

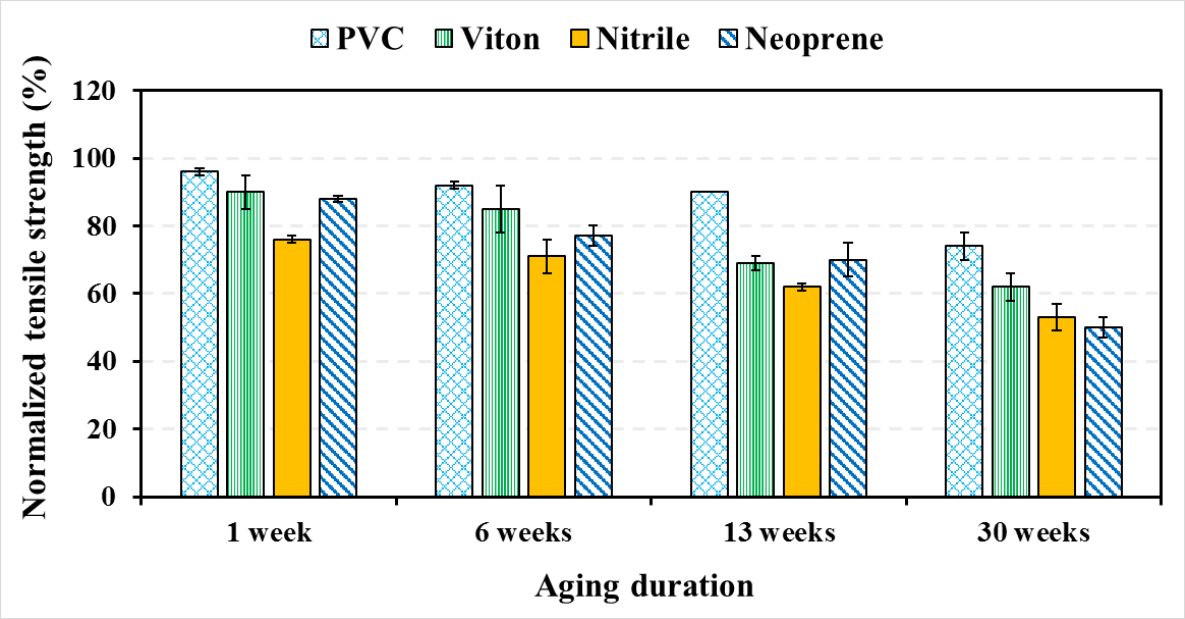

Figure 7: Tensile strength of PVC and rubber specimens exposed to benzene aqueous solution at an aging temperature of 68 ºF.

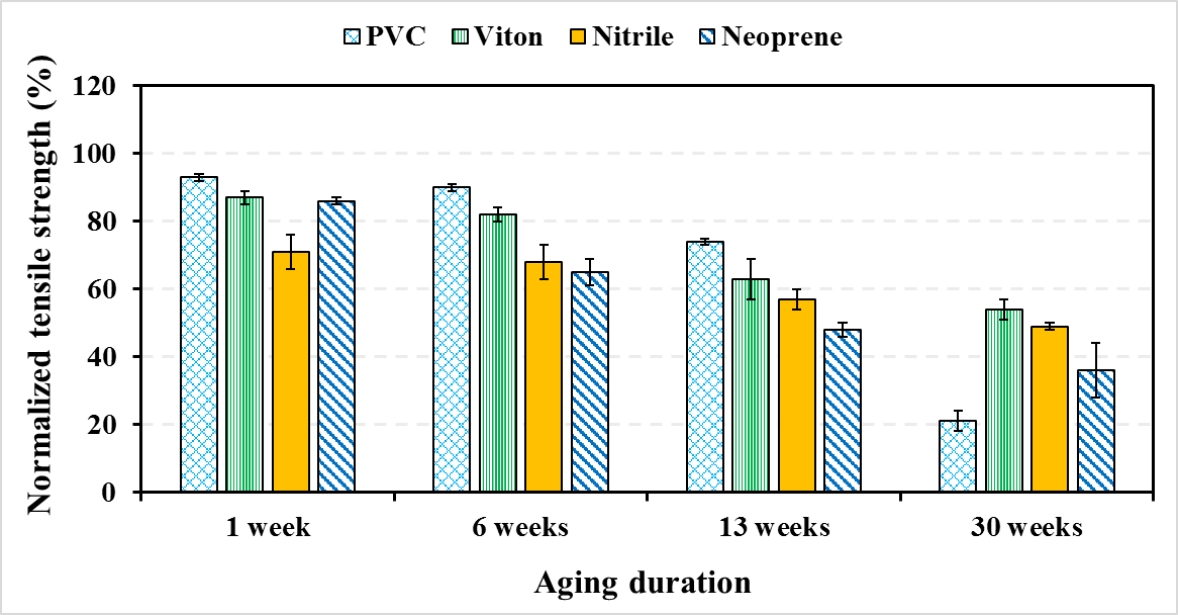

Figure 8: Tensile strength of PVC and rubber specimens exposed to benzene aqueous solution at an aging temperature of 104 ºF.

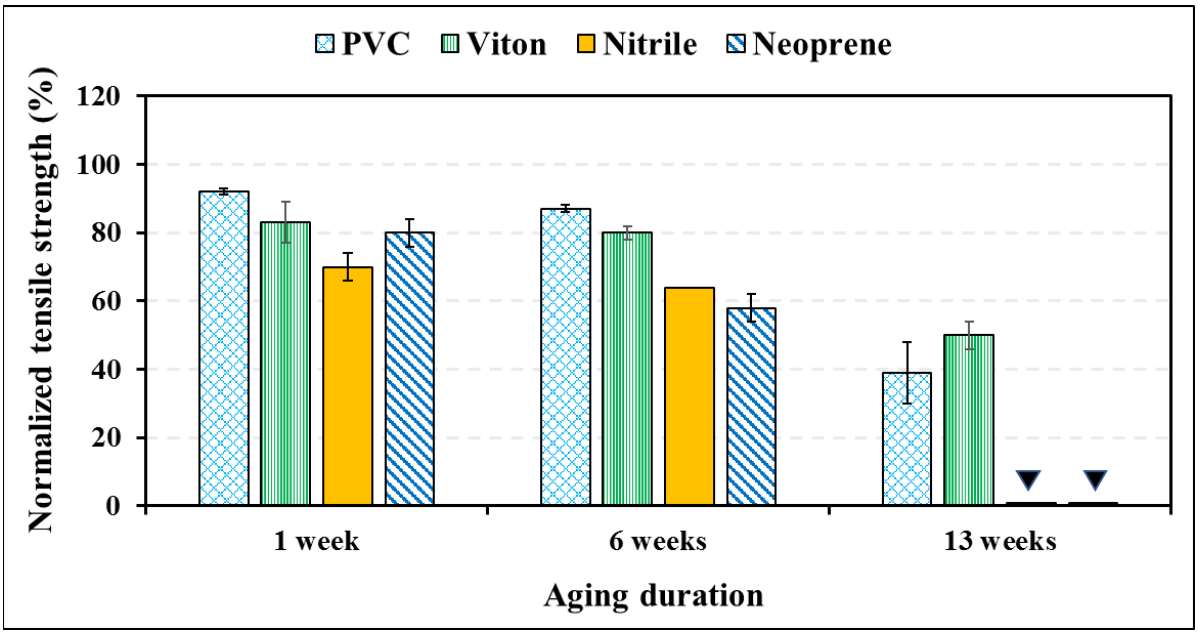

▼ Due to the severity of degradation of neoprene specimens after 13 weeks of exposure at 140 ºF, tension test could not be performed.

Figure 9: Tensile strength of PVC and rubber specimens exposed to benzene aqueous solution at an aging temperature of 140 ºF.

Figure 10: Swelling of neoprene specimen due to the prolonged exposure to benzene (13 weeks) at a high temperature of 140 °F. Left: Swollen specimen. Right: Unaged specimen for comparison.

Highlights: When exposed to benzene aqueous solution (at its solubility limit), Viton® performed far better than the other two gasket materials i.e., neoprene and nitrile.

Extensive swelling was observed when neoprene and nitrile specimens were exposed to benzene solution at elevated temperature of 140 °F.

The large reductions in tensile strength of PVC and rubber gasket materials once exposed to benzene solution indicate that benzene's effect is more detrimental, with regard to tensile strength degradation, than PCE.

4.2. Tensile strength degradation modeling

Following the process shown in Figure B5 (Appendix B), the calculated model parameters for each material type exposed to different contaminants are shown in Table 1. In Table 1, the models are in the form of exponential function as shown in Equation (3).

$$T_N = ae^{-bt} \quad (3)$$

where the T_N is the remaining tensile strength of the material as a fraction of the initial tensile strength at each specific time (t in days) and ambient temperature. Parameters a and b are the coefficients of the exponential models found in Table 1.

Table 1: Tensile strength degradation models for pipe and gasket materials exposed to contaminated water.

Material type	Exposure media	Model coefficients	
		a	b
Neoprene	PCE aqueous solution	0.91	0.0018
	benzene aqueous solution	0.86	0.0025
Nitrile	PCE aqueous solution	0.87	0.0010
	benzene aqueous solution	0.73	0.0016
Viton	PCE aqueous solution	0.90	0.0010
	benzene aqueous solution	0.89	0.0019
PVC	PCE aqueous solution	0.96	0.0003
	benzene aqueous solution	1.02	0.0015

It should be noted that the models obtained herein are based on the aqueous solutions of benzene and PCE at their solubility limits i.e., 1790 mg/L and 206 mg/L, respectively. However, even 20% of solubility limits of these chemicals are considered to be a high level of environmental pollution in contaminated groundwater (Mao, 2008). The high concentrations are mainly

encountered in the field in close proximity to a nonaqueous phase liquid (NAPL) (Mao, 2008). Accordingly, the proposed models are conservative for the field applications and the degradation rate in the field is likely to be lower than the one predicted by the models.

Concentration of organic compounds in aqueous solutions has a great influence on diffusion rates of solvents through plastics and rubbers (*Mao, 2008*). The sorption rate decreases dramatically as the concentration of contaminant reduces. Equation 4 introduces a modified model for the tensile strength degradation of the materials tested by applying a function (β) to the exponent of Equation 3 to account for the saturation level of exposure media (i.e., the ratio of concentration of contaminant of interest in a media to its solubility limit in that media). Note that β is applied to the exponent of tensile strength degradation models to avoid altering the assumed form of degradation models i.e., exponential function yet showing a reduction in the extent of tensile strength degradation by decreasing the saturation level of the water contaminants.

Two different functions can be considered for β: Linear and nonlinear. The linear function is simply the concentration of the contaminant over the saturation level. For example, in the case of exposure to benzene at a concentration of 179 mg/L, β = 179/1790 = 0.10. In the nonlinear approach the function β is calculated using Equation 5. The nonlinear approach is more conservative than the linear approach at low concentrations (less than 20%) which is the case for the majority of chemical spillage into the groundwater; at high concentration the value of β also rapidly approaches 1.0. It should be noted that Equation 5 is similar at low concentration to widely used models of sorption isotherms for polymers. Figure 11 shows both linear and nonlinear β functions ($0 < \beta \leq 1$).

$$T_{N,m} = ae^{-b\beta t} \tag{4}$$

$$\beta = Ln\left(\frac{\frac{S}{100}}{1-\frac{S}{100}}\right) \tag{5}$$

where $T_{N,m}$ is the modified normalized tensile strength and S is the saturation level or percentage of solubility limit of contaminant of interest in the aqueous exposure media in percent. The solubility limits for benzene and PCE are 1790 mg/L and 206 mg/L, respectively.

As can be seen in Figure 11, after 20% of saturation, β increases rather constantly up to 80% saturation level for the contaminant of interest. After this point, it rapidly goes up to reach unity and represents the saturation level which is the case in the vicinity of gross spillage of chemicals.

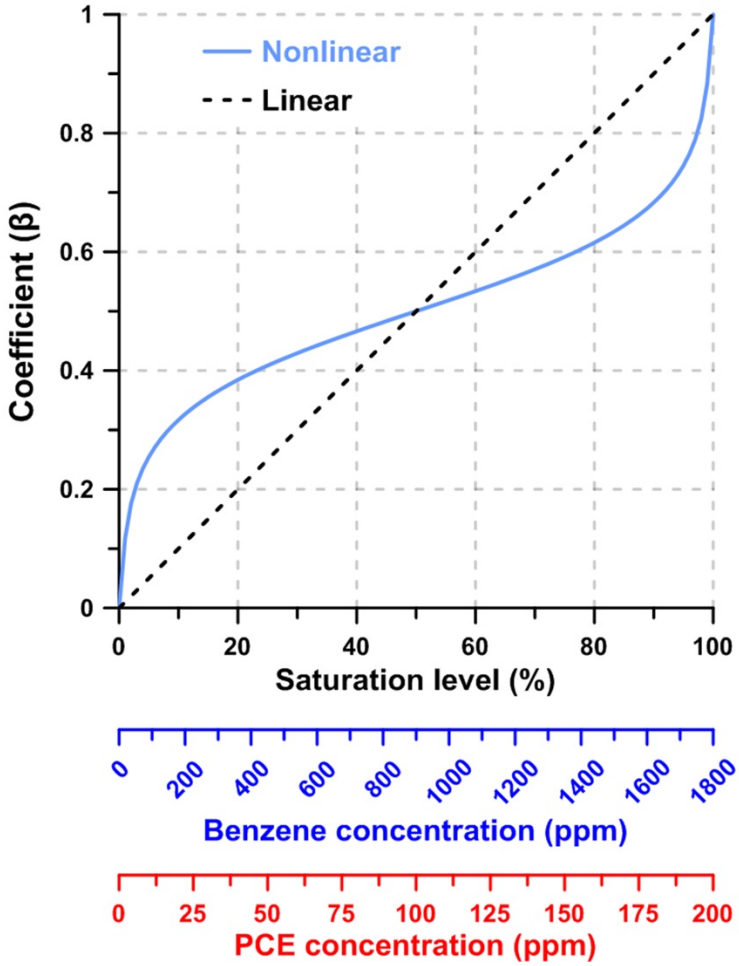

Figure 11: Conceptual models for the calculation of saturation dependence constant factor (β). Note that saturation or solubility limits for benzene and PCE in water are 1790 mg/L and 206 mg/L, respectively.

4.3. Concrete pipe

4.3.1. Compressive strength test

The results of the compressive strength of mortar specimens (with the same mixture proportion as concrete used in pipe production) aged in benzene and PCE aqueous solutions at their solubility limits i.e., 1790 mg/L and 206 mg/L for benzene and PCE, respectively, and uncontaminated water are presented in Figure 12. The compressive strength of mortar aged up to 6 months in clean and contaminated water was 9.24 ± 0.43 ksi and 9.01 ± 0.51 ksi, respectively. In addition, after 12 months of exposure, the compressive strength of mortar specimens was 10.11 ± 0.24 ksi and 9.81 ± 0.39 ksi for clean and contaminated water, respectively. This means no statistically significant change in compressive strength of mortar specimens was detected due to

water contamination after 6 and 12 months of exposure, and therefore, the mechanical stability of concrete pipes would not be altered by water contamination at the contaminants' solubility limits.

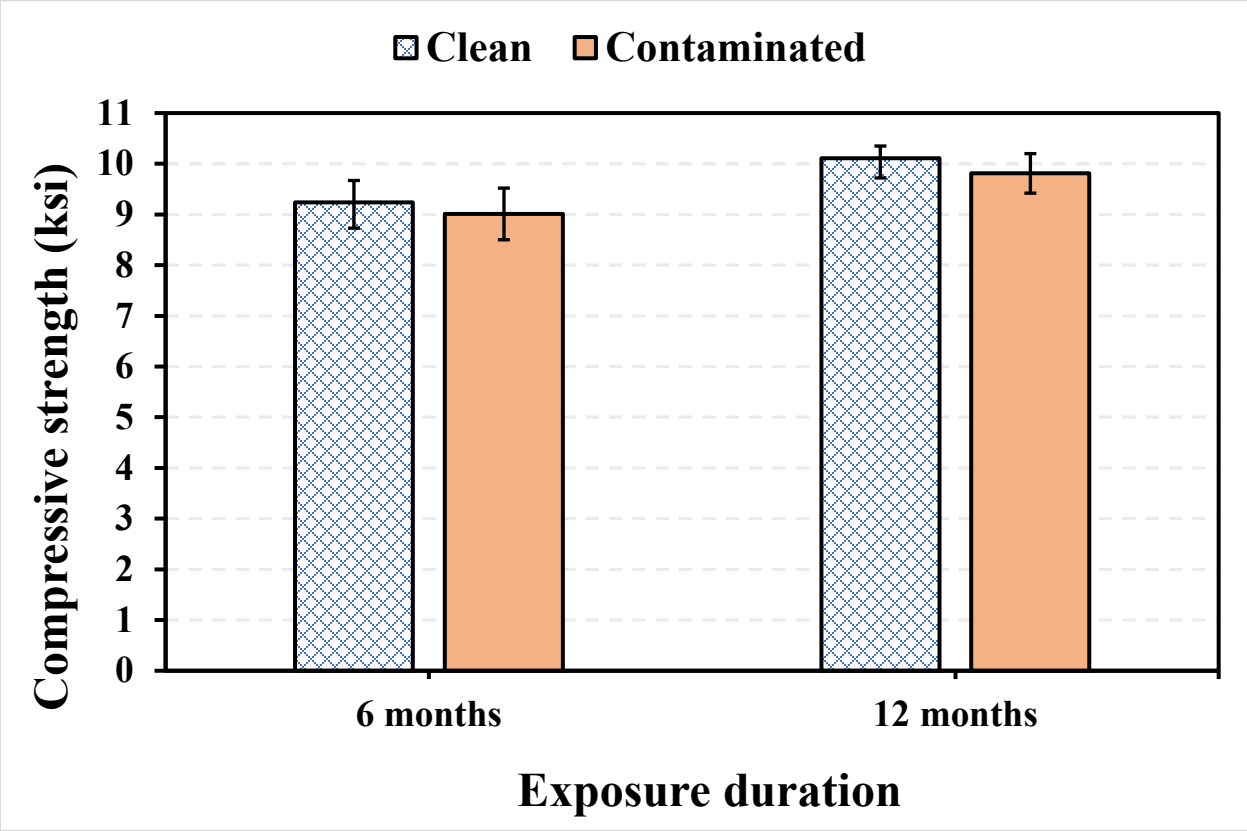

Figure 12: Compressive strength of mortar exposed to contaminated and uncontaminated water.

Highlights: Contamination of water with aromatic and chlorinated hydrocarbons at their solubility limits did not affect the compressive strength of concrete pipe materials. This is expected since concrete materials are inorganic in nature and low concentration organic compounds have negligible effect on the mechanical properties of concrete.

4.3.2. Unsaturated sorption test

The average values and standard deviations for absorbed water in each set of concrete pipe specimens in contact with pure water or PCE aqueous solution are shown in Figure C2 (see Appendix C, section C.2 for more details). Results suggest that the changes in liquid absorption for both categories of specimens overlap; this means that PCE, even at its solubility limit, does not

have a significant influence on sorptivity of concrete specimens. The initial and secondary rates of absorption were calculated based on the sorption results (Figures C3 and C4 and Table 2). As can be observed in Table 2, there is no significant difference in initial and secondary sorption rates between absorption of water and PCE aqueous solution at its solubility limit (i.e. 206 mg/L). These findings show that since the solubility limit of aromatic and chlorinated hydrocarbons in water is very low at ambient temperature, they cannot affect the unsaturated sorption of concrete pipe.

Table 2: Sorption rates of pure and contaminated water for concrete pipe specimens.

Specimens category	**Initial sorption rate (10^{-3} in/s$^{0.5}$)**	**Secondary sorption rate (10^{-3} in/s$^{0.5}$)**
Pure water exposure	0.33 ± 0.02	0.01 ± 0.001
PCE aqueous solution exposure	0.35 ± 0.01	0.01 ± 0.004

The results of water absorption over time for mixtures with and without Xypex® are shown in Figures C5 and C6 for clean and PCE aqueous solution, respectively (Appendix C). According to Figures C5 and C6, at each measurement time, the total sorption of contaminated or uncontaminated water for the specimens with Xypex® is less than that absorbed by control specimens.

The initial and secondary rates of sorptivity calculated based on Figure C7 to Figure C10, is reported in Table 3; there is slight difference (only 5% reduction) in the initial rate of absorption for the Xypex®-incorporated mixture compared to the control mix while exposed to clean water. The decrease in the initial rate of absorption is 7% by the incorporation of Xypex® in case of PCE solution exposure. Moreover, compared to the control mixture, no discernable difference could be detected with the addition of Xypex® as the specimens were in contact with PCE aqueous solution at its solubility limit (i.e. 206 mg/L).

Table 3: Sorption rates of clean and contaminated water for mortar specimens.

Type of exposure	**Specimen category**	**Initial sorption rate (10^{-3} in/s$^{0.5}$)**	**Secondary sorption rate (10^{-3} in/s$^{0.5}$)**
Pure water exposure	Control (without Xypex®)	0.43 ± 0.03	0.02 ± 0.001
Pure water exposure	Mixture containing Xypex®	0.41 ± 0.03	0.02 ± 0.002

PCE aqueous solution exposure	Control (without Xypex®)	0.44 ± 0.01	0.02 ± 0.002
PCE aqueous solution exposure	Mixture containing Xypex®	0.41 ± 0.01	0.02 ± 0.001

Highlights: The unsaturated sorption rates of concrete pipes did not change when exposed to hydrocarbon contaminated water (at their solubility limit) as compared with pure water as exposure medium. This indicates that the rate of water absorption can be used as a good estimate for the rate of absorption of water containing VOCs.

Xypex® did not change the sorption rates of mortar specimens in any statistically meaningful manner either in the absence or presence of contaminants.

4.3.3. Diffusion measurements

The results of calculation of diffusion coefficient of benzene and PCE vapors through saturated concrete are presented in Table 4. Diffusion coefficient of benzene vapor through mortar specimens with and without Xypex® can also be found in Table 4. Note that since benzene showed a higher value of diffusion coefficient than PCE in concrete, it was selected to further investigate the effect of Xypex® on VOCs vapor diffusion coefficient.

According to data in Table 4, diffusion of benzene through saturated concrete pipe is one order of magnitude faster than that of PCE. This can be attributed to the smaller molecular size of benzene compared to PCE and lower solubility limit of PCE (Mao, 2008), which in turn cause lower concentration of PCE vapor to be exposed to the surface of concrete pipe specimen.

As can be seen in Table 4, by the application of Xypex® admixture, the diffusion coefficient of benzene was reduced by almost 24% compared to the control mixture (without the admixture). Although no information is available on the composition of Xypex®, it seems that this decrease in the diffusion coefficient of benzene may be related to the finer pore structure of mortar after using the Xypex® due to its interaction with the matrix.

Table 4: Diffusion coefficient of VOCs vapors through cement-based materials

Type of material	Description	Diffusive vapor	Diffusion coefficient ($\times 10^{-12}$ m^2/s)
Concrete	Concrete pipe	benzene	2.88 ± 0.50
Concrete	Concrete pipe	PCE	0.24 ± 0.08
Mortar	Without Xypex®	benzene	9.91 ± 0.81
Mortar	With Xypex®	benzene	7.55 ± 0.64

Highlights: The diffusion coefficient of benzene vapor through concrete pipe is one order of magnitude higher than that of PCE vapor.

Xypex® reduced the diffusion coefficient of benzene vapor through concrete by 24% as compared to concrete that does not contain Xypex®.

4.4. Saturated soil modeling

4.4.1. Model development

The modeling work was focused on evaluating the effect of a continuous source of contamination on the contaminant distribution regime within the installed pipe trench. The analyses assumed intact and damaged conditions for pipe and gaskets. While there is information in the literature on the hydraulic conductivity of the concrete material for intact pipes, such information is neither available for the various gasket materials nor damaged concrete materials. The input parameters, were not specific to a given type of gasket; rather, the hydraulic conductivity of the undamaged gasket was assumed to be equal to that of the intact concrete in analyses presented herein. For representing a damaged gasket, the value of the hydraulic conductivity of the gasket was increased by orders of magnitude, depending on the presumed level of damage.

The focus of modeling work was on gasoline leakage from underground storage tanks with resultant contamination in a shallow underlying aquifer with subsurface concrete pipe located in a nearby trench. The contaminant considered in this study is benzene since it has the highest transported volume in the aqueous phase (Powers et al. 2001) and is one of the prevalent species found in NCDOT right of ways. Visual MODFLOW Flex, by Waterloo Hydrogeologic, coupled with MT3DMS engine, was used to model gasoline leakage from an underground storage tank (UST) with an adjacent subsurface concrete pipe installed in a trench. The modeled 3-D domain was developed for the profile illustrated in Figure 13.

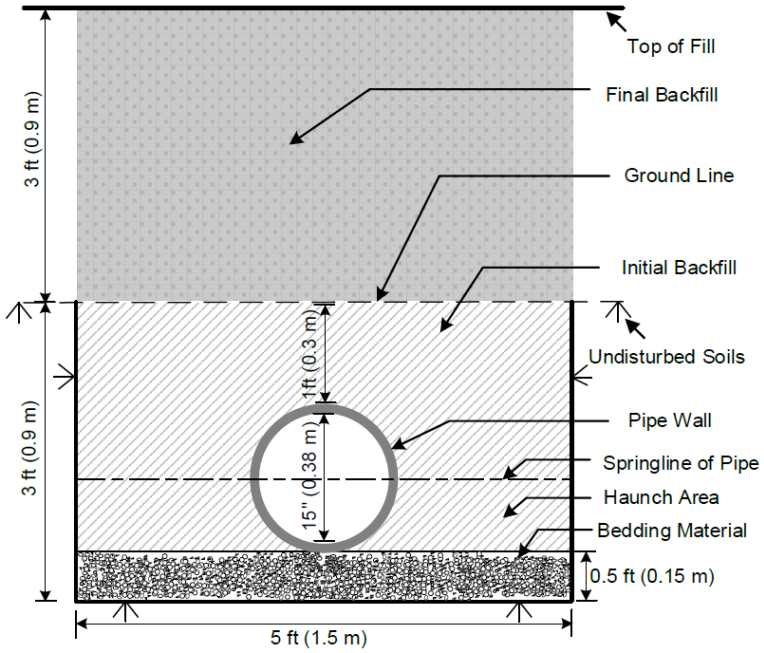

Figure 13: Profile section for installed drainage concrete pipe in a trench.

The contamination source was considered to be a continuous source of aqueous phase benzene generated from a leaking underground storage tank. Figure 14 shows a schematic of the site map being simulated in the analysis, including the UST location in a pit and the location of the contaminant source in relation to the subsurface pipe. The flow and contaminant transport simulations were run for 20 years.

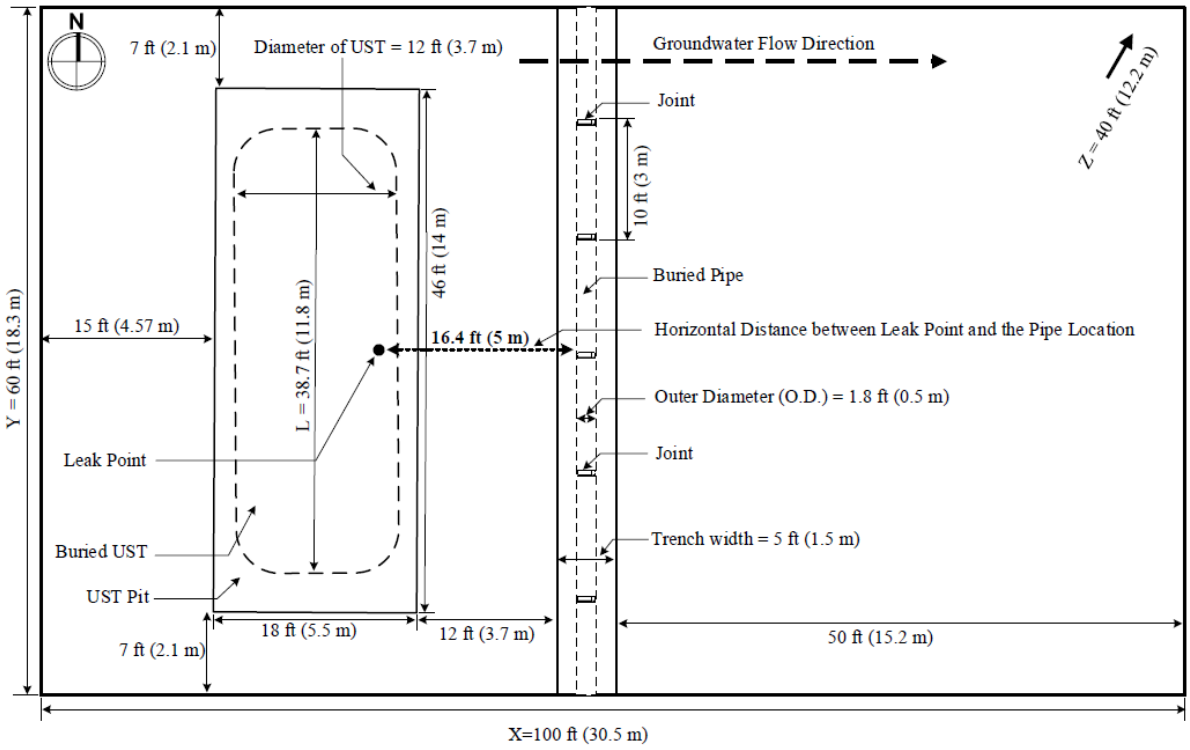

Figure 14: Site Map showing the UST location in a pit, contaminant source point, the subsurface concrete pipe location, and the groundwater flow direction.

Zones within the layers' domain were assigned hydraulic conductivity (k) and effective porosity (n_e) values. These k and n_e values, and the soil zones to which they are assigned, are schematically shown in Figure 15. Constant head values were used as the west and east boundaries of the model domain and were defined as 12.5 m (41 ft) at the western boundary and 12.2 m (40 ft) at the eastern boundary (Figure 15) for a cross-site gradient of 1%. A drained boundary was applied at the southern end of the pipe to allow the outflow through the pipe from the model domain. This flow is driven by the difference between the head in the aquifer and drainage pipe elevation. The pipe was assumed to flow half full. Thus, the total head inside the pipe is represented by the elevation corresponding to the mid-height of the pipe (10.7 m). This configuration models drained condition inside the pipe (i.e., no built-up of pressure head is allowed).

The source of contamination was designated as a point leak at the base of the underground storage tank (Figure 15). The mechanism of contamination is through a source of aqueous phase that may occur due to the presence of the free product in contact with the water phase. A specified flux boundary condition was applied at the base of UST (3.7 m below ground surface), assuming the flux rate of aqueous benzene equal to 0.02 m/d. The concentration of benzene in groundwater found at a site in North Carolina is 21.1 mg/L or 21,100 µg/L (based on the measurements obtained from a site located at 1707 Lejeune Boulevard, Jacksonville, Onslow County, NC). This value is assigned to the leak point in the model.

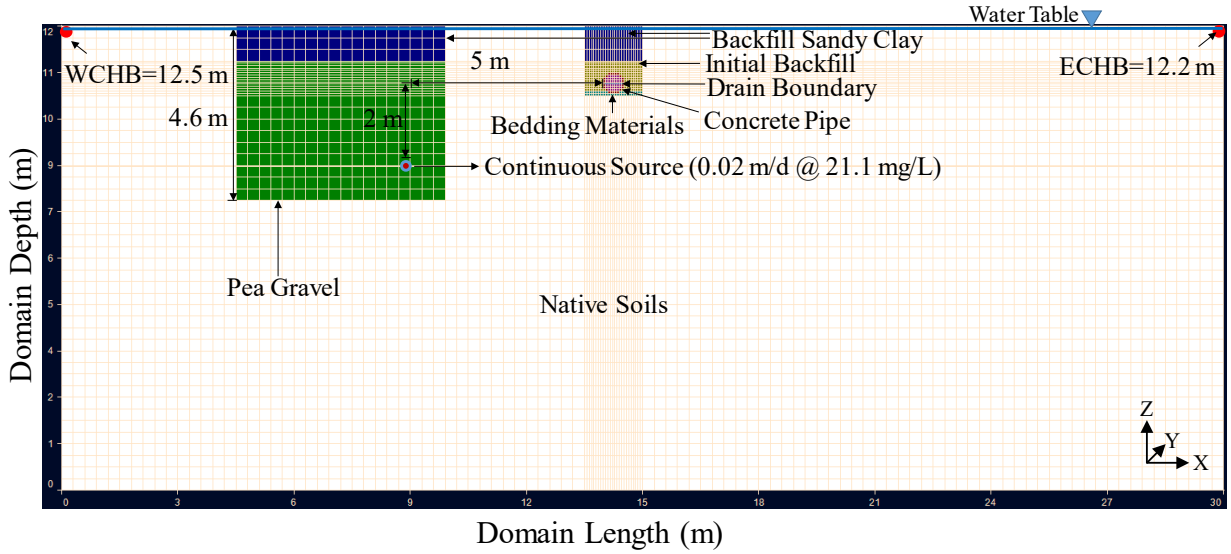

Figure 15: Cross-section view of MODFLOW grid and model design.

As mentioned earlier, the values of hydraulic conductivity and the definition of the level of damaged of various types of gaskets used with concrete pipes are not found in the literature. However, as the k-values of the gasket were compared to the k-values of the pipe, it was assumed that $k_{gasket} \leq k_{pipe}$, is classified as a good gasket condition and the $k_{gasket} > k_{pipe}$ is classified as a damaged gasket condition. Damage gasket refers to incorrect installation, and degradation or cracking with time. The input parameters, therefore, were not specific to a given type of gasket. Scenarios representing "damaged and undamaged" gaskets are considered with three levels of pipe damage modeled using a range of the equivalent hydraulic conductivity values. The value of hydraulic conductivity of an undamaged gasket is 10^{-9} cm/s, which is the value for intact concrete. The three levels of damage to gasket were therefore assumed as follows (with each level assumed to increase the k value by two orders of magnitude:)

(i) k-value of low-level damage is 10^{-7} cm/s,
(ii) k-value of moderate-level damage is 10^{-5} cm/s, and
(iii) k-value of severe-level damage is 10^{-3} cm/s.

The concrete pipe is assumed to be in good condition for these three scenarios of damaged gaskets. On the other hand, damaged and undamaged pipes are also considered in this analysis with three levels of damage as follows:

(i) k-value of low-level is 10^{-8} cm/s,
(ii) k-value of moderate-level is 10^{-6} cm/s, and
(iii) k-value of severe-level is 10^{-4} cm/s.

The gasket is assumed to be in good condition for these three scenarios of the damaged pipe, albeit the pipe will be more exposed to contaminant since the pipe has a higher surface area. Two native

soil types, sandy clay soils ($k=10^{-5}$ cm/s) and sandy soils ($k=10^{-3}$ cm/s), were evaluated in the analysis.

4.4.2. Modeling results

4.4.2.1. Gasket material condition

The benzene concentration breakthrough with time for the three assumed levels of damage to the gaskets and with the two different native soils (sandy soils; k_{soil} =10^{-3} cm/s, and sandy clay soils; k_{soil} =10^{-5} cm/s) is shown in Figure 16. No aqueous phase benzene was detected above the Maximum Contaminant Level (MCL), which is 5 µg/L at t = 20 years. This was the case for the three levels of the damaged gasket with the native soil having saturated hydraulic conductivity of 10^{-5} cm/s (sandy clay soils). In this case, the aqueous phase benzene was preferentially transported through the higher hydraulic conductivity layers and upwardly toward the backfill. The benzene concentration started to break through the "severely" damaged gaskets when the native soil was modeled as sandy soils (k_{soil} = 10^{-3} cm/s) at approximately 1-year period with a concentration of ~ 0.2 µg/l. The benzene concentration was found to permeate through the pipe with the three levels of the damaged gaskets at an approximately 2-year period, followed by an increase in the concentration with time. However, these concentrations at 20 years were below the MCL.

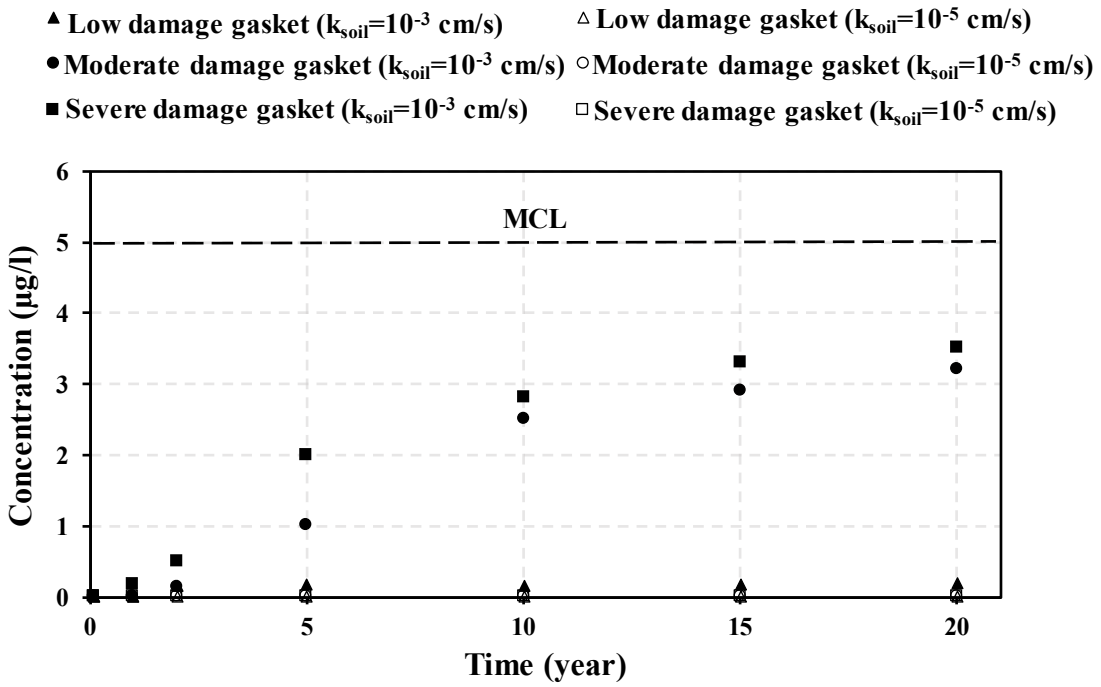

Figure 16: Peak aqueous phase benzene concentration detected inside the pipe for damaged gasket level, as a function of time with two different native soil types: (i) sandy soils; k_{soil}=10^{-3} cm/s, and (ii) sandy clay soils; k_{soil}=10^{-5} cm/s.

The results were further compiled as the mass of benzene in the aqueous phase flowing out of the pipe over the simulation time. Figure 17shows the mass of benzene flowing out of the pipe, as a function of time, for the assumed three levels of damage to the gaskets and with the two different native soil types. There was no mass of benzene flowing out of the pipe at t = 20 years for the three levels of the damaged gasket when the sandy clay soil condition (k_{soil} = 10^{-5} cm/s) was used in the analyses. On the other hand, when the native soil was sandy soils (k_{soil} = 10^{-3} cm/s), the mass of benzene flowing out of the pipe increased to nearly 33 mg, 600 mg, and 660 mg over the 20-year simulation time for the low, moderate, and severely damaged gasket cases, respectively.

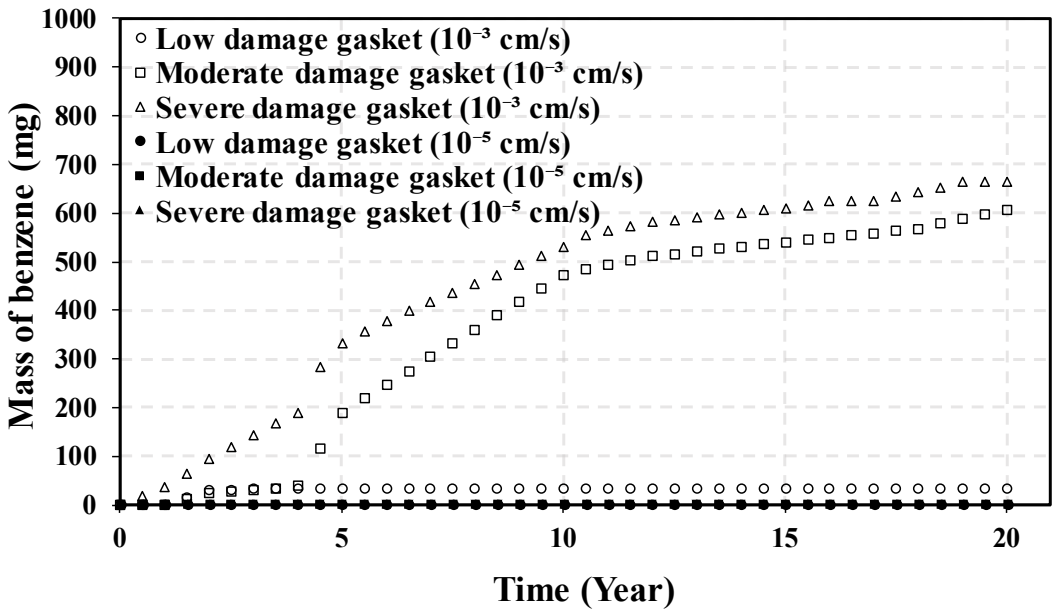

Figure 17: The total mass of benzene flowing out of the pipe from the damaged gasket level, as a function of time with two different native soil types: (i) sandy soils; k_{soil} =10^{-3} cm/s, and (ii) sandy clay soils; k_{soil} =10^{-5} cm/s.

Highlights: The breakthrough of benzene into the subsurface pipe is dependent on the saturated k-values of the native soil. Given the analyses parameters, there was no benzene estimated within the pipe with the damaged gaskets during the 20-years simulation time with k_{soil} = 10^{-5} cm/s. In this case, solute was transported upwardly into the backfill soil with the higher k-value. Thus, a damaged gasket, as described herein, should not be a concern when the native soils have low hydraulic conductivity ($k \leq 10^{-5}$ cm/s).

4.4.2.2. Pipe material condition

In comparison to results from scenarios accounting for the gasket condition, the results from scenarios assuming different levels of damaged pipe are shown in Figure 18. For the three levels of damaged pipe with k_{soil}=10^{-5} cm/s (sandy clay soils), the concentration of the aqueous phase benzene detected at the 20 years was below the MCL. The aqueous phase benzene concentration began to permeate through the pipe at an approximately 1-year period for the three levels of damage and with k_{soil} = 10^{-3} cm/s (sandy soils). This breakthrough is followed by an increase in the concentrations with time. The concentrations at 20 years approximately reached the MCL. The overall breakthrough of aqueous benzene concentration for the scenarios of damaged pipe levels is significantly higher than the breakthrough of aqueous benzene concentration for the scenarios of damaged gasket levels. The reason is associated with the higher surface area for the

pipe compared to gaskets as the analyses results presented herein assume that the whole length of the modeled pipe is damaged.

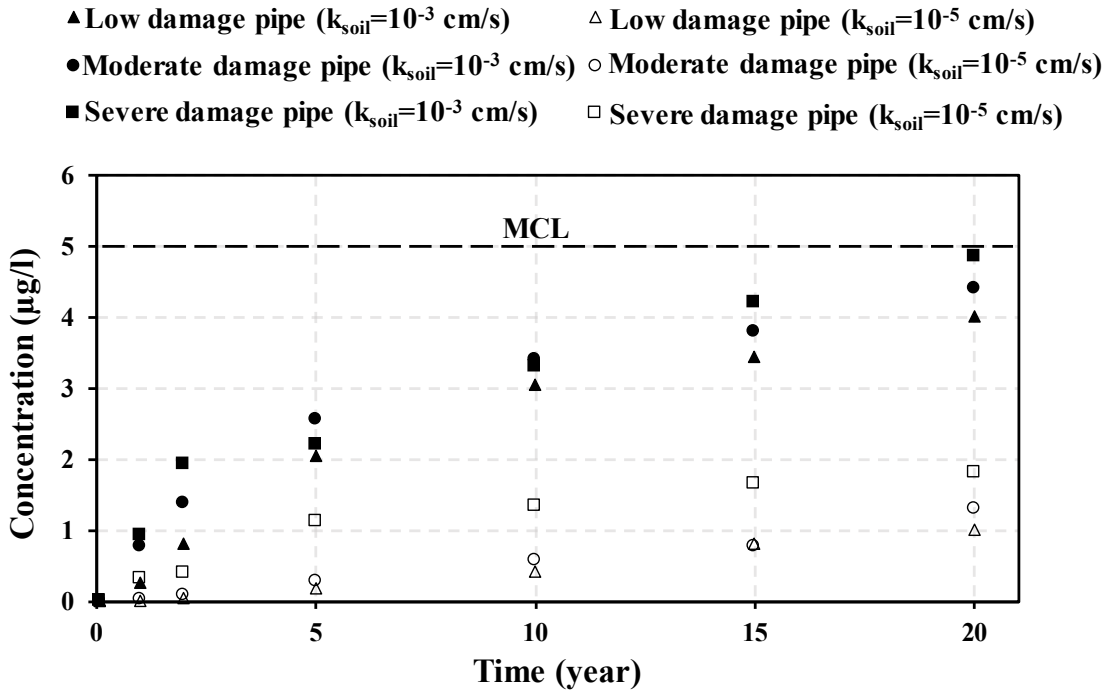

Figure 18. Peak aqueous phase benzene concentration detected inside the pipe for damaged pipe level, as a function of time with two different native soil types: (i) sandy soils; k_{soil}=10^{-3} cm/s, and (ii) sandy clay soils; k_{soil}=10^{-5} cm/s.

The mass of benzene flowing out of the pipe with time for the three levels of damage with the two native soil types (10^{-3} cm/s, and 10^{-5} cm/s) assumed in the analysis is shown in Figure 19. The masses of benzene flowing out of the pipe at t = 20 years for the low, moderate, severe damaged pipe with sandy clay soil (k_{soil} = 10^{-5} cm/s) are 189, 245, and 344 mg, respectively. For k_{soil} of 10^{-3} cm/s, the masses of benzene flowing out of the pipe ranged approximately from 780 for low damage to 920 mg for severe damage. The breakthrough mass of benzene for the scenarios of damaged pipe levels is higher than the mass of benzene for the scenarios of damaged gasket levels.

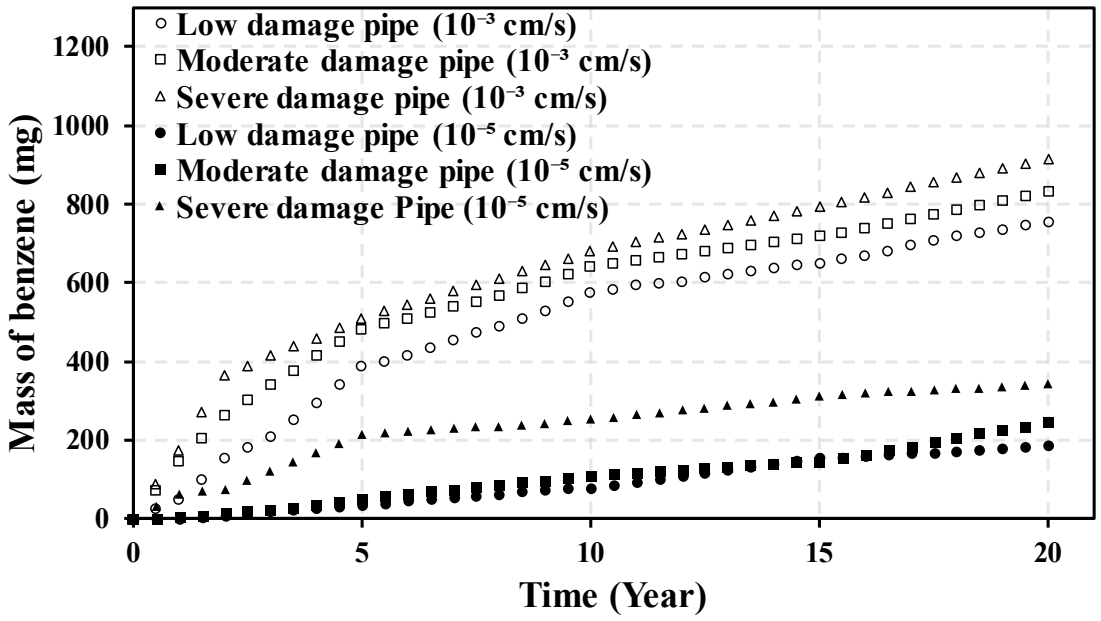

Figure 19: The total mass of benzene flowing out of the pipe from the damaged pipe level, as a function of time with two different native soil types: (i) sandy soils; $k_{soil} = 10^{-3}$ cm/s, and (ii) sandy clay soils; $k_{soil} = 10^{-5}$ cm/s.

Highlights: The highest potential of benzene breaking through the pipe, and the mass of benzene flowing out of the pipe, was when the damaged pipe was assumed, rather than the damaged gasket, with sand soil having k on the order 10^{-3} cm/s. The reason is associated with the larger surface area through which breakthrough occurs. Thus, the damage to the pipe can potentially be more critical compared to the damage to the gaskets for the occurrence of contamination breakthrough the subsurface pipe.

4.5. Unsaturated soil modeling

4.5.1. Model development

Benzene transport scenarios through unsaturated subsurface profile and pipe trench corridor were analyzed. The simulations investigated multiphase multicomponent transport considering the effects of several variables including water table levels, pipe material quality, gasket condition, the source size and the unsaturated soil hydraulic properties. The concentrations inside the pipe in gas and aqueous phases have been evaluated. In addition, the mass ingress into the pipe, in the various phases is calculated. The effect of volatilization through the atmospheric layer has been considered in the analyses. The numerical model is developed using TOUGH and Petrasim numerical code T2VOC (Falta et al. 1995). As mentioned earlier, the code considers simultaneous flow of three phases (aqueous, gaseous and NAPL). Transport of the three phase components occurs by advection in all three phases and by multicomponent diffusion in the gas phase.

4.5.1.1. Site description

The study site used as a guide to develop the model input parameters is located in Jacksonville, Onslow County, North Carolina. Gasoline leakage was detected at the site which has a nearby subsurface concrete pipe. This gasoline leakage led to contamination of underlying soil layers. The nearby subsurface drainage concrete pipe is installed in a trench located along Western Boulevard adjacent to the gasoline station, as shown in Figure 20. The information presented herein is from reports by Delta (2000), Antea (2016) and Terracon (2018). Soils at the subject location are moderately to well drained silt, and silty to sandy clay. According to reported results from slug testing, the hydraulic conductivity of the geologic material ranged from 6.24×10^{-5} cm/s (1.77×10^{-1} ft/day) to 9.07×10^{-5} cm/s (2.57×10^{-1} ft/day) with an average of 7.33×10^{-5} cm/s (2.08×10^{-1} ft/day) (Delta 2000). The average hydraulic gradient of groundwater flow is 1% with northeast direction. Figure 20 shows the site map with model domain dimensions used in unsaturated analyses. The gas station, the monitoring well locations, and groundwater flow contours are also shown on Figure 20. As presented in the reports by Antea (2016) and Terracon (2018), benzene persisted at concentrations above the regulatory limit. They reported petroleum hydrocarbon as NAPL thickness of 0.47 m (1.53 ft) at MW-12. The reader is referred to the later section 4.5.2.4 of the report for NAPL thickness used in the analyses and the influence of the assumed NAPL thicknesses on the analyses results. Benzene, toluene, ethylbenzene, and xylenes (BTEX) were reported with solid phase concentration of 3207 mg/kg (Antea, 2016, Terracon, 2018).

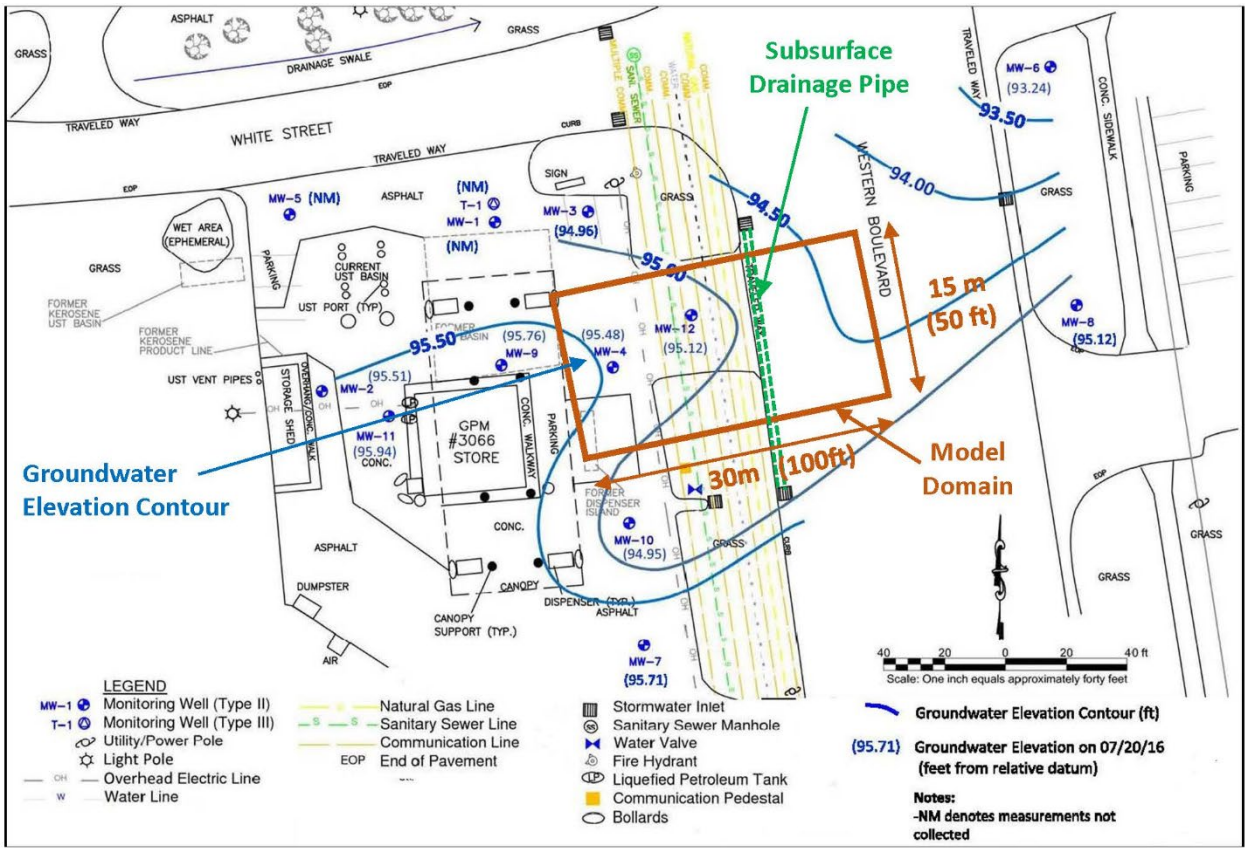

Figure 20: Jacksonville site map and model domain dimensions being simulated in unsaturated analyses (Antea, 2016).

4.5.1.2. Model configuration

The soil domain is simulated by 3D rectilinear geometry. The domain dimensions are 30 m × 15 m × 6 m (100 × 50 × 20 ft). A schematic sketch of the model domain is shown in Figure 21. A 0.5 m diameter pipe is located at 1.5 m (5 ft) below the ground surface. The domain's horizontal distance (x direction) is large enough to minimize boundary effects. The simulated domain contains MW-4 and MW-12; these are the monitoring wells with the highest contaminant concentrations (Antea, 2016). Pipe gaskets are modeled at 2.5m (8 ft) from each other. The distance of 15m (50 ft) along z direction (horizontal axis along pipe) includes five joints or gaskets. In the vertical direction (y axis), the model depth encompasses the extent of contamination which doesn't exceed 6m (20 ft) from the ground surface, according to data from monitoring well (MW4) data. (Delta, 2000).

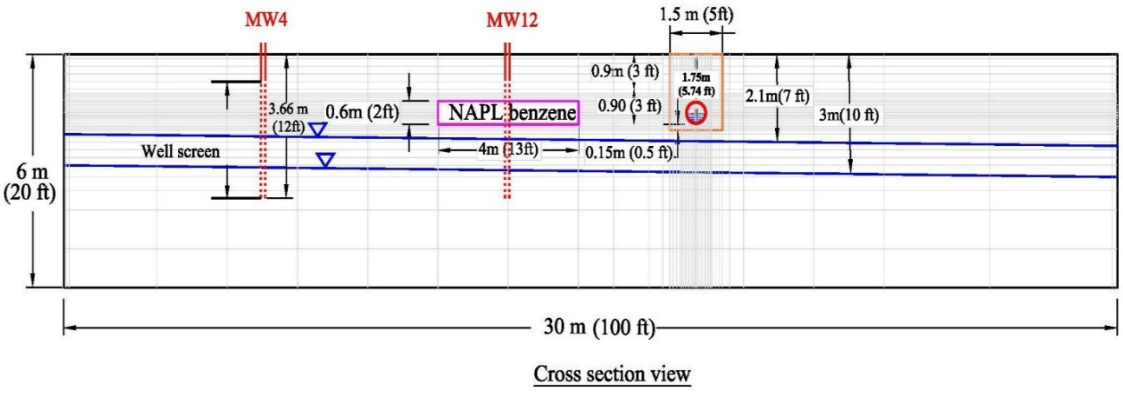

Cross section view

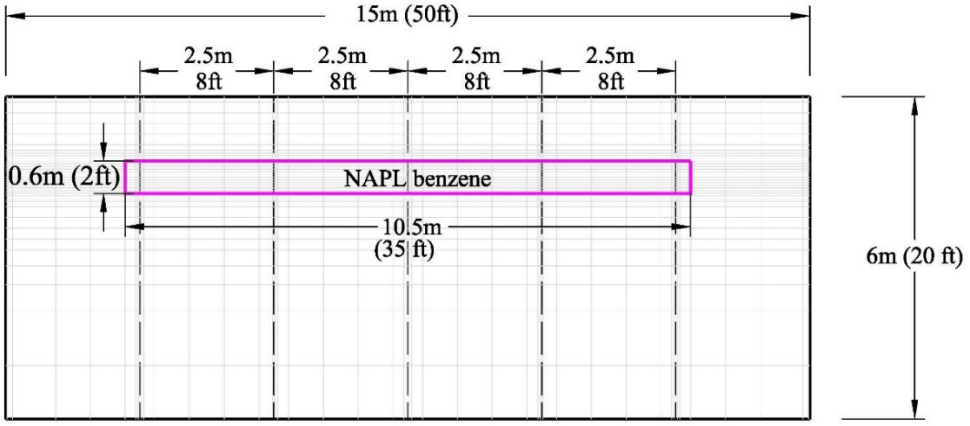

Profile view

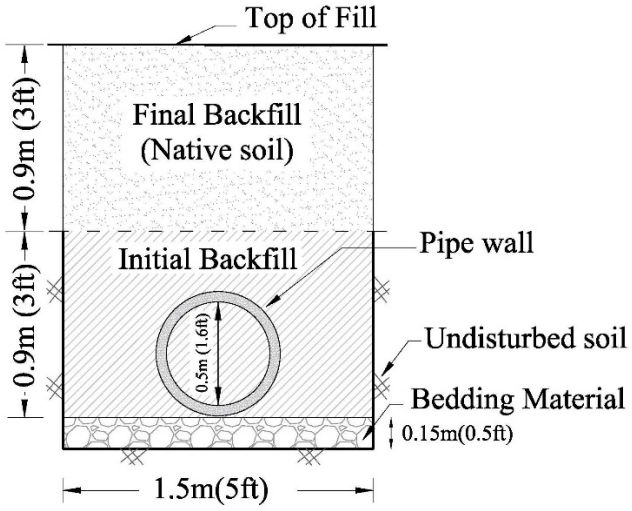

Section detail view

Figure 21: Schematic sketch of Model

The discretized domain and pipe as well as gaskets are shown in Figure 22 and Figure 23, respectively. The mesh is constructed of 76,140 cells and the grid size becomes finer toward the location of the pipe. A series of mesh sensitivity analyses (ex. 15 to 33m model dimension in x dir.; and 0.8 to 2m grid sizes outside the trench) was executed to assess the proper dimensions and ascertain that no or minimal effect of the mesh size on the results. The effect of groundwater table elevation investigated assuming two possible levels of ~ 3m (10 ft) in one scenario and 2.1 m (7 ft) from surface in a second scenario. The water table is located at 1.25m (4.1ft) and 0.35m (1.15ft) from pipe invert in first and second scenarios, respectively. The results were compared to assess the effect of groundwater table depth on benzene transport in the unsaturated zone. The flow gradient of 1% (1ft difference in depth between left and right boundaries) was used in the analysis. A top layer with 0.005 m (0.016 ft) thickness is applied to model atmospheric layer boundary condition at the ground surface.

Benzene is released as NAPL and as percentage of maximum detected BTEX (3207 mg/kg) in soil. The assume degree of saturation of benzene within the void space (S_n)= 0.1 at 1.2 m to 1.8 m (4 ft - 6 ft) depth from ground surface. The contamination was assumed over an area of 4×10.5 m (13×35 ft) around MW12. This is the location where NAPL was detected (data from Antea, 2016). The area of benzene as NAPL release is schematically indicated in Figure 21 and Figure 22. Model parametrization, and the simulation process are described in Appendix D.

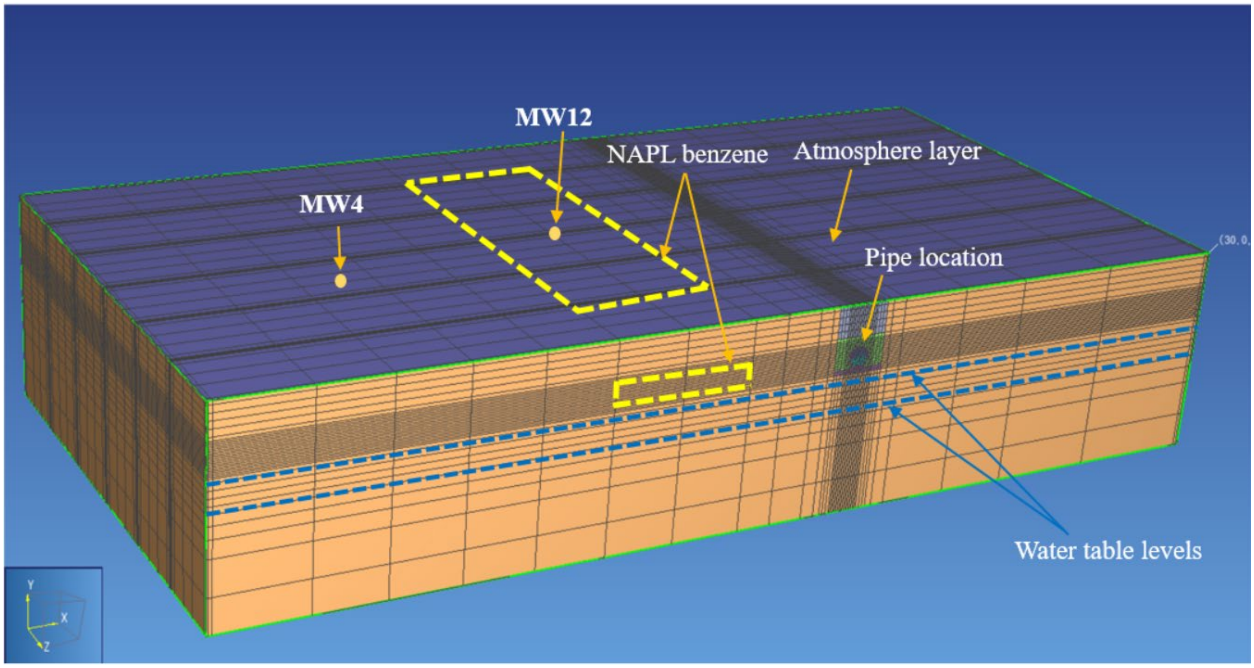

Figure 22: The Model and created Mesh (pipe is located in unsaturated zone).

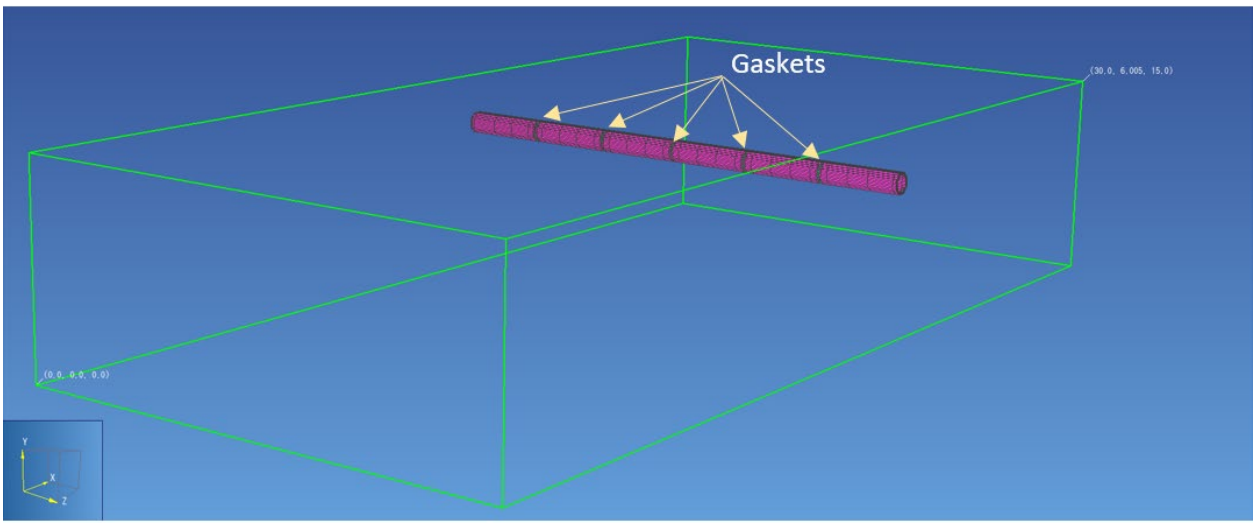

Figure 23: The discretized mesh with pipe and gaskets (Distances of gaskets are 2.5 m or 8 ft).

4.5.2. Modeling results

Factors investigated included the effect of depth to groundwater table, pipe material quality, damaged-undamaged gaskets, soil parameters, NAPL thickness at source location and evaporation to the atmosphere. Since the NAPL plume was defined as a finite volume in a specific region it cannot develop further from source and reach pipe location. The model results indicated that the initial NAPL saturation (S_n=0.1) at the source location around MW12 is depleted through partitioning into gas and aqueous phases approximately two and half years after release. The relatively fast time to depletion is related to the assumed initial condition of un-contaminated profile (except for the location of the initial benzene release is depicted in Figure 21).

4.5.2.1. Water table level

The results indicated the mass transfer through the unsaturated profile is mostly dominated by gas phase diffusion rather than advection in gaseous, aqueous or NAPL phases. VOC diffusion coefficients in the gas phase are up to 4 orders of magnitude higher than the coefficients for the aqueous phases (Rivett et al. 2011). The modeled scenario with the higher water table resulted in lower benzene concentration and mass breaking through the pipe than for the lower water table scenario. This is due to the larger unsaturated thickness of soil domain and the greater availability of air voids for the mass exchange to take place.

Furthermore, the greater thickness of contaminated unsaturated zone with the lower water table increases the gaseous contaminant diffusion thereby permitting greater transport of benzene into the pipe. Figure 24 shows benzene concentration in aqueous (Figure 24a) and gaseous (Figure 24b) phases inside the pipe for the two modeled water table levels of 1.25m (4.1ft) and

0.35m(1.15ft) from pipe invert. Benzene breaks through the pipe gradually increases within eight years after release and the mass and concentration begin to drop as the NAPL source is depleted. The peak concentration along the pipe reaches 11.3 µg/l (aqueous phase) and 2.2 µg/l (gas phase) when water table level at pipe location is 1.25m below the pipe invert. These peak values decrease to 0.7 µg/l and 0.13 µg/l, respectively, when water table level is raised to 0.35 from the pipe invert. It should be noted that the concentrations are at one location along the pipe and transport by flow advection will lead to decrease in these concentrations. These concentrations are above 5 µg/l (MCL, EPA, 2002) and $1.2x10^{-4}$ µg/l (AAL, NCDEQ 2018) as indicated in Table D1 in Appendix D.

In a second analyses scenario, the source of NAPL contamination was assumed floating on water table, with the water table below the pipe. A benzene saturation of 0.01 was applied above groundwater table, located at 1.25m and 0.35m from pipe invert.As such, this NAPL migrated toward the pipe as the watertable level was raised. Results from these analyses indicated higher magnitude of concentration and mass transfer into the pipe as the watertable level was raised. Table 5 presents a comparison between the concentrations in both cases after one year. As shown in Table 5, more concentrations in all phases can penetrate into the pipe when water table transports NAPL benzene toward the pipe. However, as shown in Figure 24 and Figure 25, when NAPL benzene is located in unsaturated zone well above the groundwater level and some horizontal distance from the pipe, low lateral gas diffusion hinders contaminant breakthrough to the pipe in case of water table is raised closer to the ground surface and the pipe.

Table 5: Concentrations inside and outside the pipe when NAPL benzene is raised with water table fluctuations
In case of NAPL benzene is located above water table level below the pipe -Sn=1%

Water table level from pipe invert	Concertation inside the pipe after one year aqueous phase	Concertation inside the pipe after one year gas phase	Concertation outside the pipe in the trench after one year- aqueous phase	Concertation outside the pipe in the trench after one year gas phase
	µg/l	µg/l	µg/l	µg/l
0.35m (1.15ft)	$1.6x10^{-2}$	$3.0x10^{-3}$	38.00	7.50
1.25m (4.1ft)	$1.0x10^{-2}$	$2.0x10^{-3}$	6.30	1.20

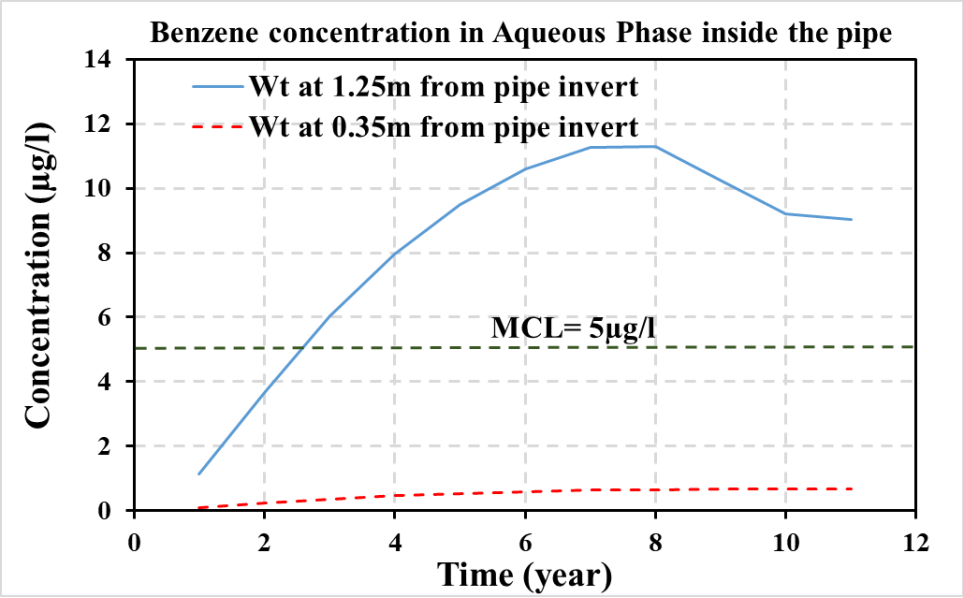

a) Aqueous benzene

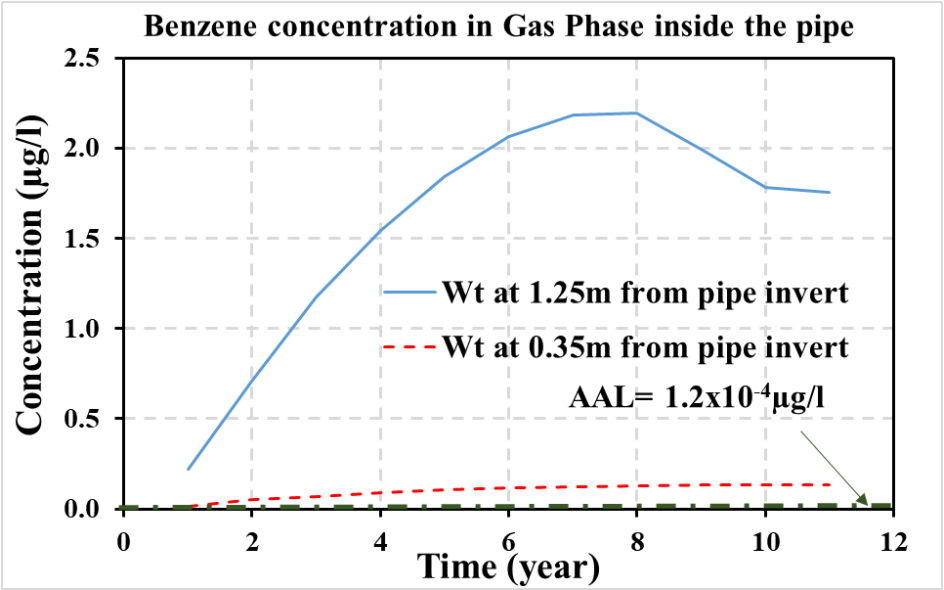

b) Gaseous benzene

Figure 24: Benzene quantity inside the pipe flow for two water table levels a) Aqueous phase, and b) Gas phase

The cumulative masses of benzene breaking through the pipe in aqueous and gaseous phases are computed by adding up the product of gas and aqueous fluxes at individual cells of the pipe surface at the specific period of time in which those fluxes were calculated:

$$Cumulative\ mass = \sum_{t=1}^{n\ (time\ periods)} Flux\ of\ VOC\ in\ gas\ or\ water\ \left(\frac{mg}{s}\right) x\ \Delta t\ (s) \qquad (6)$$

The mass calculations are plotted in Figure 25 for the two water table levels. The main point inferred from results is although lateral gas diffusion is responsible for contaminant transport from source to the trench, most of accumulated mass in the trench breaks through the pipe as aqueous flux. At this point it should be mentioned that the wall of concrete pipe is fully saturated due to the matric suction of the concrete forming wall. The initial total mass released as NAPL phase in the domain is 840×10^6 mg from which only 2,355 mg and 237 mg enter the pipe in aqueous phase during simulation time for water table levels of 1.25m and 0.35m from pipe invert, respectively. The mass ingress in gas phase is 19 mg and 2 mg for water table at 1.25m and 0.35m, respectively. The lower mass fluxes in gas phase are reasonable given the high water content in the saturated pores of concrete material of pipe and the high capillary pressure preventing the gas diffusion through the pipe wall. After contaminant breaking through the pipe walls, it is partitioned into both aqueous and gas phases as the concentrations are in equilibrium with each other. The concentration in gas phase can locally reach greater values than the regulatory limit. These concentrations can be exacerbated especially when a damage occurs in pipe wall or gaskets as the analyses results show relatively high concentrations in the pipe trench (70,000 µg/l in aqueous phase and 13,000 µg/l in gas phase).

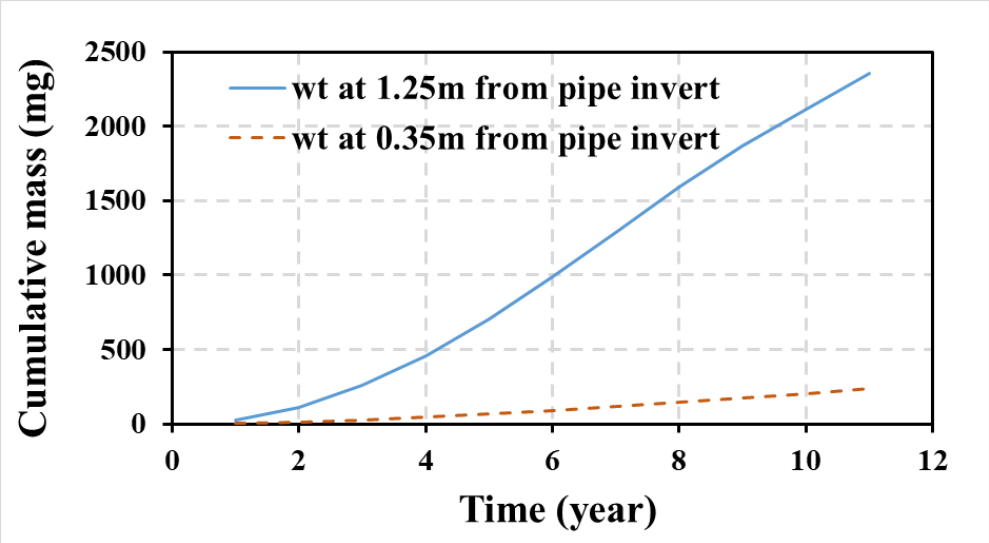

a) Aqueous benzene

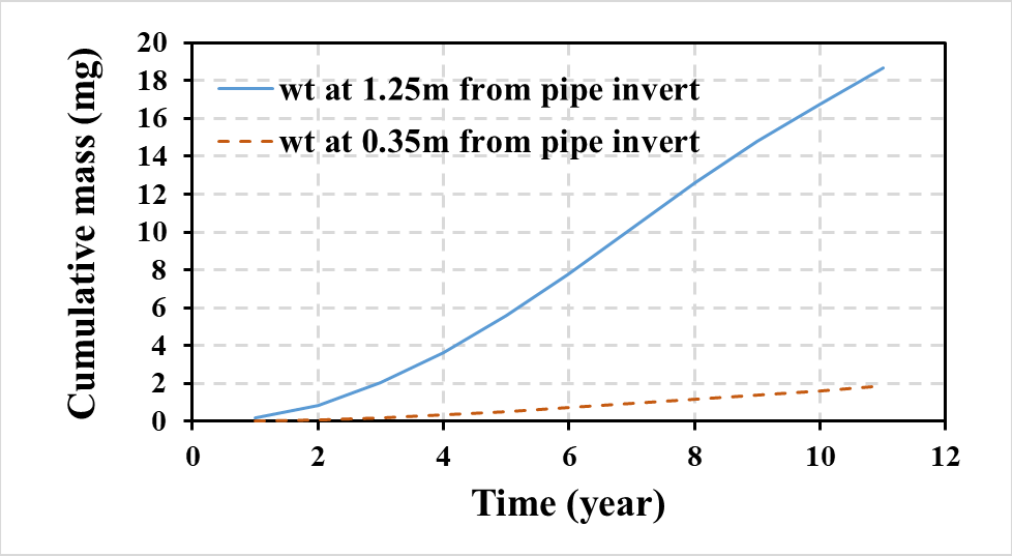

b) Gaseous benzene

Figure 25: Cumulative mass breaking through the pipe for two water table levels a) Aqueous, phase and b) Gas phase

Highlights: The water table level has a significant effect on mass transport into the pipe. The mechanism of transport in unsaturated domain is dominated by vapor phase diffusion for benzene (VOCs). When water table rises toward the ground surface, the concentrations inside the pipe decrease due to low lateral diffusive gas phase spreading within the domain as a result of increased water content of the soil in the vadose zone. If however the source of NAPL contamination was assumed floating on water table, this NAPL migrates toward the pipe as the watertable level is raised and leads to higher magnitude of benzene concentration and mass transfer into the pipe.

4.5.2.2. Pipe material quality

The unsaturated transport properties of concrete materials are dependent on the mixture proportions and water-to-cement (w/c) ratio of the mix. Change in the mixture proportions and w/c ratio affect the saturated hydraulic conductivity, water retention and relative permeability behavior of the formed concrete. The unsaturated transport properties of concrete are particularly sensitive to w/c ratio. At a given capillary suction, the degree of saturation is higher for concrete with a lower w/c ratio. This is because of the presence of smaller size of pores with the lower w/c ratio concrete mixes which then would require larger suction pressures to desaturate (Kumar et al. 2010). The simulations were implemented with three assumed conditions of concrete materials denoted by low, medium and high quality material for which the assumed properties are

shown in Tables D2 and D3. In all simulations herein, water table level is kept at 1.25m (4.1ft) from pipe invert.

It is found from analyses that the fitting parameters defining the unsaturated properties of concrete for low, medium and high quality concrete significantly impact the level of contaminants breaking through the pipes. As shown in Figure 26, the benzene concentrations in aqueous and gas phases inside the pipe reach peak values after eight years and gradually decreases thereafter to reach steady state condition in the eleventh year. The peak values in aqueous phase are 18.7, 11.3 and 2.6 µg/l and in gas phase are 3.6, 2.2 and 0.5 µg/l for low, medium and high quality materials respectively. The total released NAPL ($840x10^6$ mg) has been partitioned into adsorbed mass to the soil, NAPL, aqueous and gas phases. Approximately, 5,030 mg in aqueous phase breaks through the pipe in case of low quality material. These values are 2,355 mg and 811 mg for medium and high quality materials, respectively, a shown in Figure 27. The mass in gas phase permeating through the pipe is calculated as 40 mg, 19 mg, and 6 mg for low, medium, and high quality pipes, respectively. Using the medium quality material of pipe as a "base case," the peak concentrations in both aqueous and gas phases inside the pipe increase by 65% in case of low quality material and decrease by 77% in case of high quality pipe. The cumulative mass penetrating the pipe decreases by 65% and increases by 114% in case of high and low quality material respectively compared to the base case.

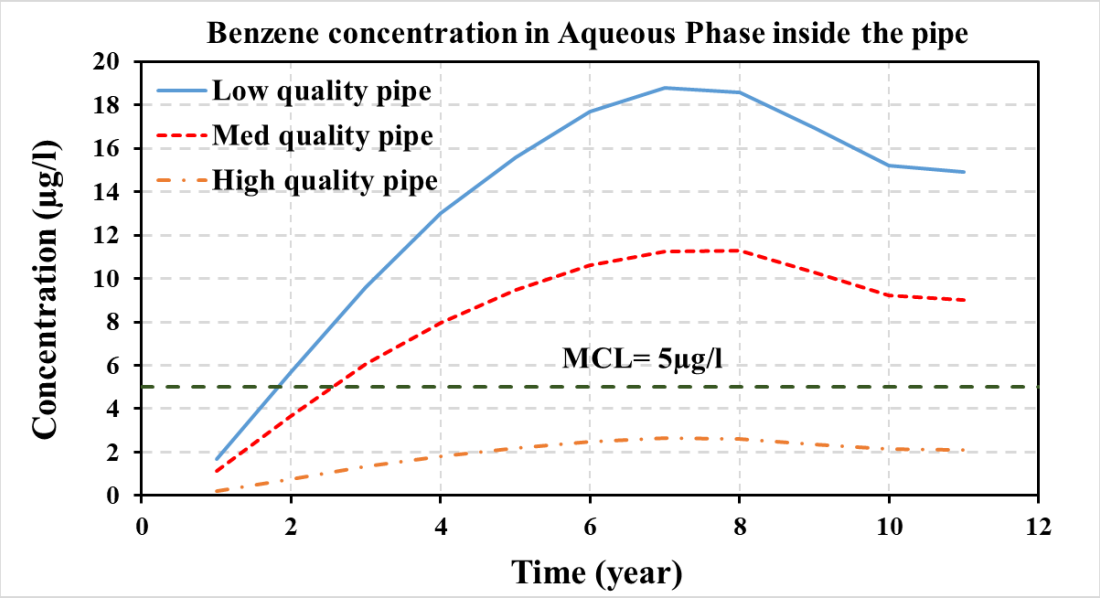

a) Aqueous benzene

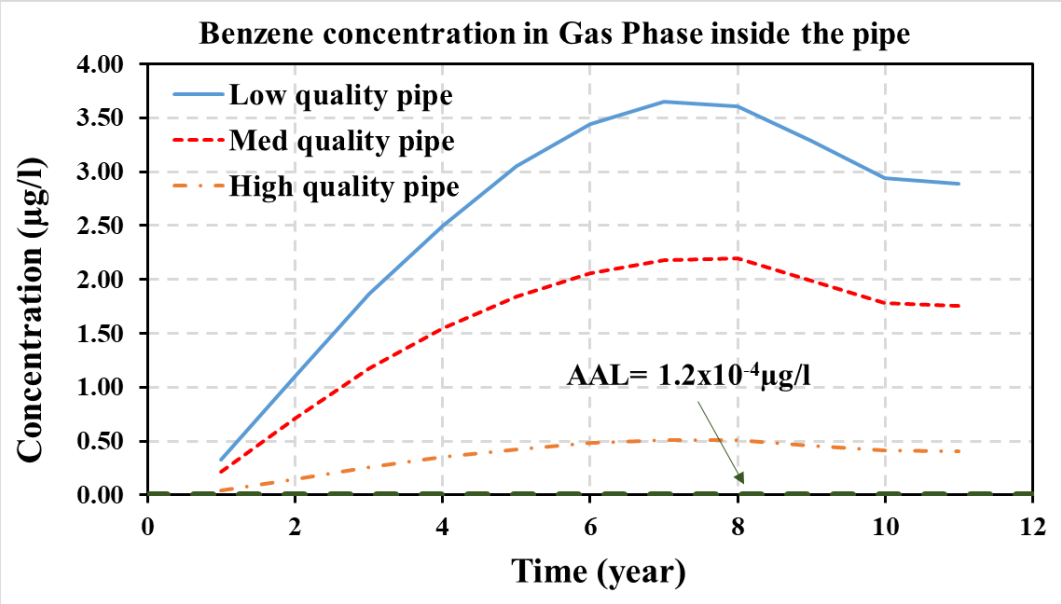

b) Gaseous benzene

Figure 26: Benzene quantity inside the pipe flow for different pipe material quality a) Aqueous phase, and b) Gas phase

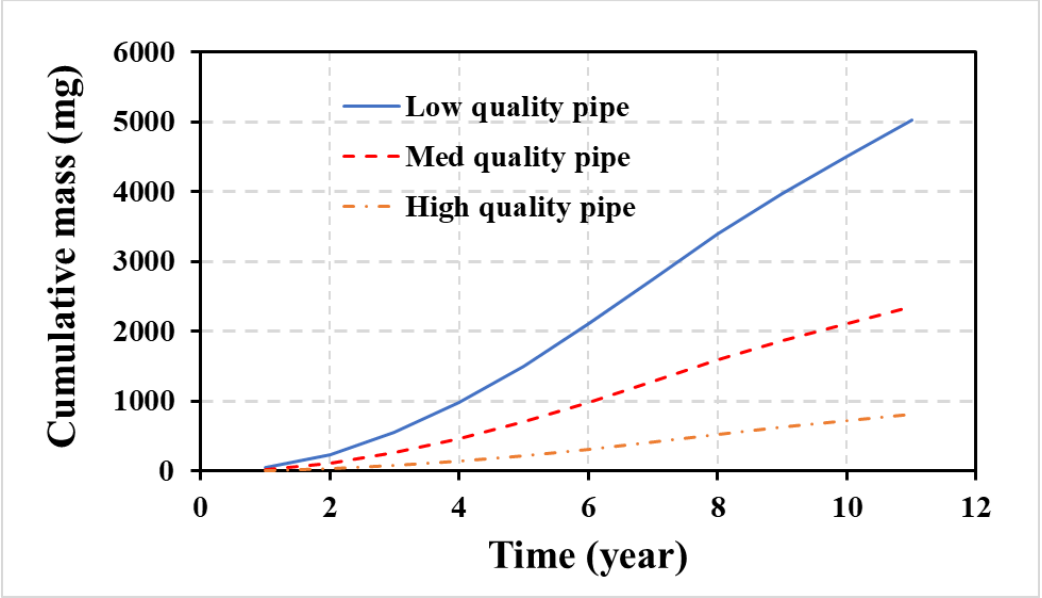

a)Aqueous benzene

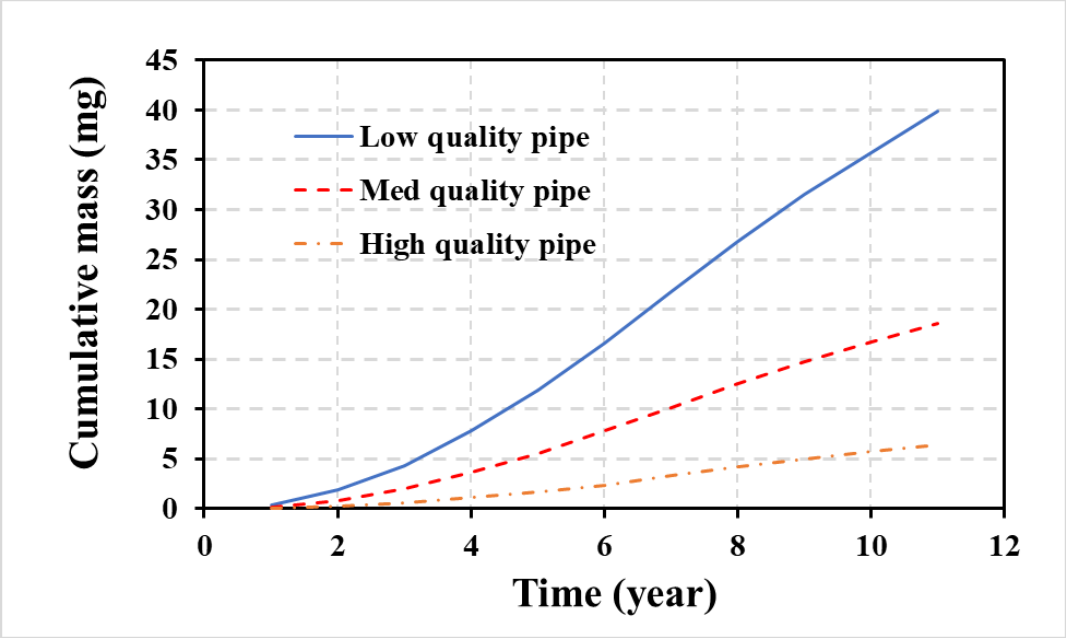

b)Gaseous benzene

Figure 27: Cumulative mass breaking through the pipe for different pipe material quality a) Aqueous phase, and b) Gas phase

Highlights: The simulations assuming three qualities of pipe materials (or conditions as manifested by the hydraulic conductivity of the pipe) show the peak concentrations inside the pipe increases by 65% for low quality pipe and decreases by 77% for high quality pipe compared to concentrations estimated for the medium quality pipe. Cumulative mass transfer into the pipe is 114% and 65% of the values estimated for the base case, in case of low and high quality material respectively. Most of the transported mass of benzene breaks through the pipe as aqueous flux through pipe surface due to high capillary pressure of concrete leading to pipe wall saturation and regressing gas diffusion.

4.5.2.3. Gasket material condition

When damage occurs in pipe wall or joints, there is potential for the contaminant within the pipe trench to break through the pipe. The contaminant transport in two scenarios of damaged and undamaged gaskets are compared herein in terms of aqueous and gaseous phases inside the pipe. In this scenario, the water table level is located at 1.25m (4.1 ft) from pipe invert.

As shown in Figure 28 , and in case of damaged gasket, the benzene concentration inside the pipe reaches 2800 µg/l in aqueous phase and 550 µg/l in gas phase within 2 years after release. In comparison, concentration of 11.3 µg/l in aqueous phase and 2.2 µg/l in gas phase is gradually accumulated during eight years in case of good-condition gaskets. For the damaged gaskets, the high mass of contaminant accumulated in the trench breaks through the pipe two years after release. The cumulative mass breaking through the pipe in case of damaged gasket increases to 284,000 mg in aqueous phase and 2245 mg in gas phase compared to the mass in case of good-condition gasket (2,355 mg in aqueous phase and 19 mg in gas phase,) Figure 29.

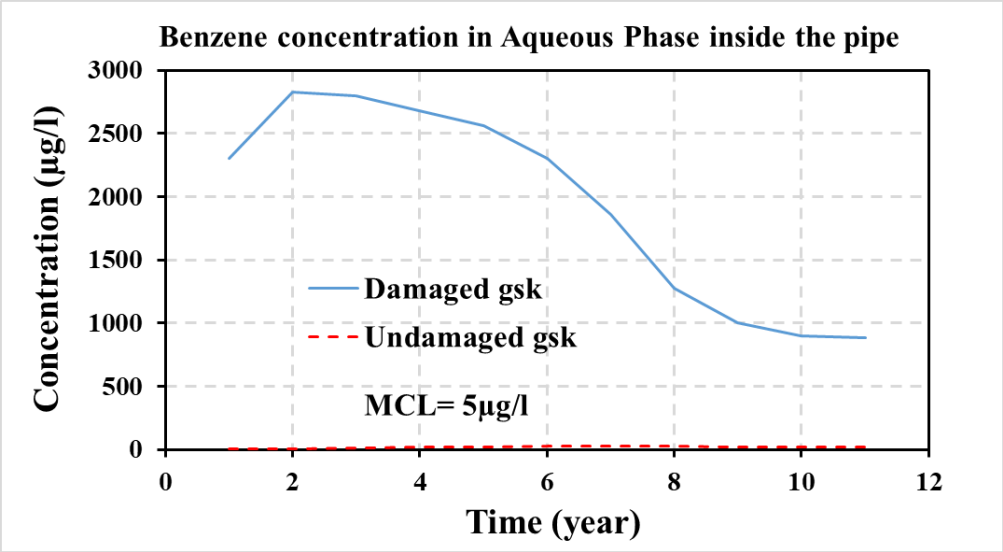

a) Aqueous benzene

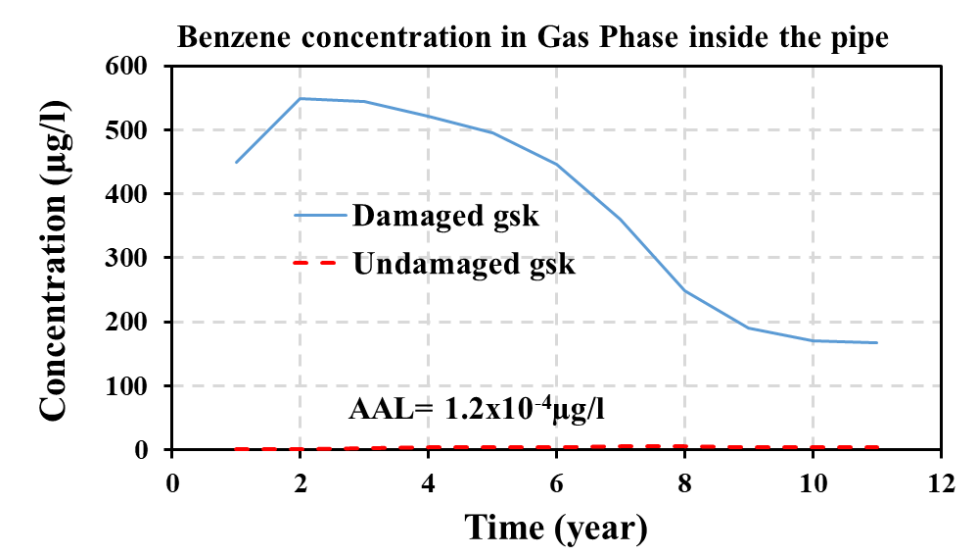

b) Gaseous benzene

Figure 28: Benzene quantity inside the pipe in case of damaged and undamaged (good condition) gaskets a) Aqueous phase, b) Gas phase

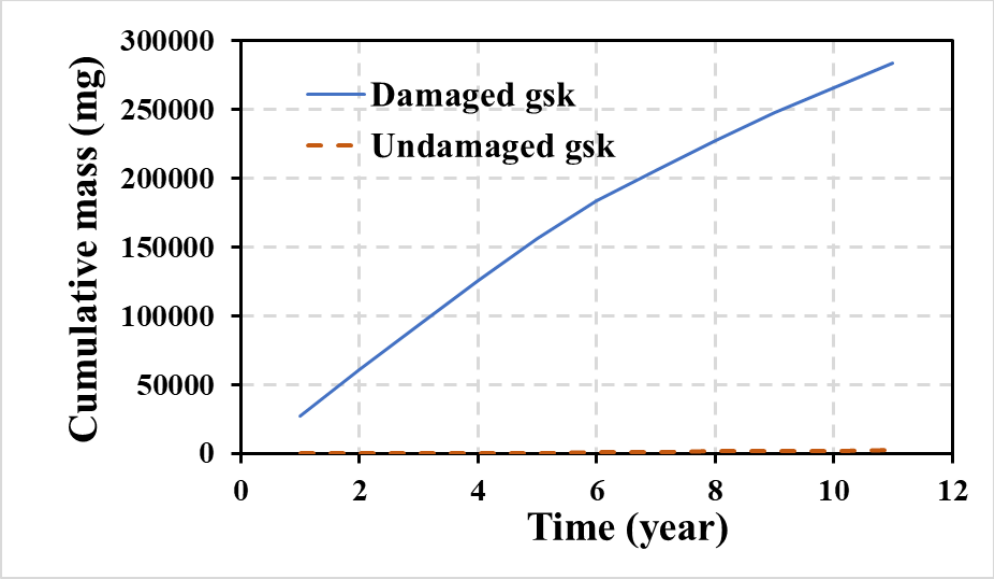

a) Aqueous benzene

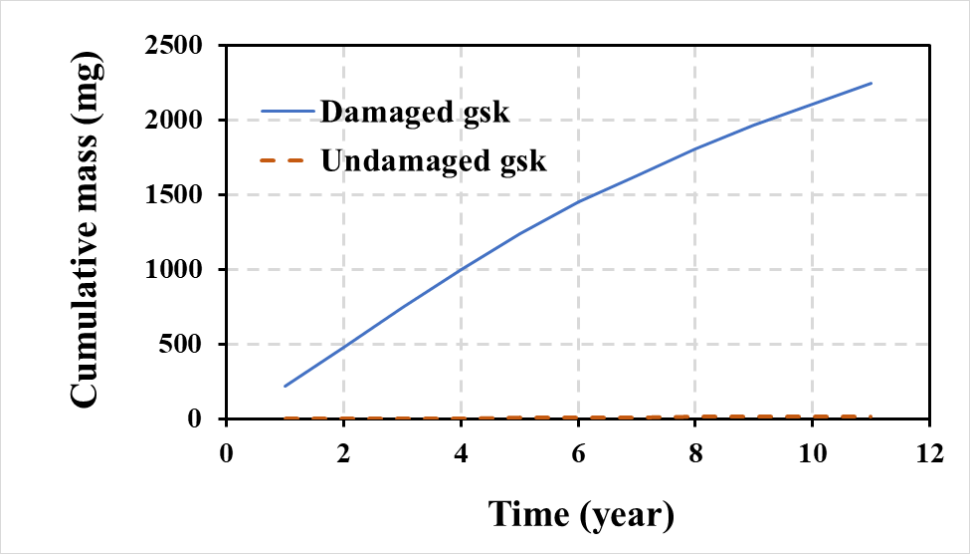

b) Gaseous benzene

Figure 29: Cumulative mass breaking through the pipe for two gasket conditions a) Aqueous phase and b) Gas phase

Highlights: Considering damaged versus undamaged gaskets, severely damaged gaskets can increase the concentrations and mass transfer into the pipe by more than two orders of magnitude. The high concentrations accumulated in the trench percolate into the pipe within two years after NAPL release.

4.5.2.4. NAPL phase thickness

The thickness of NAPL found in MW12 at the Jacksonville site was reported to be 0.5 m (1.53 ft). The NAPL thickness measured in monitoring wells usually exceed the NAPL-saturated formation thickness in the surrounding soil by a factor between 2 and 10 (Mercer and Cohen 1990). However, as the groundwater table (and therefore also the NAPL) fluctuates, residual NAPL will remain in part of the pore spaces it initially occupied. The residual NAPL entrapment in pores may result in reduced migration when the water table rises toward the ground surface and eventually lead to a decrease in NAPL thickness monitored the in wells (Fetter, 1999).

As the observed NAPL thickness in monitoring wells may not be representative of NAPL thickness in whole contaminated area, two scenarios considering the NAPL thickness as 0.3m and as 0.6m are investigated in the analysis. By reducing the thickness of initial NAPL benzene at source, the concentrations inside the pipe decrease by 13% after three years in both aqueous and gas phases, as shown in Figure 30. In this case, the peak concentrations reduced from 11.3 µg/l to 9.8 µg/l in the aqueous phase and from 2.2 to 1.9 µg/l in the gas phase along the pipe. The cumulative mass as a function of the simulated NAPL thickness is shown in Figure 31.

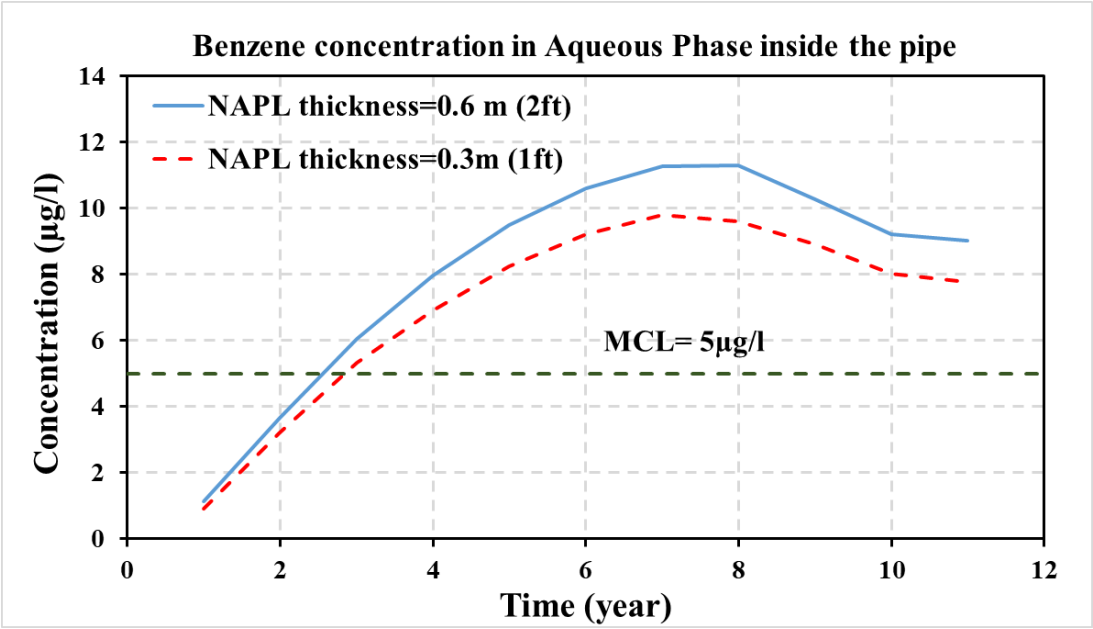

a) Aqueous benzene

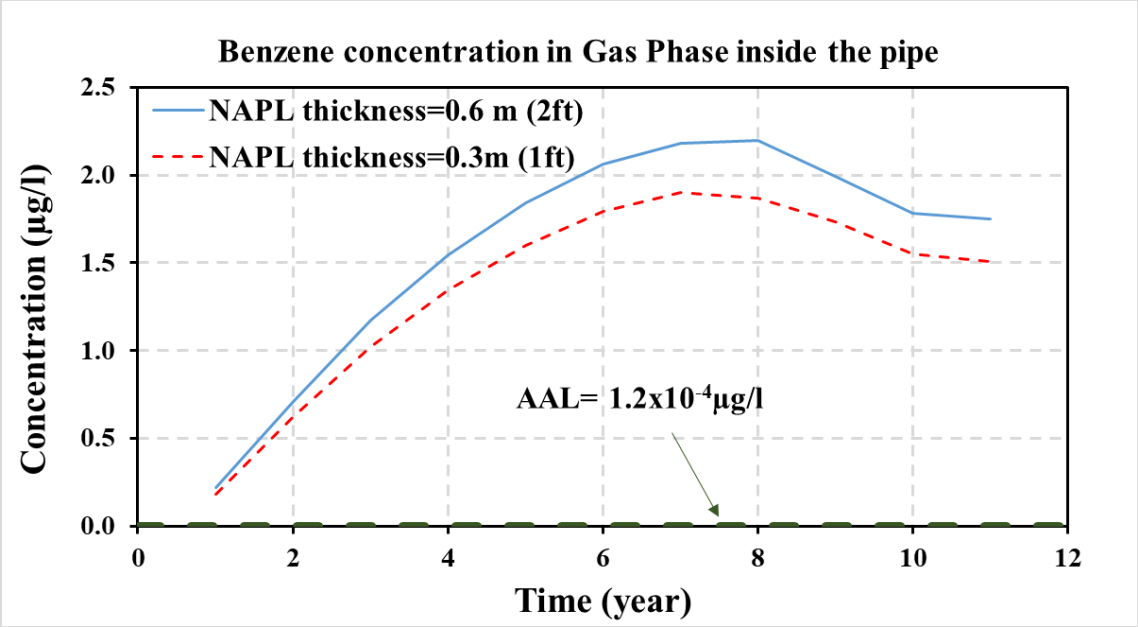

b) Gaseous benzene

Figure 30: The concentration inside the pipe flow for different NAPL thicknesses at source a) Aqueous phase, and b) Gas phase.

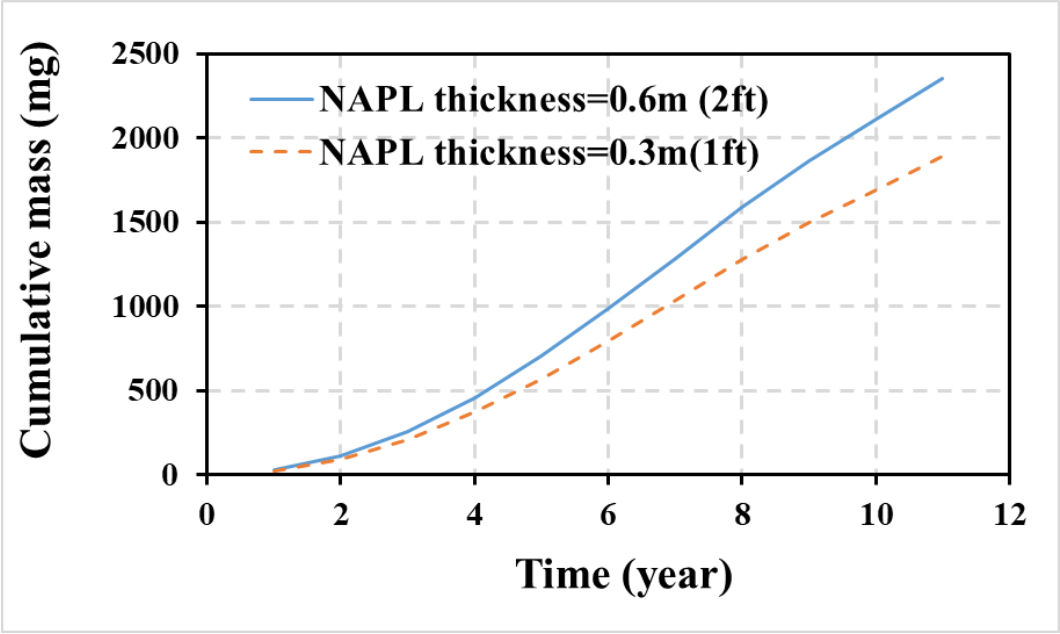

a) Aqueous benzene

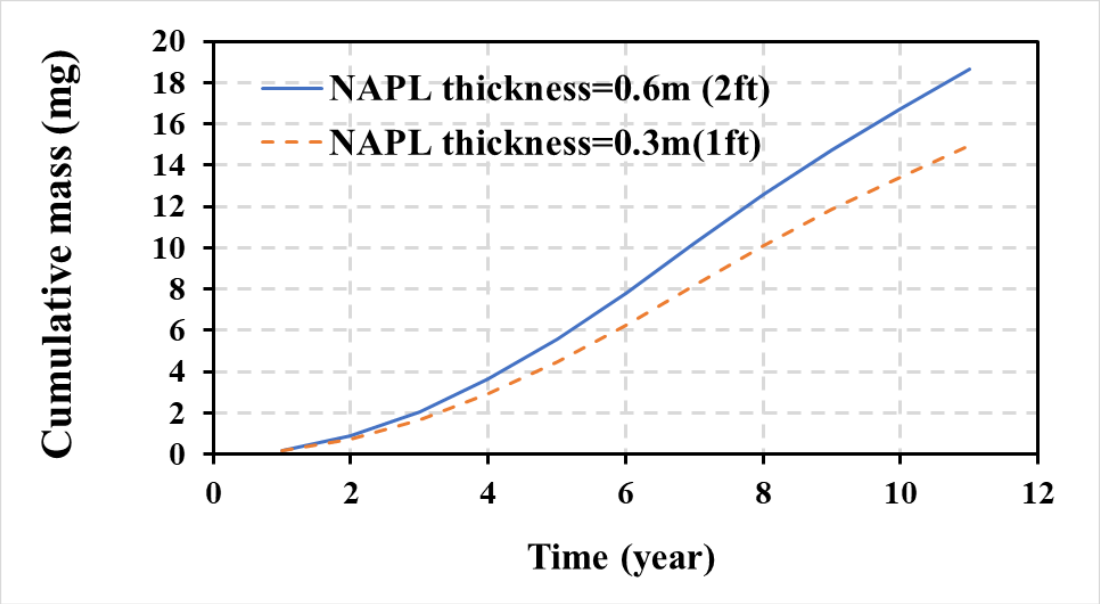

b) Gaseous benzene

Figure 31: Cumulative mass breaking through the pipe for different NAPL thicknesses a) Aqueous phase, and b) Gas phase

Highlights: The NAPL thickness at source has a secondary effect on concentration and mass transfer into the pipe; reducing the free NAPL thickness by a factor of two may lead to the decrease in the peak concentrations in both aqueous and gas phases by 13%.

4.5.2.5. Effect of native soil hydraulic conductivity

The analyses were conducted while using sandy clay soil with saturated hydraulic conductivity on the order of 10^{-5} cm/s as shown in Table D2 and unsaturated properties as shown in Table D3. The results show the coarser materials with lower water content facilitates the gas phase diffusion. Accordingly, higher mass transport of benzene into the pipe is observed from the analyses. When the saturated hydraulic conductivity increases about two order of magnitude, the concentrations in both aqueous and gas phases increase by approximately 6 times. The concentrations in the pipe flow is raised to the 9.8 µg/l in aqueous and 1.9 µg/l in gas phase 1 year after release compared to the 1.7 and 0.32 µg/l in aqueous and gas phases respectively when the sandy clay material is used as the native soil.

4.5.2.6. Atmosphere layer

The cumulative mass emitted to the atmosphere was calculated using mass fluxes in gas phase at surface boundary layer. By comparing the mass leaving out of the system at each time period and cumulative mass volatilized to the atmosphere, it is revealed that more than 98% of

mass is lost through emission to the atmosphere. The total mass of VOC remained in the system after eleven years, and in the case of water table at 1.25m, was estimated to be $1.5x10^6$ mg while the initial released mass was equal to $845x10^6$ mg. Adsorption to the soil mass retards the benzene migration considerably even with only small fraction of organic carbon in domain (about 0.1%.) The percentage of adsorbed mass compared to the total mass can vary from 4% in first year to 34% in eleventh year at which steady state condition has been established.

Highlights: An increase in saturated hydraulic conductivity of native soil by two orders of magnitude led to an increase in the concentrations breaking through the pipe in both aqueous and gas phases by approximately a factor of 6 after one year. Benzene loss through volatilization to the atmosphere lessens the contaminant transfer into the pipe. The results show 16% of benzene emitted to the atmosphere after 1 year and most of it dissipates after eleven years. Adsorption to the soil mass retards the benzene migration considerably for assumed fraction of organic carbon in the domain of 0.1%.

4.6. Mitigation strategies

The contaminated gasoline site in Jacksonville was used to develop the parameters to evaluate the effect of the contamination on a nearby drainage concrete pipe and assess the efficacy of two mitigation practices and the use of the anti-seep collar. Benzene was detected to be the primary target contaminant at the study site. Groundwater flow and solute transport model were established using Visual MODFLOW for forecasting the contaminant transport in groundwater and assessing the effects of flowable fill, clay liner, and anti-seep collar on the contaminant transport within the pipe domain.

4.6.1. Mitigation measures simulation

The Jacksonville site was used for the study of mitigation measures. The model domain dimensions simulated in saturated analysis and the estimated horizontal extent of benzene in groundwater are shown in Figure 32.

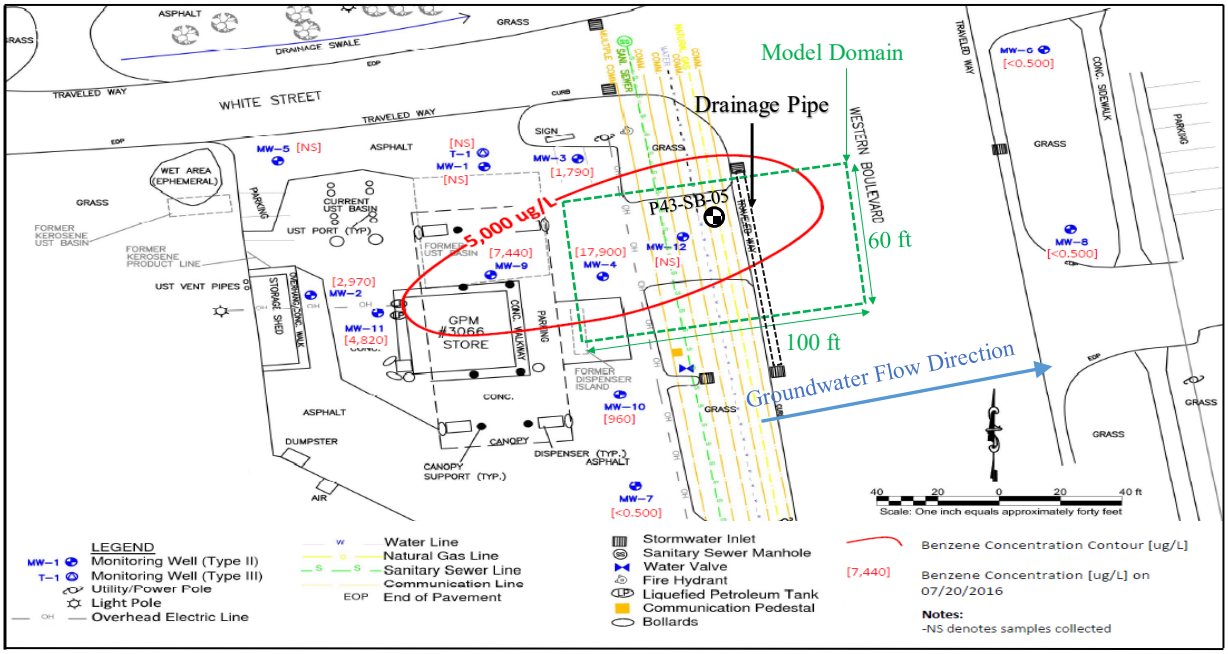

Figure 32: Jacksonville site map showing gas station and the monitoring well locations, groundwater flow direction, the estimated horizontal extent of benzene in groundwater, and model domain dimension being simulated in this analysis (Antea, 2016).

Zones within the layers' domain were assigned hydraulic conductivity (k), effective porosity (n_e), and bulk density (ρ_b) values based on the character of the material as schematically depicted in Figure 33. Pipe and gaskets are considered to be in good conditions in this analysis. The mechanism of contamination is a source of aqueous phase that occurs due to the presence of a free product in contact with the water phase. In the year of 2000, the highest concentration of benzene in groundwater was 19,100 µg/L (Delta, 2000). This concentration was based on the measurements obtained from the site, at MW-4. The initial distribution of benzene concentration assigned in the model with an area of 46 ft x 45 ft and a depth of 12 ft. This distribution is developed by tracing the approximated contours in the horizontal and vertical extent of the plume at the MW-4 that reported at Delta (2000), as indicated in Figure 33. The K_d values were assigned in the model as 8.5×10^{-11} L/µg.

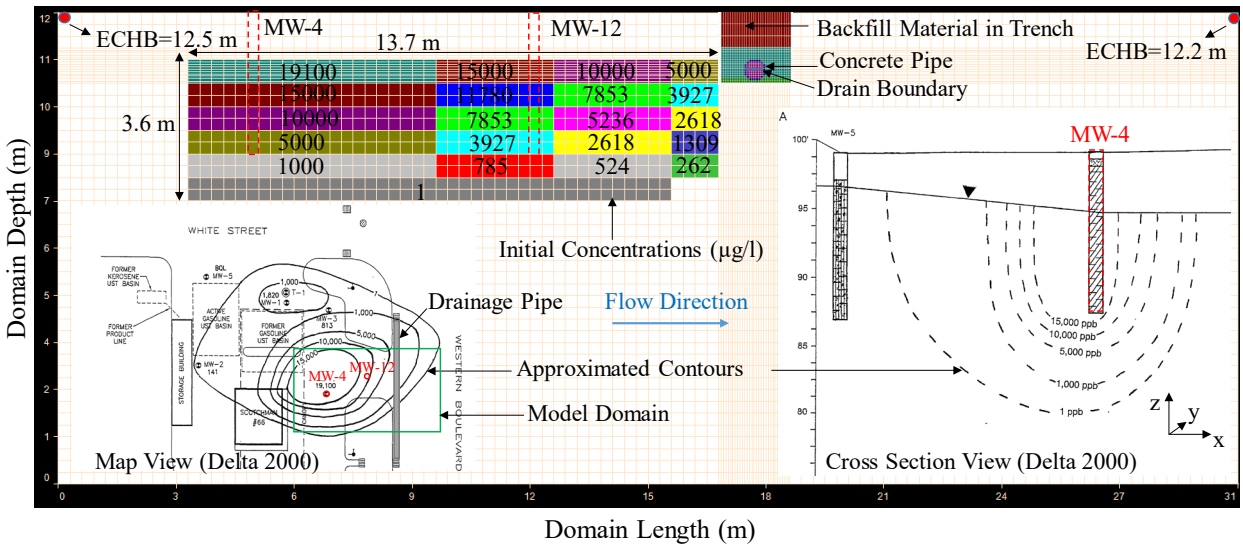

Figure 33: Cross-section view of MODFLOW grid design with assigned initial benzene concentration (in µg/L) distribution.

4.6.1.1. Clay barrier

A clay barrier is constructed by lining the trench with low hydraulic conductivity soil with the objective of cutting off the contaminant transport pathway and altering the transport direction to control further contamination diffusion. The clay barrier configuration is shown in Figure 34. In this case, the clayey barrier was placed between the trench and the native soils. The permeability coefficient of the clay barrier was set 10^{-7} cm/s, and the thickness was set at 1 ft. The k, n_e, and ρ_b values of the clayey barrier are listed in Table E1.

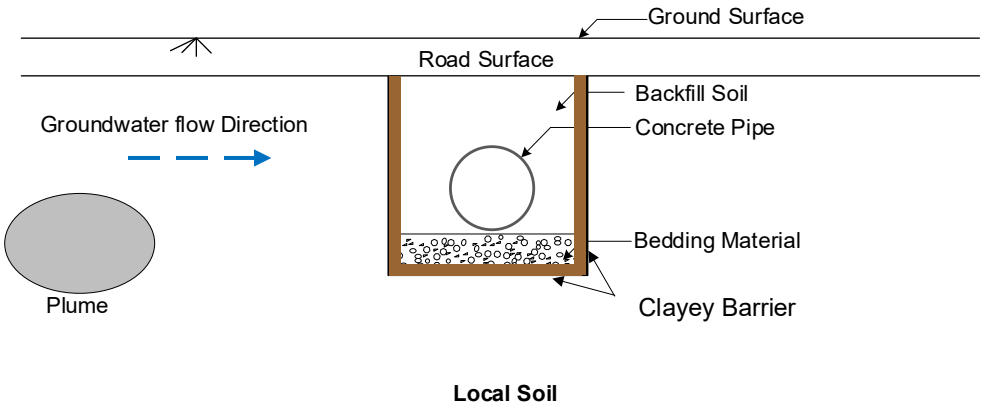

Figure 34: Clayey barrier configuration.

4.6.1.2. Flowable fill

Flowable fill is a cementitious slurry consisting of a mixture of fine aggregate or filler, water, Portland cement, pozzolanic materials, and other cementitious materials like coal fly ash. Flowable fill is used as backfill around the pipe instead of compacted earth. Flowable fill has a wide range of hydraulic conductivity values based on the ingredient of the flowable fill mixture. Parameters of the flowable fill utilized in the past by the Wisconsin Department of Transportation (WDOT) were used in this analysis. In an endeavor to achieve low hydraulic conductivity characteristics, WDOT includes sodium bentonite clay and coal combustion fly ash as the cementitious ingredient to achieve $k \leq 10^{-7}$ cm/s. Figure 35 shows the flowable fill being placed during the installation of the concrete pipe at Greenville, NC. The k, n_e, and ρ_b values of the flowable fill are listed in Table E1.

Figure 35: Placement of flowable fill along the trench.

4.6.1.3. Anti-seep collar

Anti-seep collar is a plumb migration prevention device used in conjunction with hardened drainage structures. Anti-seep collars are used around the pipes in discrete locations to mitigate the migration of contaminants along the utility corridor. Anti-seep collars used for concrete pipe are typically constructed with cast-in-place or prefabricated concrete. The configuration of the anti-seep collar is shown in Figure 36. The 1.5 m x 1.5 m (5 ft x 5 ft) anti seep collars are modeled along the pipe at 10 ft from each other. The k, n_e, and ρ_b values of the anti-seep collar are listed in Table E1. The initial distribution of benzene concentration assigned in the model is indicated in Figure 37. Natural gradients of 1.6 %, 0.5 %, 0.05 %, 0.01 % were considered to investigate the

effect of natural gradient on the potential of contaminant getting into the pipe in the presence of an anti-seep collar.

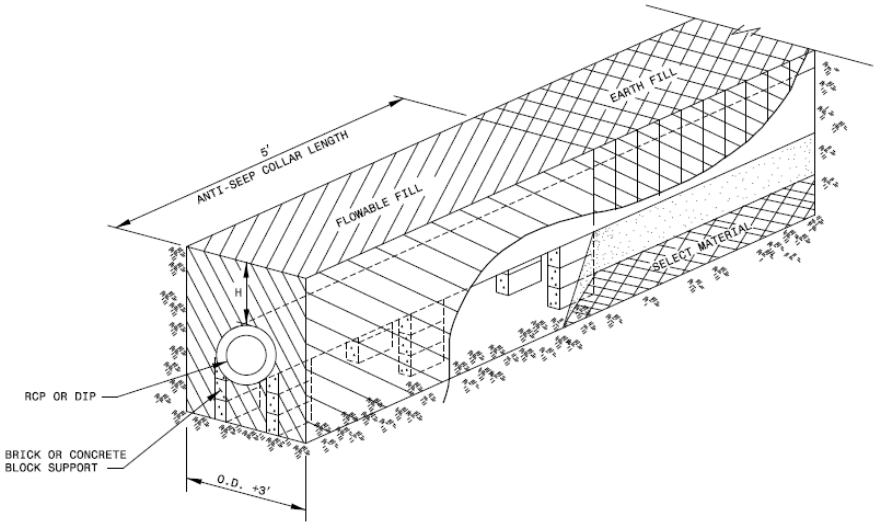

Figure 36: Anti-seep collar configuration.

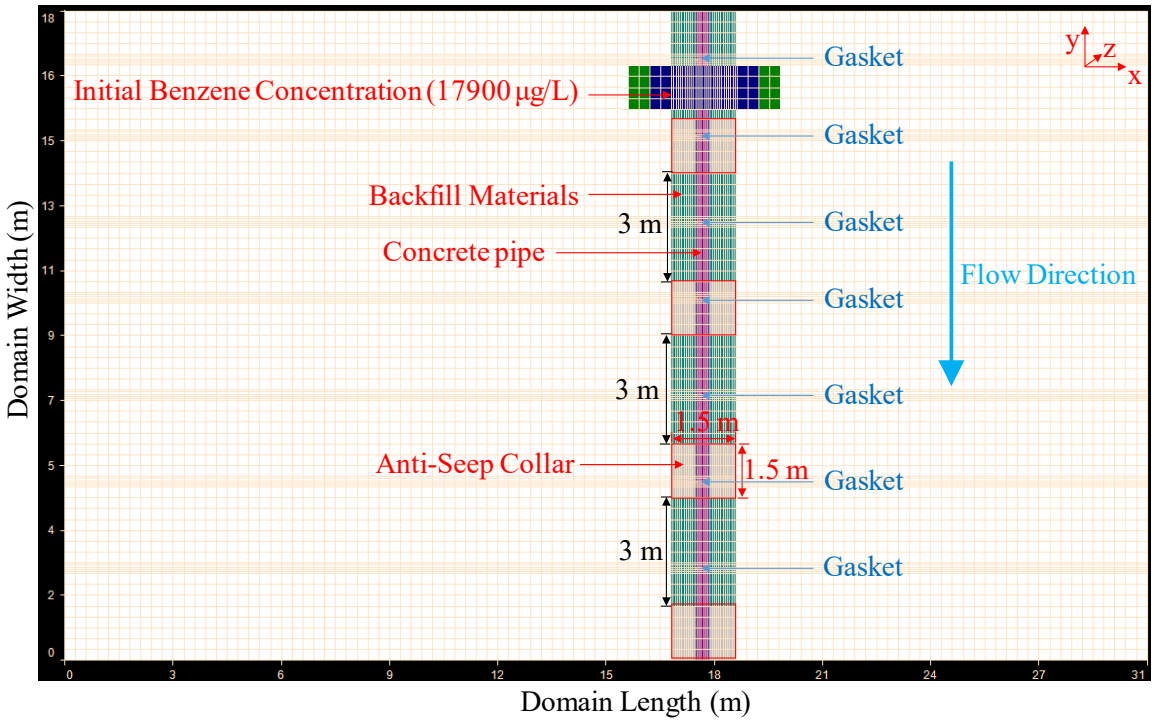

Figure 37: Map view of MODFLOW grid design for anti-seep collar scenarios with assigned initial benzene concentration (in µg/L) distribution.

4.6.2. Results - saturated model

The simulated domain with the subsurface drainage concrete pipe adjacent to the gas station is shown in Figure 38. This section view shows the distribution of the initially contaminated soil and groundwater with the depth that was detected at the location of MW-4 (where the data are available for the benzene concentration in the year of 2000 and reported by Delta, 2000). Also, shown are the changes in the plume size and migration through the subsurface domain conforming to the west-east dominant flow regime (using a 1 % gradient across the site). The benzene concentration permeated through the concrete pipe at the 20 years simulation period was 4,389 µg/L. The mass of benzene flowing out of the pipe increased to nearly 860 g over the 20 years of simulation time. As can be seen in Figure 38, the magnitude of the benzene contour in the vicinity of MW-4 and MW-12 is similar in order of magnitude to 5000 µg/l (Figure 32) measured at the site. Also, the benzene contours did not reach to the far eastern side of the pipe, showing agreement with the aqueous benzene concentrations at MW-6, and MW-8 which were reported as being less than the MCL.

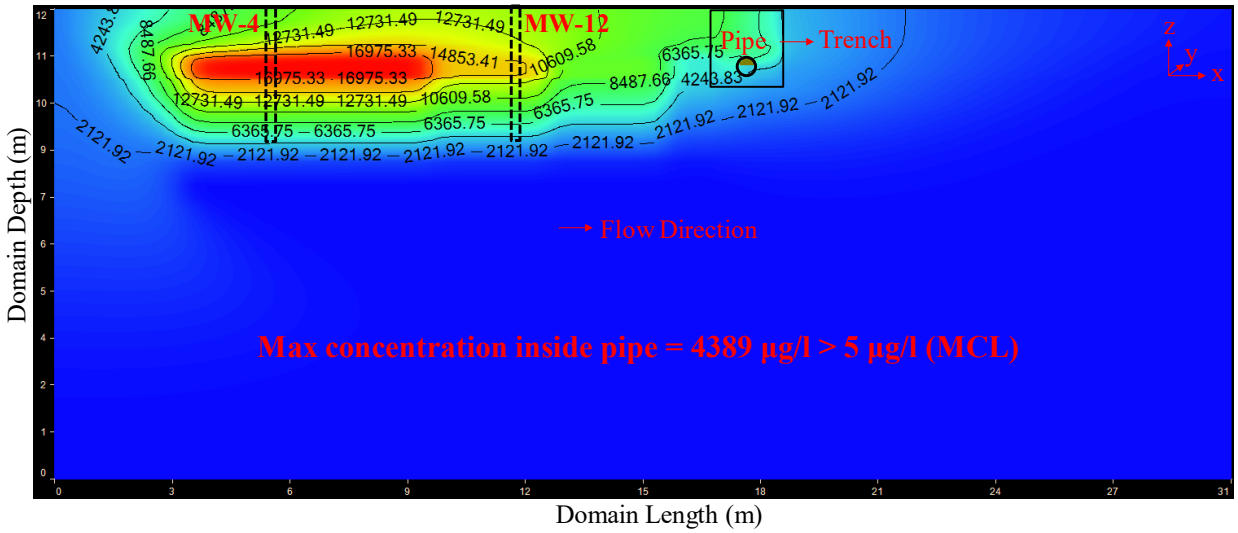

Figure 38: Cross-section views of the base case scenario for simulated aqueous benzene concentration (in µg/L) through the subsurface domain and subsurface drainage concrete pipe at 20 years.

4.6.2.1. Effect of clay barrier

The clay barrier reduced the concentration of benzene breaking through the subsurface concrete pipe by initially cutting off the plume migration from reaching the trench. However, the

total amount of contaminants did not decrease. By contrast, and as shown in Figure 38 versus Figure 39, the plume transport distance was shorter compared to the case of no clayey barrier. The plume circumvents the clay barrier and further contaminates the trench and the pipe after 5 years. Therefore, within a given time range, the clay barrier might effectively protect the trench and subsurface pipe. However, for the continuous point source, the hardening effect of the clay barrier, as a function of time, was effective, but not sustained.

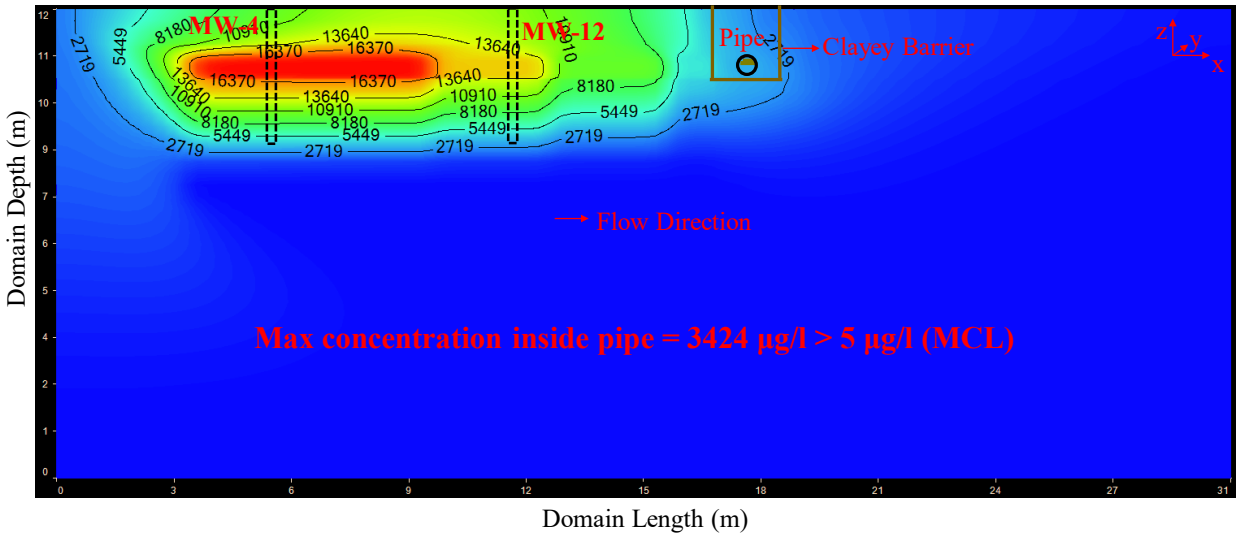

Figure 39: Cross-section views of the clayey barrier for simulated aqueous benzene concentration (in µg/L) through the subsurface domain and subsurface drainage concrete pipe at 20 years.

The total mass of benzene flowing out of the pipe for the clay barrier scenario as a function of time is shown in Figure 40. In this scenario, the groundwater flow direction is from the west to the east boundary. The cumulative mass of benzene flowing out of the pipe increased to nearly 320 g and 600 g after the 5 and 20 years, respectively, with the presence of the clay barrier. The concentration of benzene is, however, mitigated by 71.6% and 22% compared to the no clay barrier case over the 5, and 20 years of simulation time, respectively. The corresponding mass of benzene flowing out of the pipe is decreased by 53.6% and 30% for the 5 and 20 years of simulation time, respectively.

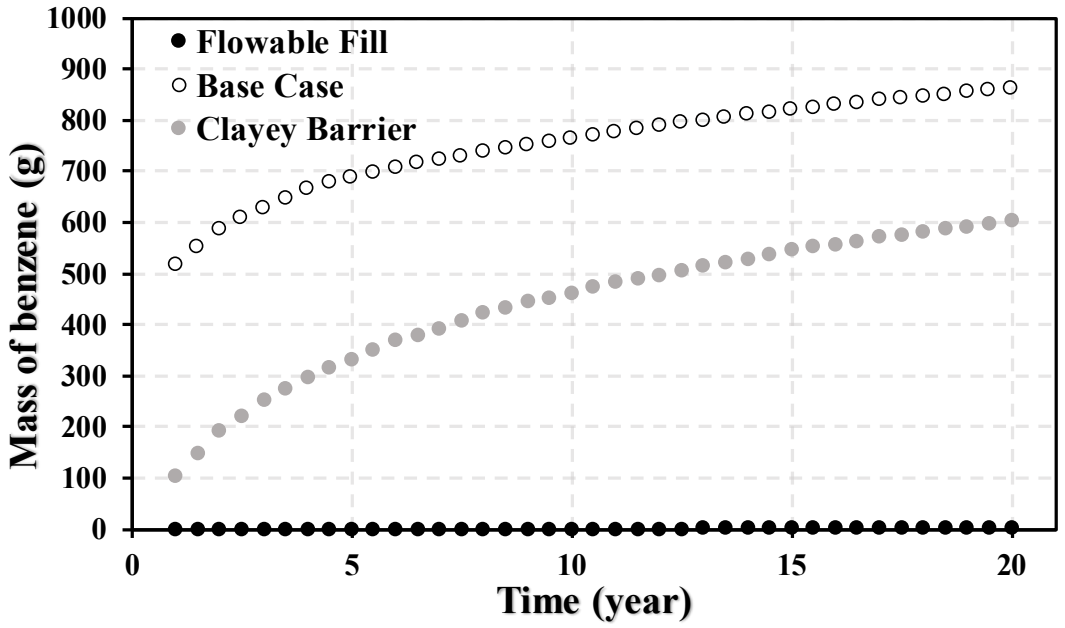

Figure 40: The total mass of benzene flowing out of the pipe for the clayey barrier scenario, and flowable fill scenario as a function of time.

Highlights: When clay barrier is ued, the concentration of benzene is reduced by 22 % compared to the case of no clay barrier case for 20 years of simulation time. The mass of benzene flowing out of the pipe is decreased by 30 % for the same period. Therefore, the clay barrier could be an effective method to protect the trench and subsurface pipe for the specified time.

4.6.2.2. Effect of flowable fill

The simulated domain with the presence of the flowable fill overlaying the concrete pipe is shown in Figure 41. The aqueous phase benzene concentration began to permeate through the gasket of the pipe after approximately 10 years, with the benzene concentrations inside the pipe at 20 years being 1.4 µg/L (below 5 µg/L). In none of the flowable fill analysis scenarios, a benzene concentration permeated through the gasket above 5 µg/L (MCL). The concentration of benzene is mitigated by 99.9 % compared to the case of no flowable fill case at the 20 years of simulation time.

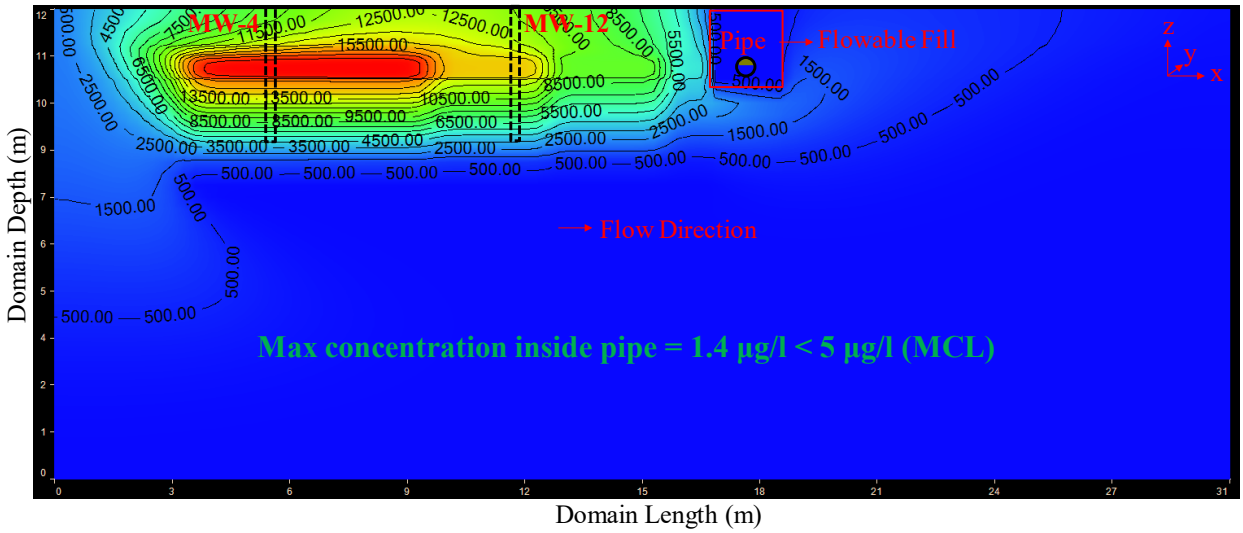

Figure 41: Cross-section views of the flowable fill scenario for simulated aqueous benzene concentration (in µg/L) through the subsurface domain and subsurface drainage concrete pipe at 20 years.

The total mass of benzene flowing out of the pipe for the flowable fill as a function of time is shown in Figure 40. In this scenario, the groundwater flow direction is from the west to the east boundary. The cumulative mass of benzene flowing out of the pipe is nearly 250 mg after the 20 years of simulation time. The mass with the installation of the flowable fill is decreased by 99.9 % compared to the no flowable fill case.

Highlights: The use of flowable fill leads to a 99.9 % reduction in the concentration of benzene permeated through the pipe for 20 years. The mass of benzene flowing out of the pipe is decreased by 99.9 %. Therefore, the flowable fill method is a long-term engineering control to mitigate the potential contamination that may breakthrough the subsurface pipe.

4.6.2.3. Effect of anti-seep collar

The results from the simulated domain with the presence of the anti-seep collar are presented in Figure 42. In this configuration, the anti-seep collar lengthens the drainage path and lengthens the time for contaminants reaching the pipe. However, the aqueous phase benzene, do permeate through the pipe after 2 years at a concentration above the MCL. The breakthrough concertation increases with time. The benzene is preferentially transported through the utility corridor, which is more permeable than the surrounding soil and then breaks through the gasket or the pipe.

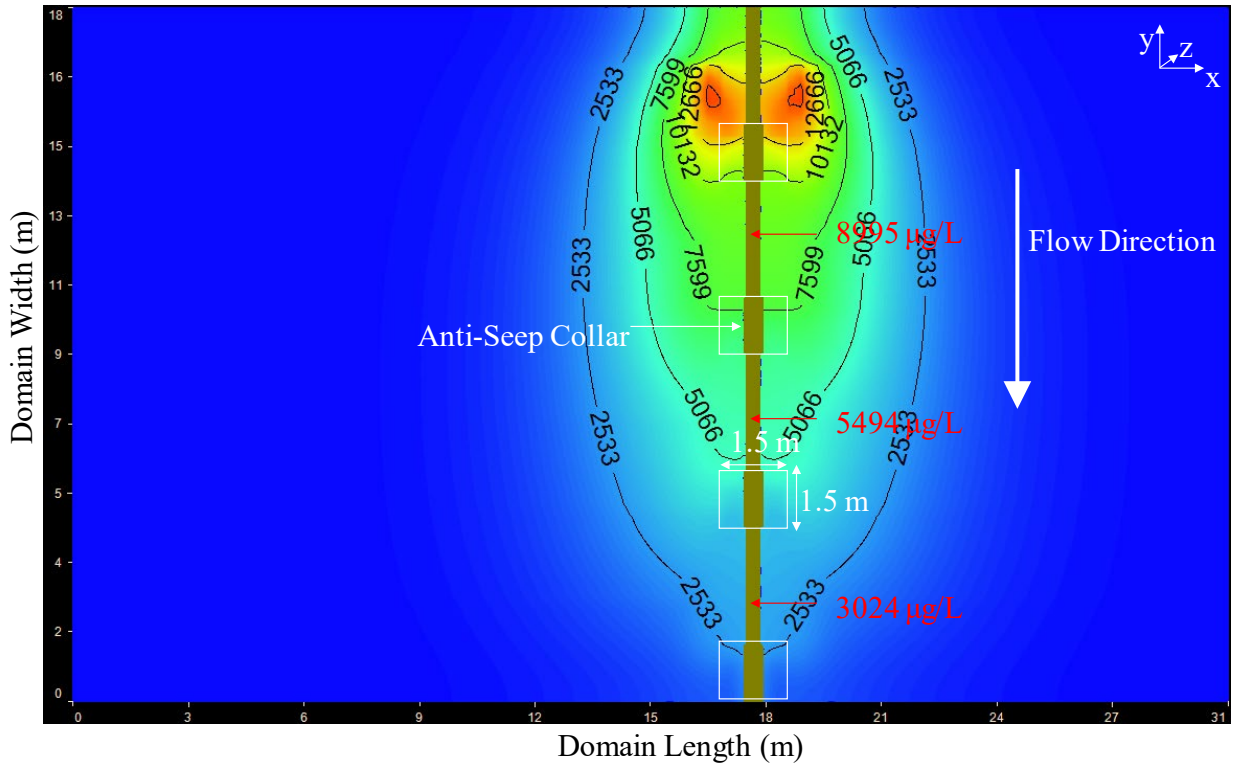

Figure 42: Map view of the anti-seep collar scenario for simulated aqueous benzene concentration (in µg/L) through the subsurface domain and subsurface drainage concrete pipe at 20 years.

The comparison between the effect of the base case (not installing anti-seep collar) and installing a collar at the plume boundary is shown in Figure 43. In this case, the normalized concentration of aqueous phase benzene profiles at 20 years along the trench soils indicated that the collar is an effective deterrent to creating a preferential pathway along with the backfill material. The effect of the natural gradient with the installation of the anti-seep collar on the mass of benzene flowing out of the pipe is shown in Figure 44. As the natural gradient increases, the mass of benzene breaking through the pipe increases. The cumulative mass of benzene flowing out of the pipe is nearly 1350 g, 1140 g, 1000 g, and 900 g over the 20 years of simulation time for i = 1.6 %, 0.5 %, 0.05 %, and 0.01 %, respectively. In comparison, for the case having no anti-seep collar, the cumulative mass of soluble phase benzene flowing out of the pipe is nearly 2400 g, 2000 g, 1510 g, and 1180 g over the 20 years for i = 1.6 %, 0.5 %, 0.05 %, and 0.01 %, respectively. The mass after the 20-year period is decreased by 44 %, 43 %, 34 %, and 24 % with the installation of the anti-seep collar for i = 1.6 %, 0.5 %, 0.05 %, and 0.01 %, respectively.

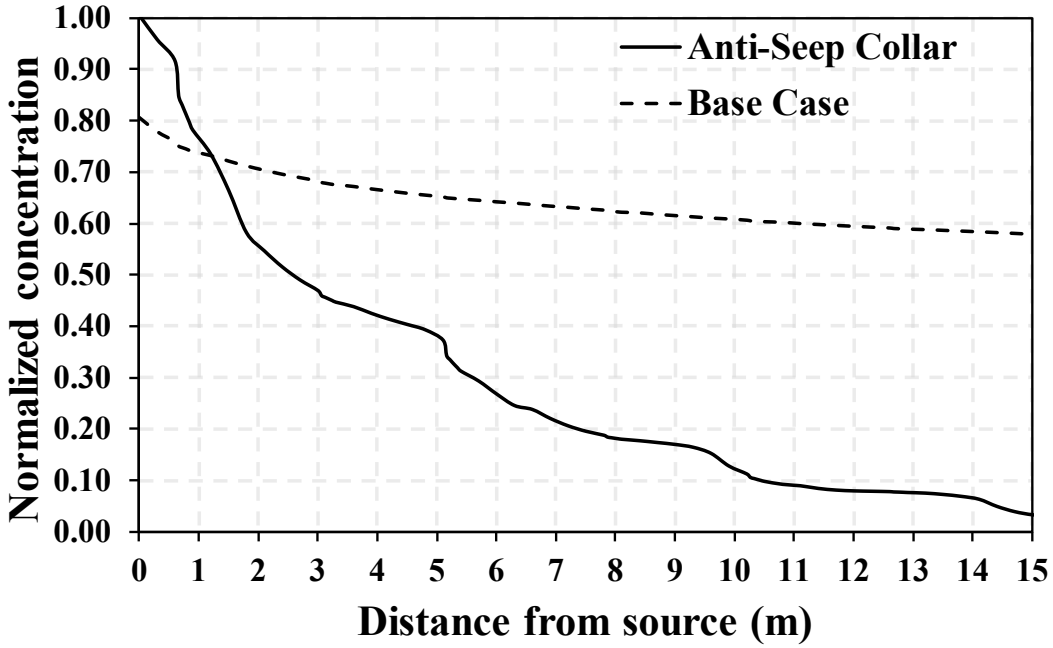

Figure 43: The concentration of benzene profiles at 20 years along with the trench soils for the base case and the anti-seep collars.

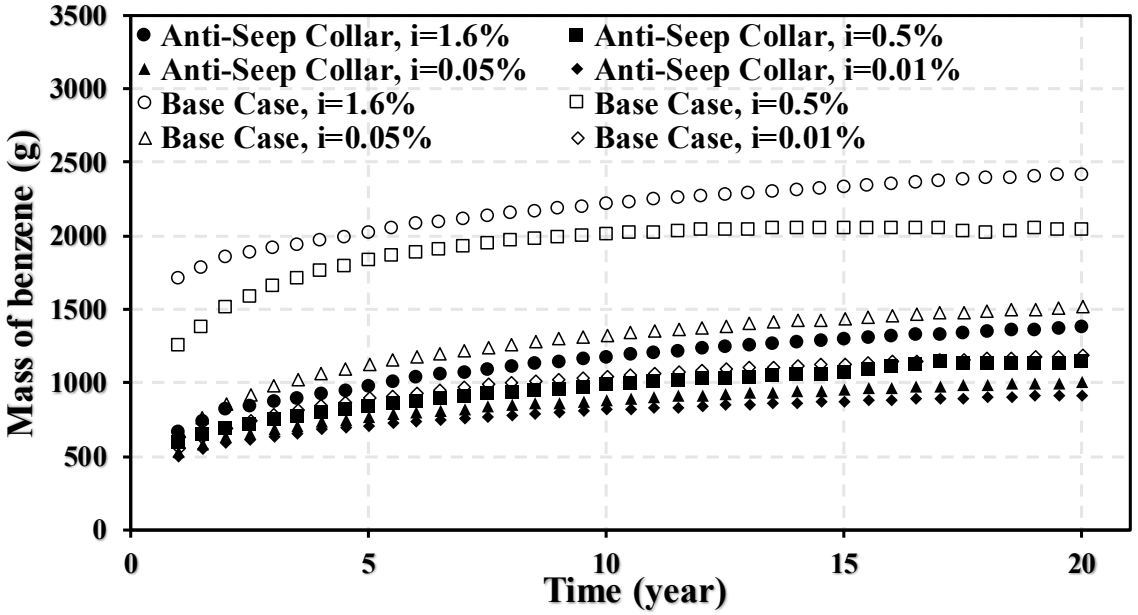

Figure 44: The total mass of benzene flowing out of the pipe for the anti-seep collar scenario as a function of time under different hydraulic gradients.

Highlights: Anti-seep collar leads to a 60 % reduction in the concentration of benzene permeated through the pipe for the 20 years simulated time. The mass of benzene flowing out of the pipe has decreased by up to 44 %. However, these results should be viewed in light of the assumptions made regarding the model parameters and the flow regime.

The natural hydraulic gradient of the site affects the level of contamination breaking through the pipe. With lower gradients, a smaller mass of contamination was found to break through the pipe. Thus, the existing hydrogeology of the site and the properties of the subsurface pipe need to be ascertained during the design and modeling phase and then ensured during the construction phase.

4.6.3. Plumb migration prevention: unsaturated model

To mitigate the contamination breaking through the pipe, the 1.5mx1.85 m (5ft x6 ft) anti seep collars are simulated along the pipe at 3m (10 ft) installation interval. The unsaturated properties of anti-seep collars are presented in Tables D2 and D3 in Appendix D. The anti-seep collar WRC (water retention Curve) is shown in Figure D1 in Appendix D. The low quality pipe material was employed to assess the worst case scenario. Figure 45 shows the analysis domain with the anti-seep collars installed along the pipe. The hydraulic gradient is assumed equal to 1%.

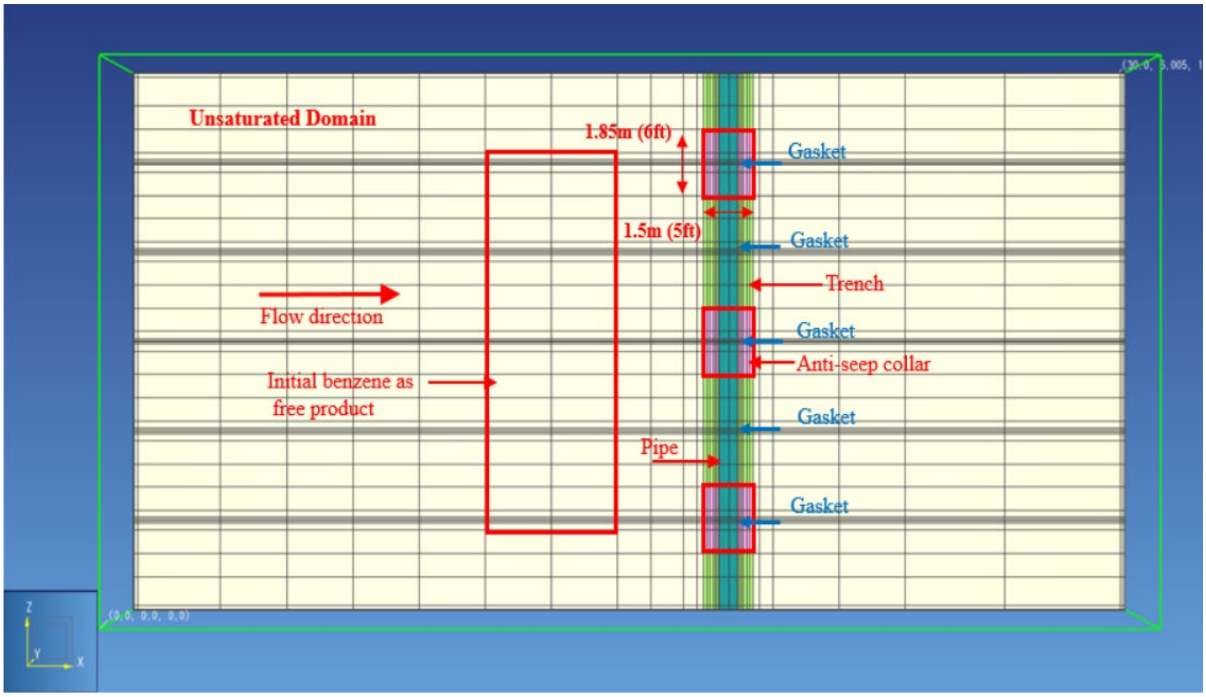

Figure 45: Anti-seep collar in unsaturated model

4.6.4. Results for unsaturated model

Anti-seep collars with very low hydraulic conductivity and unsaturated properties close to concrete properties can mitigate the contaminant breaking through the pipe as indicated in Figure 46. Using anti-seep collar the breakthrough concentrations decreased from 18.7 to 0.65 µg/l in aqueous phase and from the 3.60 to 0.12 µg/l in gas phase compared to the case without anti-seep collars; in this case, the cumulative mass transfer into the pipe is decreased by 96% (191 mg in aqueous phase and 1.5mg in gas phase), Figure 47.

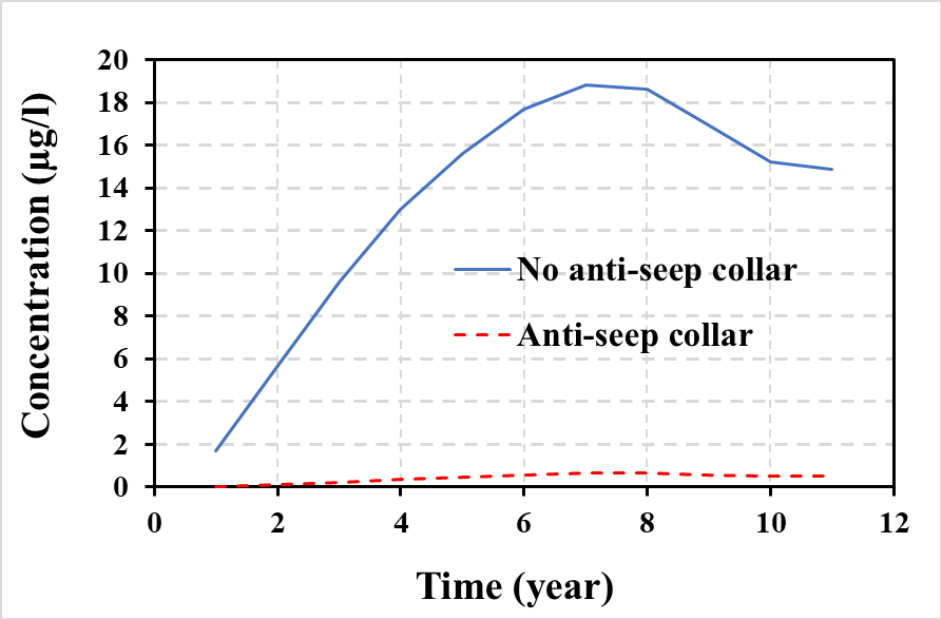

a) Aqueous phase

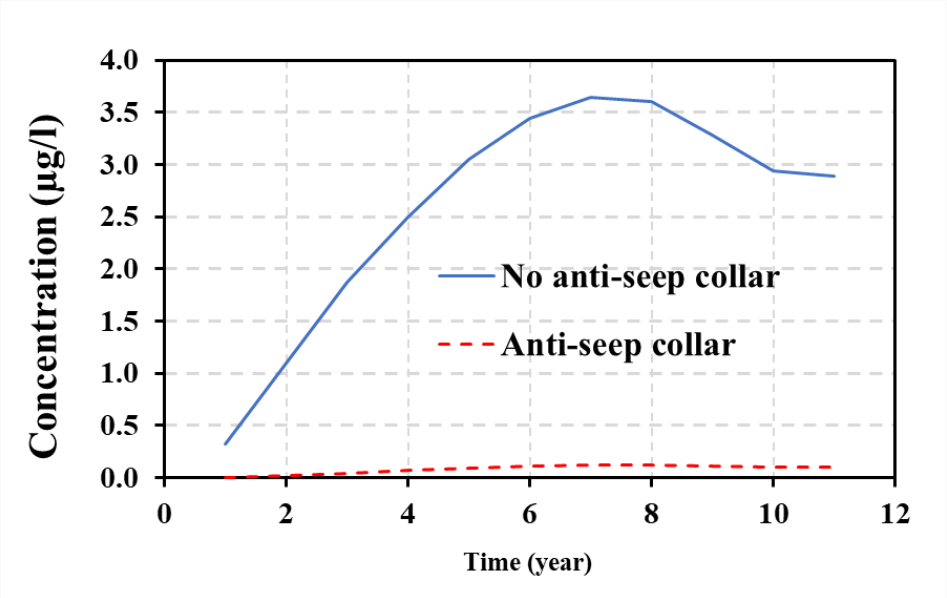

b) Gaseous phase

Figure 46: Comparison between benzene concentration inside the pipe flow for two scenarios of without anti-seep collar and using anti-seep collar a) Aqueous phase and b) Gas phase

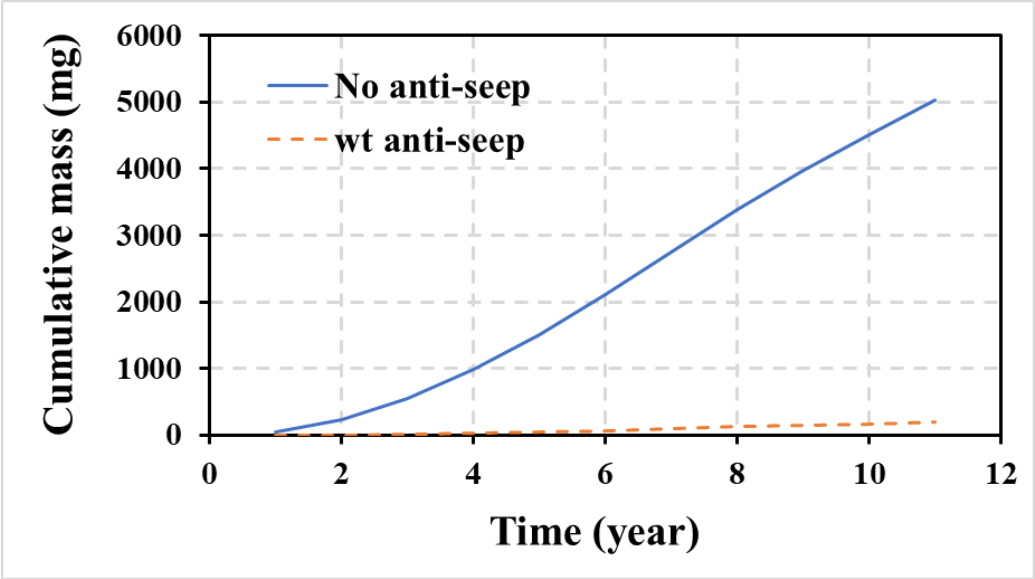

a) Aqueous phase

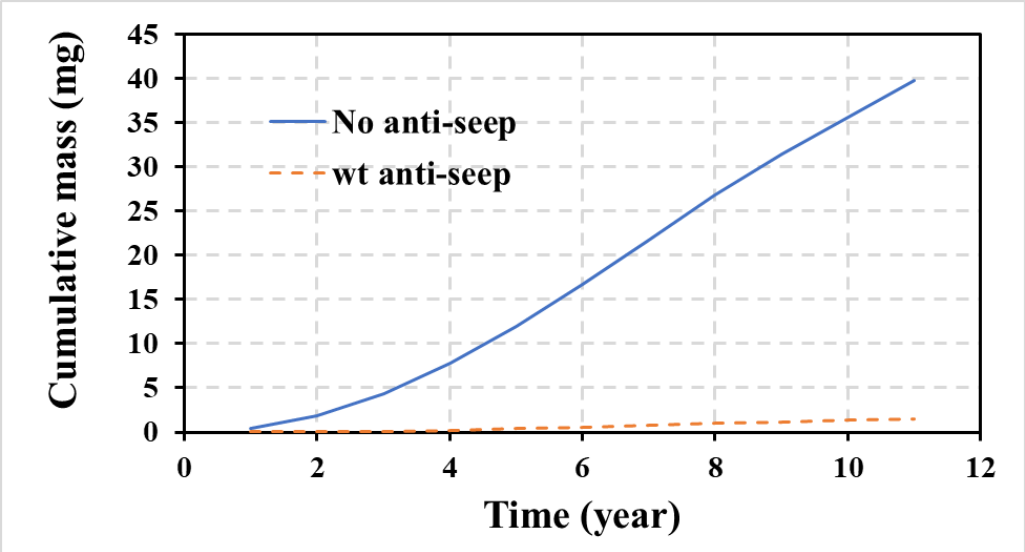

b) Gaseous phase

Figure 47: Cumulative mass breaking through the pipe for two scenarios of without anti-seep collar and using anti-seep collar a) Aqueous phase, and b) Gas phase

Highlights: Using anti-seep collar in unsaturated zone can mitigate mass breakthrough the pipe. The results show more than 90% decrease in the concentrations and cumulative mass transfer into the pipe with installed anti-seep collar.

5. Findings and Recommendations

Based on the content of this report, the following conclusions and recommendations are reported:

5.1. Experimental Results

Based on the results obtained from the experimental program, the following conclusions can be drawn:

- After 7 months of exposure, water (here deionized water) has no effect on the mechanical properties of PVC.
- Similar to Viton® specimens, nitrile specimens showed good stability while they are in contact with uncontaminated water for long time even at elevated temperatures.
- Compared to PCE, benzene has a more detrimental effect on the durability of plastic and rubber materials. More caution should be exercised when installations occur in benzene-contaminated areas. The degradation rate of plastic and rubber materials increases as the exposure time and/or temperature increase.
- After 7 months of exposure, the reduction in the tensile strength of neoprene was the highest among all gasket materials (i.e., neoprene, nitrile, and Viton®).
- In all exposure media (i.e., deionized water, PCE, and benzene solutions), Viton® performed the best among all gasket materials.
- After 7 months of exposure at different temperatures, among all rubber gasket specimens, Viton® performed far better than the other two. The degradation of nitrile was lower than that of neoprene. It should be noted that as the tensile strength of nitrile is much higher than that of neoprene, even at equal degradation percentage, the remaining strength of nitrile is greater than that of the neoprene specimens.
- A major issue with using neoprene or nitrile gaskets in heavily contaminated areas with benzene is their swelling which can arbitrarily deform the pipeline joints. This issue is more pronounced when neoprene is employed.
- Water contamination with aromatic and chlorinated hydrocarbons at their solubility limits did not show statistically significant effect on the compressive strength of mortar up to one year of exposure.
- According to the data obtained from unsaturated sorption test, contamination of water with aromatic or chlorinated hydrocarbons up to their solubility limits would not change the initial and secondary sorption rates of concrete pipe specimens.

- Application of Xypex® did not change the sorption rates of mortar specimens when exposed to clean or contaminated water.
- The diffusion coefficient of PCE vapor through saturated concrete pipe is one order of magnitude less than that of benzene vapor.
- The diffusion coefficient of benzene vapor was reduced by 24% through utilizing Xypex®. However, it is not possible to explain why this reduction occurred as no information is available on the composition of the admixture used in this study.
- Models for estimating tensile strength degradation of PVC and rubber gasket materials were developed.

5.2. Modeling

5.2.1. Saturated soil model

- The breakthrough of benzene concentrations into the subsurface pipe is dependent on the saturated hydraulic conductivity (k-value) of the native soil. Given the analyses parameters, there was no benzene estimated within the pipe with the damaged gaskets 20-years simulation scenarios under sandy clay soils ($k_{soil} = 10^{-5}$ cm/s). In this case, solute transported upwardly into the backfill soil with the higher k-value. Thus, the damaged gasket should not be a concern when the native soils have low hydraulic conductivity ($k \leq 10^{-5}$ cm/s).
- The highest potential of benzene concentration breaking through the pipe, and the mass of benzene flowing out of the pipe, was when the damaged pipe was assumed, rather than the damaged gasket case. This is due to the larger surface area through which breakthrough occurs. Thus, the damage to the pipe is more critical compared to the damage to the gaskets, for the potential occurrence of contamination breakthrough.

5.2.2. Unsaturated soil model

- Given the model assumptions in the unsaturated vadose zone and after two and half years, the source mass contamination will completely disappear through partitioning into the solid, aqueous and gas phases. In such case, the contaminant is transported to the pipe by diffusion in gas phase or advection in aqueous and gaseous phases.
- The water table level has a significant effect on mass transport into the pipe. The mechanism of transport in unsaturated domain is dominated by vapor phase diffusion for benzene (VOCs). The results show when water table rises toward the ground surface the concentrations inside the pipe decrease due to low lateral diffusive gas phase

spreading within the domain as a result of increased water content of the soil in the vadose zone.

- The mass calculations show the most of transported mass of benzene breaks through the pipe as aqueous flux through pipe surface. The high capillary pressure of concrete in this case regresses gas diffusion, however, the concentrations inside the pipe in both phases are in equilibrium and could be locally higher than allowable concentrations provided by standard guidelines.
- The simulations for three qualities (or condition as manifested by the hydraulic conductivity of the pipe) of pipe materials show the peak concentrations inside the pipe increases by 65% for low quality pipe and decreases by 77% for high quality pipe compared to concentrations estimated for the medium quality pipe. Cumulative mass transfer into the pipe is 114% and 65% of the values estimated for the base case or medium quality, in case of low and high quality material respectively.
- The analysis results for damaged versus undamaged gaskets show that severe-damaged gaskets can increase the concentrations and mass transfer into the pipe by more than two orders of magnitude. The high concentrations accumulated in the trench percolate into the pipe within two years after NAPL release.
- It was found the NAPL depth at source has a secondary effect on concentration and mass transfer into the pipe; reducing the NAPL thickness by a factor of two may lead to the decrease in the peak concentrations in both aqueous and gas phases by 13%.
- Considering the coarse-type soil material versus the sandy clay as the native soil, an increase in saturated hydraulic conductivity by two orders of magnitude led to an increase in the concentrations break through the pipe in both aqueous and gas phases by approximately 6 times after one year.
- Benzene was lost through volatilization to an atmospheric layer at top of the model domain. Such loss lessens the contaminant transfer into the pipe. The results show 16% of benzene emitted to the atmosphere after 1 year and most of it dissipates after eleven years in case of water table at 3m (10ft) below the surface (1.25m (4.1ft) from pipe invert).
- Adsorption to the soil mass retards the benzene migration considerably for a fraction of organic carbon in the domain of about 0.1%. The percentage of adsorbed mass compared to the total mass can vary from 4% in first year to 34% in eleventh year in which steady state has been established.

5.3. Mitigation strategies

- When clay barrier is used, the concentration of benzene is reduced by 22 % compared to the case of no clay barrier case for 20 years of simulation time. The mass of benzene flowing out of the pipe is decreased by 30 % for the same period. Therefore, the clay

barrier could be an effective method to protect the trench and subsurface pipe for a specific time.

- The use of flowable fill leads to a 99.9 % reduction in the concentration of benzene permeated through the pipe for 20 years. The mass of benzene flowing out of the pipe is decreased by 99.9 % compared to no flowable fill case. Thus, the flowable fill method is a long-term engineering control to mitigate the potential contamination that may break through the subsurface pipe.
- Anti-seep collar leads to a 60 % reduction in the concentration of benzene permeated through the pipe for the 20 years simulated time. The mass of benzene flowing out of the pipe has decreased by up to 44 %. However, these results should be viewed in light of the assumptions made regarding the model parameters and the flow regime.
- The natural hydraulic gradient of the site affects the level of contamination breaking through the pipe. With lower gradients, a smaller mass of contamination was found to break through the pipe. Thus, the existing hydrogeology of the site and the properties of the subsurface pipe need to be ascertained during the design and modeling phase and then ensured during the construction phase.
- Using anti-seep collar in unsaturated zone can mitigate mass and concentration break through the pipe. The results show more than 90% decrease in the concentrations and cumulative mass transfer into the pipe with installed anti-seep collar.

6. References

Abriola, L. M., and G.F. Pinder. A Multiphase Approach to the Modeling of Porous Media Contamination by Organic Compounds 1. Equation Development, Water resources research, 1985, January, 21(1): 11-18.

American Water Works Association (AWWA). Standard for polyethylene (PE) pressure pipe and fittings, 4 in (100 mm) through 63 in (1,575 mm), for water distribution and transmission, ANSI/AWWA C906-99, 1999, Denver, Colorado.

Antea. Groundwater Monitoring Report, GPM 3066 (Scotchman 3066), September 2016, Incident No. 20072.

Baehr, Arthur L. Selective Transport of Hydrocarbons in the Unsaturated Zone due to Aqueous and Vapor Phase Partitioning, Water Resources Research, 1987, VOL. 23, NO. 10: 1926-1938.

Battisteli, A. Modeling Multiphase Organic Spills in Coastal Sites with TMVOC V.2.0, Vadose zone journal, 2008, 7(1): 316-324.

Berens AR. Prediction of organic chemical permeation through PVC pipe. Journal American Water Works Association. 1985; 77(11):57-64.

Biczok I. Concrete corrosion and concrete protection. Publishing House of the Hungarian Academy of Sciences, 1964, Budapest, Hungary.

Brown RP. Practical Guide to the Assessment of the Useful Life of Rubbers, Rapra Technology Ltd., Shropshire, UK, 2001.

Burn S, Davis P, Schiller T, Tiganis B, Tjandraatmadja G, Cardy M, Gould S, Sadler, P, Whittle AJ. Long-term performance prediction for PVC pipes. Water Research Foundation (AwwaRF), 2005, Denver, Colorado.

Cheng CL, Gaunt JA, Mao F, Ong SK. Permeation of gasoline through DI pipe gaskets in water mains. Journal of American Water Works Association, 2012; 104(4): 73,74.

Chevron Phillips Chemical Co. Performance Pipe (CPCCPP): Engineering Manual. Chevron Phillips Chemical Co., 2003, Piano, Texas.

Class, H., R. Helmig, and P. Bastian. Numerical Simulation of Non-Isothermal Multiphase Multicomponent Processes in Porous Media, 1-An Efficient Solution Technique, Advances in water resources, 2002, 25: 533-550.

Cline PV, Delfino JJ, Rao PS. Partitioning of aromatic constituents into water from gasoline and other complex mixtures. Environmental Science & Technology, 1991; 25(5):914-920.

Corapcioglu, M. Y., Arthur L. Baehr. A Compositional Multiphase Model for Groundwater contamination by Petroleum Products, 1. Theoretical Consideration, Water Resources Research, 1987, 23(1): 191-200.

Cornelius, W. Ambient Air Quality Report, U.S. Department of Environmental and Natural Resources, Division of Air Quality, 2013.

Dafny, E. TCE Longevity in the Vadose Zone and Loading to the Groundwater-The Case of Episodic NAPL Releases from Near-Surface Source, Environmental Technology and Innovation, 2017, 7: 128-140.

Davis P, Burn S, Goul S, Cardy M, Tjandraatmadja G, Sadler P. Long-term performance prediction for PE pipes. Water Research Foundation (AwwaRF), 2007, Denver, Colorado.

Deiss, L., A. J. Franzluebbers , A. Amoozegar, D. Hesterberg, M. Polizzotto, and F. W. Cubbage. Soil Carbon Fractions from an Alluvial Soil Texture Gradient in North Carolina. Soil Science Society of America Journal, 2017, 81(5): 1096-1106.

Delle Site, A. Factors Affecting Sorption of Organic Compounds in Natural Sorbent/Water Systems and Sorption Coefficients for Selected Pollutants, J. Phys. Chem. Ref. Data, 2001, 30(1) :188-439.

Delta Environmental consultants. Comprehensive Site Assessment, Scotchman #66, 267 Western boulevard, Jacksonville, North Carolina, 2000, No. X0NC-110.

Dhaka, S., Kango, R., and Sharma, A. Groundwater flow and contaminant transport using Visual MODFLOW Flex. AGU International Journal of Science & Technology, 2016.

Dobrowolski JA. Concrete construction handbook, 4th edition, McGraw-Hill Handbooks, 1998, New York, USA.

DWI0772, Permeation of benzene, trichloroethene and tetrachloroethene through plastic pipe, Foundation for Water Research, 1997.

Environmental Protection Agency (EPA), Permeation and Leaching, EPA, 2002, Washington DC.

EPA (United states environmental protection agency), AWWA. Permeation and Leaching, 2002.

Fagerlund, F. F., Niemi, A., & Odén, M. Comparison of Relative Permeability-Fluid Saturation Capillary Pressure Relations in the Modelling of Non-aqueous Phase Liquid Infiltration in Variably Saturated, Layered Media. Advances in Water Resources , 2006, 29: 1705-1730.

Falta Ronald W., K. Pruess, S. Finsterle, and A. Battistelli, T2VOC User's guide, 1995.

Falta, Ronald W., Iraj Javandel, K. Pruess, and Paul A. Witherspoon. Density-Driven Flow of Gas in the Unsaturated Zone due to the Evaporation of Volatile Organic Compounds, Water resources research, 1989, 25(10): 2159-2169.

Falta, Ronald W., K. Pruess, I. Javandel, and Paul A. Witherspoon. Numerical Modeling of Steam Injection for the Removal of Non Aqueous Phase Liquids From the Subsurface, 1. Numerical Formulation, Water resources research, 1992, 28(2): 433-449.

Fetter, C. W. Contaminant Hydrogeology (second ed.). Upper Saddle River, New Jersey, United States of America: Prentice Hall inc., Simon & Schuster, 1999.

Freez, R. A., and J. A. Cherry. Groundwater, Prentice Hall, Englewood cliffs, N. J., 1979.

Ghoraba, S. M., Zyedan, B. A., & Rashwan, I. M. H. Solute transport modeling of the groundwater for quaternary aquifer quality management in Middle Delta, Egypt. Alexandria Engineering Journal, 2013, 52(2), 197-207.

Glaza EC, Park JK. Permeation of organic contaminants through gasketed pipe joints. Journal of American Water Works Association, 1992; 84(7):92-100.

Grube, W. E. Slurry trench cut-off walls for environmental pollution control. In Slurry Walls: Design, Construction, and Quality Control. ASTM International, 1992.

Harbaugh, A. W. MODFLOW-2005, the US Geological Survey modular ground-water model: the ground-water flow process (pp. 6-A16). Reston: US Department of the Interior, US Geological Survey, 2005.

He, L., Liu, G., & Li, X. Modeling and Predicting Groundwater Pollution Caused by Oil Pipeline Leakage Using MODFLOW and MT3D. In Bioinformatics and Biomedical Engineering, 2009. ICBBE 2009. 3rd International Conference on, (pp. 1-5). IEEE, 2009, June.

Holsen TM, Park JK, Bontoux L, Jenkins D, Selleck RE. Effect of soils on permeation of plastic pipes by organic chemicals, Journal of American Water Works Association, 1991b; 83(8):85-91.

Holsen TM, Park JK, Jenkins D, Selleck RE. Contamination of potable water by permeation of plastic pipe. Journal of American Water Works Association, 1991a; 83(8):53-56.

Islam, M. R., Jewett, D., Williams, J. R., & Hantush, M. Calibration of groundwater flow and contaminant transport modeling for Ogallala, Nebraska. In After the Rain Has Fallen: Groundwater Management Symposium, 1998, (pp. 105-110). ASCE.

Joun,W., S. Lee, Y. Koh, and K. Lee. Impact of Water Table Fluctuations on the Concentration of Borehole Gas from NAPL Sources in the Vadose Zone, Vadose Zone Journal, 2016.

Jury, W.A., W. F. Spencer, and W.J. Farmer. Behavior Assessment Model for Trace Organics in Soil: I. Model Description, J. Environ. Qual., 1983, 12(4).

Kaluarachchi J.J., and J. C. Parker. Multiphase Flow with a Simplified Model for Oil Entrapment, Transport in Porous Media, Kluwer Academic Publishers, 1992, pp 1-14.

Kelham M. A water absorption test for concrete. Magazine of Concrete Research, 40 (143), 1988, 106–110.

Koo DH. Assessment and calculation of BTEX permeation through HDPE water pipe. School of Engineering and Technology, Purdue University Indianapolis, 2012, Indiana.

Kumar, Ajeet. Water Flow and Transport of Chloride in Unsaturated Concrete, Thesis submitted to Graduate studies of university of Saskatchewan, Canada, 2010, Page 75.

Kyle BG. Soil-water equilibria for nonionic organic compounds. Science, 1981; 213(4508):683.

Lautz, L. K., & Siegel, D. I. Modeling surface and groundwater mixing in the hyporheic zone using MODFLOW and MT3D. Advances in Water Resources, 2006, 29(11), 1618-1633.

Le Saux V, Le Gac PY, Marco Y, Calloch S. Limits in the validity of Arrhenius predictions for field ageing of a silica filled polychloroprene in a marine environment. Polymer Degradation and Stability, 2014; 99:254-261.

Lea FM. The chemistry of cement and concrete, 3rd edition, Edward Arnold (Publishers) Limited, 1970, London, UK.

Li S, Willoughby J, Rojas OJ. Oil-in-water emulsions stabilized by carboxymethylated lignins: properties and energy prospects. ChemSusChem, 2016; 9:2460 -2469.

Mao F, Gaunt JA, Cheng CL, Ong SK. Microscopic visualization technique to predict the permeation of organic solvents through PVC pipes in water distribution systems. Journal of Environmental Engineering, 2011a; 137(2):137-145.

Mao F, Gaunt JA, Cheng CL, Ong, SK. Permeation of BTEX compounds through HDPE pipes under simulated field conditions. Journal of American Water Works Association, 2010; 102(3):107-118.

Mao F, Gaunt JA, Ong SK. Permeation of organic contaminants through PVC pipes. Journal of American Water Works Association, 2009; 101(5):128-136.

Mao F, Gaunt JA, Ong, SK, Cheng CL. Permeation of petroleum-based hydrocarbons through PVC pipe joints with Rieber gasket systems. Journal of Environmental Engineering, 2011b; 137(12):1128–1135.

Mao F. Permeation of hydrocarbons through polyvinyl chloride (PVC) and polyethylene (PE) pipes and pipe gaskets. Ph.D. thesis, Iowa State University, 2008, Ames, Iowa.

McDonald, M.G. and A.W. Harbaugh, A Modular Three-Dimensional Finite-Difference Ground-Water Flow Model, 1998, USGS TWRI Chapter 6-A1, 586 p.

Mercer, J. W., and R. M. Cohen. A Review of Immiscible Fluids in the Subsurface: Properties, Models, Characterization and Remediation. Journal of Contaminant Hydrology, 1990, 6: 107-163.

Murdock LJ, Blackledge GF. Concrete materials and practice, 4th edition, Edward Arnold Publishers Limited, 1968, London, UK.

Naylor T deV. Permeation Properties. In: Comprehensive Polymer Science and Supplements, Edited by B. Colin and P. Colin, Pergamon, 1989, Oxford, Great Britain.

NC DEQ, Maximum Soil Contaminant Concentrations, 2007, 15A NCAC 02L .0411.

NC DEQ, Toxic Air Pollutant Guidelines, 2018, 15A NCAC 02D.1104.

NCDEQ, Groundwater Quality Standards, 2016, 15ANCAC 2L .0202.

Nemes, A., M. G. Schaap, and F. J. Leij. UNSODA Version 2.0, Database of Unsaturated Soil Hydraulic Properties, 1999.

Olson AJ, Goodman D, Pfau JP. Evaluation of permeation of organic solvents through PVC, asbestos/cement, and ductile iron pipes. Journal of Vinyl and Additive Technology, 1987; 9(3):114-118.

Ong SK, Gaunt JA, Mao F, Cheng CL, Esteve-Agelet L, Hurburgh CR. Impact of petroleum-based hydrocarbons on PE/PVC pipes and pipe gaskets. Water Research Foundation (AwwaRF), 2008, Denver, Colorado.

Oostrom, M., Lenhard, R. J., Comparison of Relative Permeability-Saturation Pressure Parametric Models for Infiltration and Redistribution of a Light Nonaqueous-Phase Liquid in Sandy Porous Media, Advances in Water Resources 21, 1998, 2: 145-157.

Orchard DF. Concrete Technology-Properties of materials, Vol. 11, 4th edition. Applied Science Publishers, 1971, London, UK.

Park JK, Bontoux L, Holsen TM, Jenkins D, Selleck RE. Permeation of polybutylene pipe and gasket material by organic chemicals. Journal of American Water Works Association, 1991; 83(10):71-78.

Parker, J. C. , R. J. Lenhard, and T. Kuppusamy. A Parametric Model for Constitutive Properties Governing Multiphase Flow in Porous Media, Water Resources Research, April 1987, 23(4): 618-624.

Peng, S., N., Wang, and J., Chen. Steam and Air Co-Injection in Removing Residual TCE in Unsaturated Layered Sandy Porous Media, Journal of contaminant Hydrology, 2013, 153:24-36.

Petrasim User Manual, Rockware Inc., 2018, www.thunderheadeng.com.

Plastic Pipe Institute (PPI). Handbook of PE pipe, 2009, Washington, DC.

Powers, S. E., Hunt, C. S., Heermann, S. E., Corseuil, H. X., Rice, D., and Alvarez, P. J. "The transport and fate of ethanol and BTEX in groundwater contaminated by gasohol." Critical Reviews in Environmental Science and Technology, 2001, 31(1), 79-123.

Pruess, K., and A. Battistelli. TMVOC, a Numerical Simulator for Three-Phase Non-Isothermal Flows of Multicomponent HydrocarbonMixtures in Saturated- Unsaturated Heterogeneous Media. LBNL-49375 Lawrence Berkeley National Lab.: Berkeley, CA, USA, 2002.

Pye PW, Harrison HW. BRE Building elements, floors and flooring. performance, diagnostics, maintenance, repair and the avoidance of defects. Building Research Establishment, Construction Research Communications Limited, 1997, London, UK.

Rahman S, Alchin N. Rieber joint system for PVC pipe: Synopsis of a locked-in elastomeric gasket. in Proceeding of Pipes Wagga Conference, 2005, Wagga Wagga, Australia.

Ramme, Bruce W. M. Tharaniyil. Coal Combustion Products Utilization Handbook, Wisconsin Electric Power Company. TekDoc ñ Technical Documentation, Inc. Greendale, Wisconsin, 2000.

Rasmusson, K. Rasmusson, M. NAPL Spill Modeling and Simulation of Pumping Remediation, Master Thesis, Department of Earth Sciences, Air, Water and Landscape Science, Uppsala University, 2009.

Reid, R. C., J. M. Prausnitz, and B. E. Poling. The Properties of Gases and Liquids, McGraw-Hill, New York, 1987.

Saghravani, S. R., Mustapha, S. A. B., Ibrahim, S. B., Yusoff, M. K., & Saghravani, S. F. Phosphorus migration in an unconfined aquifer using MODFLOW and MT3DMS. Journal of Environmental Engineering and Landscape Management, 2011, 19(4), 271-277.

Sleep, B. E., and J. F. Skyes. Modeling the Transport of Volatile Organics in Variably Saturated Media, Water resources research, 1989, 25(1): 81-92.

Smyl, D., F. Ghasemzadeh, and M. Pour-Ghaz. Modeling Water Absorption in Concrete and Mortar with Distributed damage. Construction and Building Materials, 2016, 125: 438-449.

Sookhak Lari, K., Davis, G., Johnston, C. Incorporating Hysteresis in a Multi-Phase Multi-Component NAPL Modelling Framework; a Multi-Component LNAPL Gasoline Example, Advances in Water Resources, 2016, 96: 190-201.

Spragg RP, Castro J, Li W, Pour-Ghaz M, Huang PT, Weiss J. Wetting and drying of concrete using aqueous solutions containing deicing salts. Cement & Concrete Composites, 2011; 33:535-542.

Stone, H. L. Probability Model for Estimating Three-Phase Relative Permeability, J. Pet. Technol., 1970, 22(1): 214-218,.

Terracon Consultants, Preliminary Site Assessment of 267 Western Boulevard project, Jacksonville, July 2018 .

Thompson C, Jenkins D. Review of water industry plastic pipe practices. Water Research Foundation (AwwaRF), 1987, Denver, Colorado.

Van Geel, P. J., and J. F. Sykes. Laboratory and Model Simulation of a LNAPL Spill in a Variably-Saturated Sand, 1. Laboratory Experiment and Image Analysis Techniques, Journal of Contaminated Hydrology, 1994, 17 (1): 1-25.

Van Geel, P. J., and J. F. Sykes. Laboratory and Model Simulation of a LNAPL Spill in a Variably-Saturated Sand, 2. Comparison of Laboratory and Model Results, Journal of Contaminated Hydrology, 1994, 17 (1): 27-53.

Van Genuchten, M. T. A Closed-Form Equation for Predicting the Hydraulic Conductivity of Unsaturated Soils, Soil Sci. Soc. Am. J., 1980, 44: 892-898.

Van Genuchten, M. T., Leij, F. J., and S. R., Yates. The RETC Code for Quantifying the Hydraulic Functions of Unsaturated Soils, EPA/600/2-91/065. U.S. Department of Agriculture, Agricultural Research Service, Riverside, California, U.S. Environmental Protection Agency, 1991.

Viswanath DS, Ghosh TK, Prasad DH, Dutt NVK. Viscosity of liquids: Theory, estimation, experiment, and data, Springer, Dordrecht, 2007.

Vonk MW. Permeation of organic compounds through pipe materials. Publication No. 85. KIWA, 1985, Neuwegein, Netherlands.

Wealthall, G.P., Rivett, M.O., Dearden, R. A. A Review of Transport and Attenuation of Dissolved-Phase Volatile Organic Compounds (VOCs) in the unsaturated zone, British Geological Survey Commissioned Report, 2010.

Whelton AJ, Nguyen T. Contaminant migration from polymeric pipes used in buried potable water distribution systems: A review. Critical Reviews in Environmental Science and Technology, 2013; 43:679-751.

Wilson SA, Langdon NJ, Walden PJ, The effects of hydrocarbon contamination on concrete strength. Geotechnical Engineering, 2001; 149(3):189-193.

Yang, Q. Modelling of benzene Distribution in the Subsurface of an Abandoned Gas Plant Site after a Long Term of Groundwater Table Fluctuation, Hydrol. Process. 2012, 27: 3217–3226.

Yang, Z., Zandin, H., Niemi, A., Fagerlund, F. The role of geological heterogeneity and variability in water infiltration on non-aqueous phase liquid migration, Environ Earth Sci, 2013 68:2085–2097.

Zytner RG. Sorption of benzene, toluene, ethylbenzene, and xylenes to various media. Journal of Hazardous Materials, 1994; 38(1):113-126.

Appendix A: Literature review

In this the existing knowledge on the effect of soil and groundwater contamination on the performance of subsurface utilities such as pipes and gaskets is presented. The

A.1. Contaminant diffusion through pipes and gaskets

A.1.1. Most Common Contaminants in the US Water System

Among different classes of contaminants, petroleum-based products (e.g., resulting from spillage of underground storage tanks and fuel stations) and chlorinated organic solvents (typically released from dry-cleaning solvents) are the most common in the US (EPA, 2002; Holsen et al., 1991a; Koo, 2012). Figure A1 illustrates the percentage of contamination incidents in the US water system involving different contaminants (EPA, 2002; Holsen et al., 1991a). Clearly the largest number of incidents is related to contamination by petroleum-based products, followed by TCE (Trichloroethene) and PCE (Tetrachloroethylene) from dry-cleaning solvents.

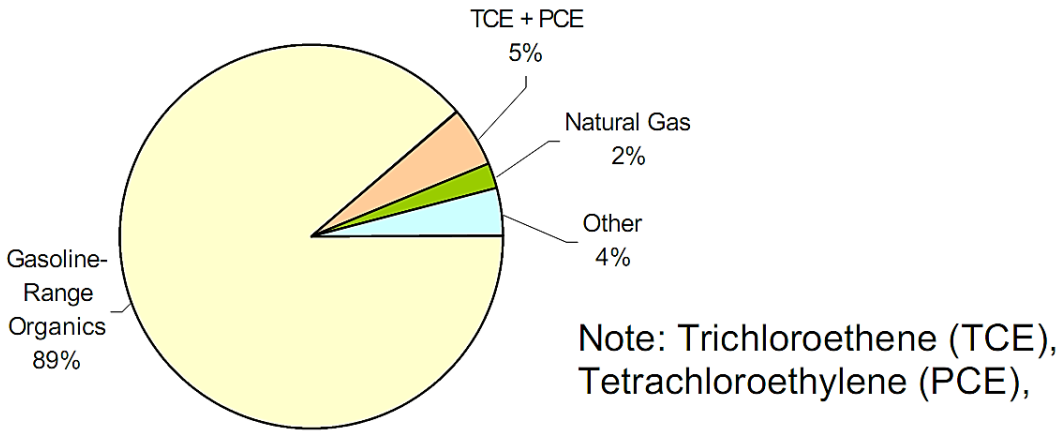

Figure A1: Percentage of contamination incidents in the US water system involving different contaminants (EPA, 2002; Holsen et al., 1991a).

A.1.2. Most Common Polymeric Pipes used in the US

The majority of the polymeric (plastic) pipes utilized in the US water pipeline system consist of polyvinyl chloride (PVC), polyethylene (PE), and polybutylene (PB) pipes (Whelton and Nguyen, 2013). Due to their low performance and rapid degradation at early stages of their service life (the first five years of service), PB pipes are not commonly used (Whelton and Nguyen, 2013). In addition, PB pipes are the most permeable pipe among the three pipe types (Whelton and

Nguyen, 2013). Figure A2 shows the results of a survey conducted in 1980s that evaluated the contribution of different pipe types to drinking water contamination incidents (Holsen et al., 1991a; Thompson and Jenkins, 1987). According to Figure A2, 43% of the contamination incidents involved PB pipes, showing the poor performance of these pipes. PE pipes also accounted for 39% of the incidents; however, PE pipes are still commonly used. In the following sections, the effect of contaminates on the properties of PVC and PE pipes are reviewed. Also, available information about the permeation of contaminants through PVC and PE pipes are included.

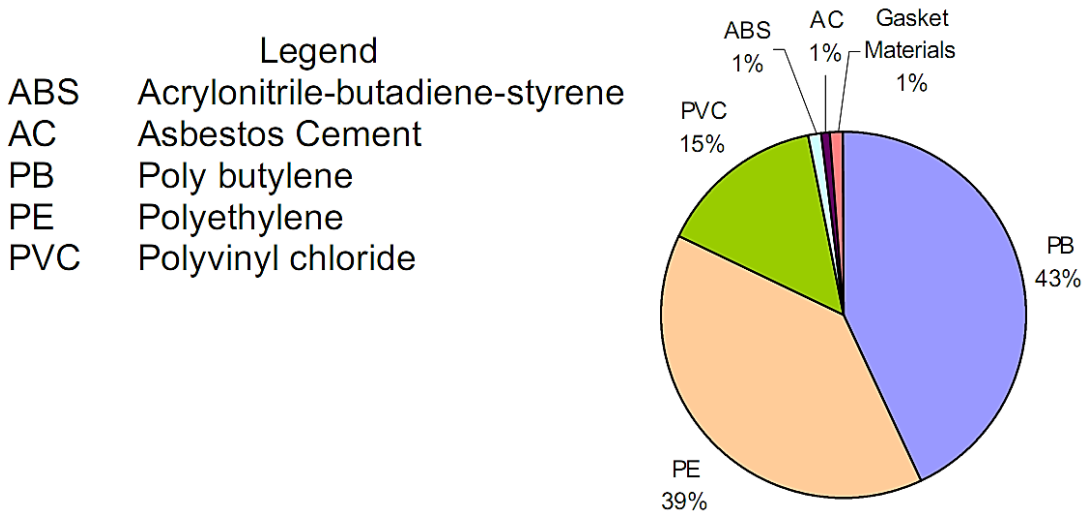

Figure A2: Percentage of pipe types involved in the US water system permeation incidents (EPA, 2002; Holsen et al., 1991a; Thompson and Jenkins, 1987).

A.1.3. Effect of contaminants on PVC pipes

PVC pipes have been among the most common pipe materials in the US since 1970s (Burn et al., 2005; Whelton and Nguyen, 2013). PVC is an amorphous thermoplastic with very limited flexibility of the polymer chains (Mao, 2008; Whelton and Nguyen, 2013). Owing to its high glass transition temperature (Tg = 179.6 ^{o}F) compared to room temperature, PVC is a glassy, rigid plastic (Whelton and Nguyen, 2013). PVC pipes are generally thought to be essentially impermeable to environmental organic contaminants but permeation through PVC pipes can be expected in heavily contaminated situations (Berens, 1985; Vonk, 1985).

Diffusivity of different contaminates through PVC materials have been well studied by many researchers. Berens (1985), investigated the diffusion of different organic solvents at a wide range of concentration in PVC powder, film, and sheet using gravimetric sorption test. He found

that at low activities (concentrations) of solvents, the estimated permeation through the PVC pipe wall is virtually zero even for long exposure times (i.e. many centuries obtained by modeling). Thus, it was concluded that except in case of a gross spillage or leakage of a strong swell-inducing solvent, rigid PVC pipes are effective barriers against permeation of the tested pollutants (Berens, 1985; Mao, 2008).

Vonk (1985), studied the diffusion of organic contaminants through PVC and PE pipes. The results revealed that because of the glassy structure of PVC, as compared to PE which is a semi-crystalline material at room temperature, PVC pipe was significantly less permeable when compared to PE pipe (Vonk, 1985).

Olson et al. (1987), evaluated the permeation of Toluene, Hexane, and TCE into full-size commercial PVC, Asbestos/Cement (AC), and Ductile Iron (DI) pipes. The tests were performed on jointed and unjointed sections of these pipes while the pipes were pressurized to 40 psi. The schematic illustration of the test assembly is shown in Figure A3.

When exposed externally to pure organic solvents, all the jointed pipes, except the hexane/ductile iron, showed permeation of organic solvents. The unjointed iron pipe did not show permeation over 42 days of exposure; however, the unjointed PVC slowly softened to point of permeation with toluene after 37 days. The asbestos/cement unjointed pipe showed permeation in a few days by toluene and TCE due to its high porosity. It should be noted that according to the test results, constant internal pressure does not prevent contamination by permeation.

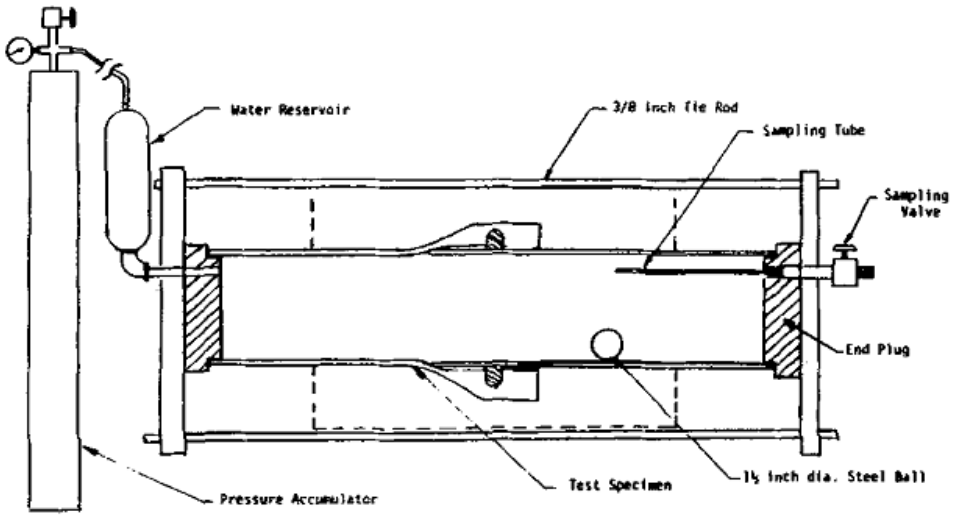

Figure A3: Testing setup of piping system (Olson et al., 1987).

Olson et al. (1987), also tested jointed and unjointed pipes exposed to water contaminated with toluene and TCE at their solubility limits for 180 days. The same trend of permeation as that of pure solvent was observed for aqueous solutions prepared at the solubility limits of contaminants; however, permeation (breakthrough) occurred at later times. Table A1 summarizes the approximated breakthrough time for all the tested pipes. Moreover, unjointed pipe had slower or no permeation. In this regard, this finding could be connected with very low concentrations of contaminants in the aqueous solutions.

Table A1: Summary of the results by Olson et al. (1987), showing time to organic solvent breakthrough.

Solvent		**Time to Organic Solvent Breakthrough (days)**								
		PVC			**DI**			**AC**		
		J1*	J2	UJ**	J1	J2	UJ	J1	J2	UJ
Toluene	Pure solvent	10	4	38	9	3	NP	3	1	7
	Solution (solubility limit)	NP***	NP	70	161	77	NP	77	77	NP
TCE	Pure solvent	22	15	NP	8	4	NP	12	5	14
	Solution (solubility limit)	NP	NP	NP	161	105	NP	70	70	NP

* Jointed pipe; ** Unjointed pipe; *** No permeation

Mao (2008), studied permeation of BTEX (benzene, toluene, ethylbenzene, and xylene) and chlorinated TCE contaminants in the forms of pure solvent, aqueous solution, and organic vapor through gasketed and ungasketed PVC and PE pipes. Mao (2008), studied different concentrations of contaminants. In addition, to simulate contaminated field conditions, Mao investigated the permeation of contaminates into pipes from contaminated soils. Different test setups were prepared, and the permeability and diffusivity of different contaminants were evaluated using three methods: pipe-bottle, gravimetric sorption, and microscopic visualization tests.

The pipe-bottle test included a glass bottle with a 1-inch PVC/PE pipe mounted horizontally through holes drilled in the bottle (Figure A4). In this test, the PVC/PE pipe was (i) directly exposed to pure solvents, (ii) directly exposed to aqueous solution of solvents, and (iii) exposed to vaporized contaminants. In all cases, the PVE/PE pipe was filled with deionized water and pipe water samples were taken daily and analyzed for the presence of the target compounds

(BTEX as petroleum-based compounds and TCE as chlorinated organic solvent) (Mao, 2008; Mao et al., 2010).

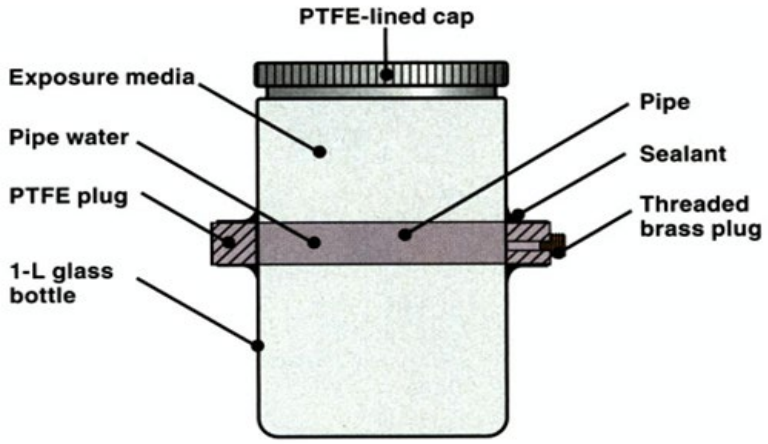

Figure A4: Schematic illustration of pipe-bottle test apparatus (Mao et al., 2010).

The permeation of TCE, toluene, and benzene through PVC were detected after 7, 16, and 20 days, respectively. Figure A5 shows the cumulative mass per unit area of the pipe wall for TCE, toluene, and benzene (Mao et al., 2011a). It can be seen that the chlorinated organic solvent (TCE) permeated through the PVC pipes more rapidly than benzene and toluene (Mao et al., 2011a). After the breakthrough, the permeation occurs at a constant rate where benzene permeated with the highest rate followed by TCE.

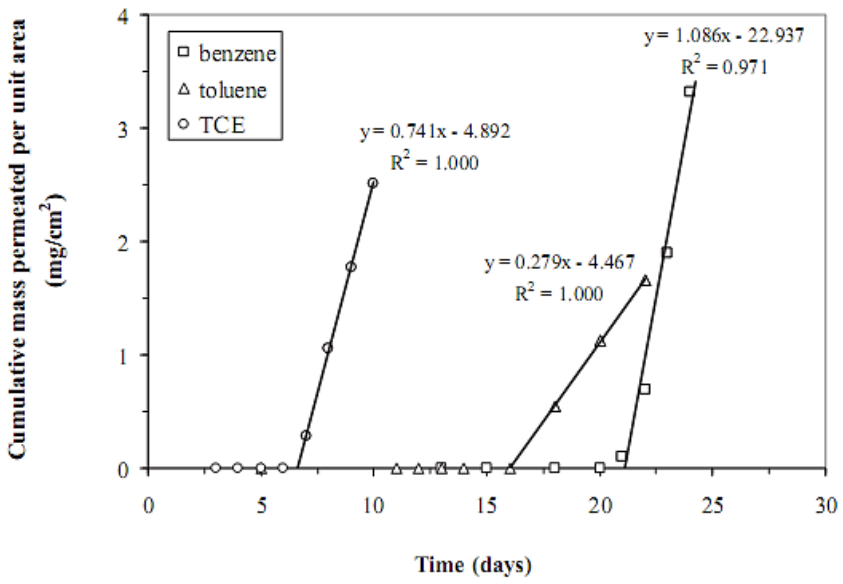

Figure A5: Cumulative mass permeated per unit area of PVC pipes exposed to pure solvents of benzene, toluene, and TCE (Mao et al., 2011a).

Using the pipe-bottle test the PVC pipes were exposed directly to pure gasoline. After two years of measurement, no detectible BTEX (from gasoline) was observed. This observation shows that PVC pipes are resistant to permeation by commercial gasoline, at least for a 2-year exposure period (Mao et al., 2011a). The resistance of PVC pipes to gasoline permeation is attributed to the relatively low activity (concentration) of BTEX in gasoline (Mao et al., 2011a).

Using the pipe-bottle test, Mao et al. (2009) evaluated permeation of solvents into PVC pipe from vapors phase. Figure A6 shows the results of the pipe-bottle test performed on PVC pipes exposed to pure solvent (same data as Figure A5) and vapor of benzene, toluene, and TCE. In Figure A6, similar to exposure to pure solvents, TCE permeated first, followed by toluene and benzene during exposing PVC pipes to contaminants' vapor. Moreover, after the breakthrough for each specific contaminant, its permeability rate is nearly similar from both pure solvent and vapor source.

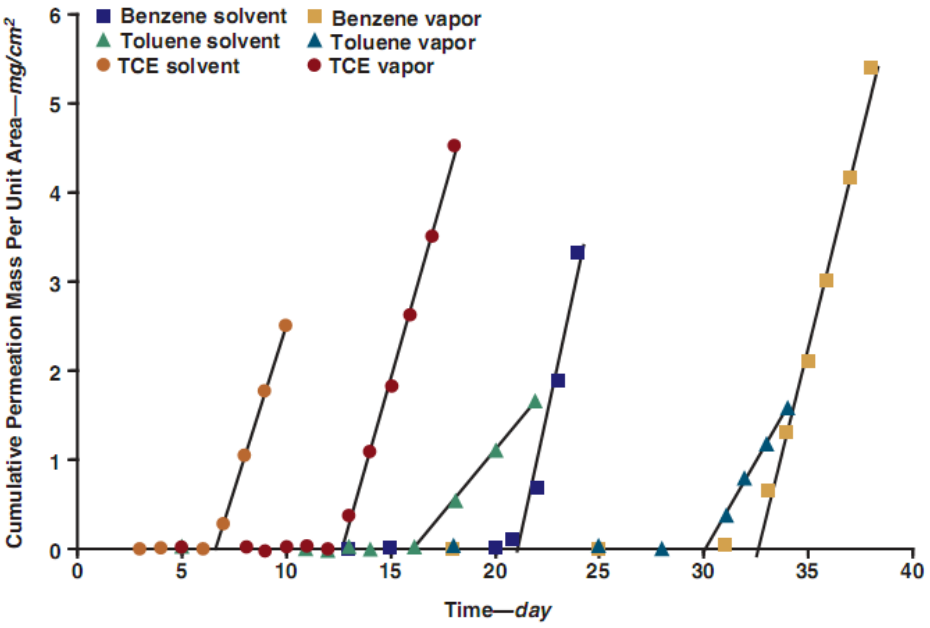

Figure A6: Cumulative mass permeated per unit area for 1-in PVC pipes exposed to pure solvent and vapor of benzene, toluene, or TCE (Mao et al., 2009).

Using the pipe-bottle test, Mao et al. (2009), also evaluated permeation of solvents into PVC pipe from the solution of water and solvent. Since the mixing action has a strong effect on both the dissolution of solvents from the nonaqueous phase liquid (NAPL) phase to the aqueous phase and the mass transfer of contaminants in aqueous solution (Mao et al., 2009), the influence of mixing action of solvents in aqueous solution during performing pipe-bottle test on the breakthrough time and the rate of diffusion of benzene and TCE through PVC pipe was investigated.

As shown in Figure A7, continuous stirring of contaminants greatly affected the breakthrough time and the rate of diffusion of each contaminant through PVC pipe. In Figure A7, the breakthrough times were shortened, and the diffusion rates were increased when continuous stirring procedure was applied. The results for toluene were not reported in Mao et al.'s work (2009) since breakthrough did not occur during the 10-month duration of the experiment after which the experiment was terminated due to technical difficulty.

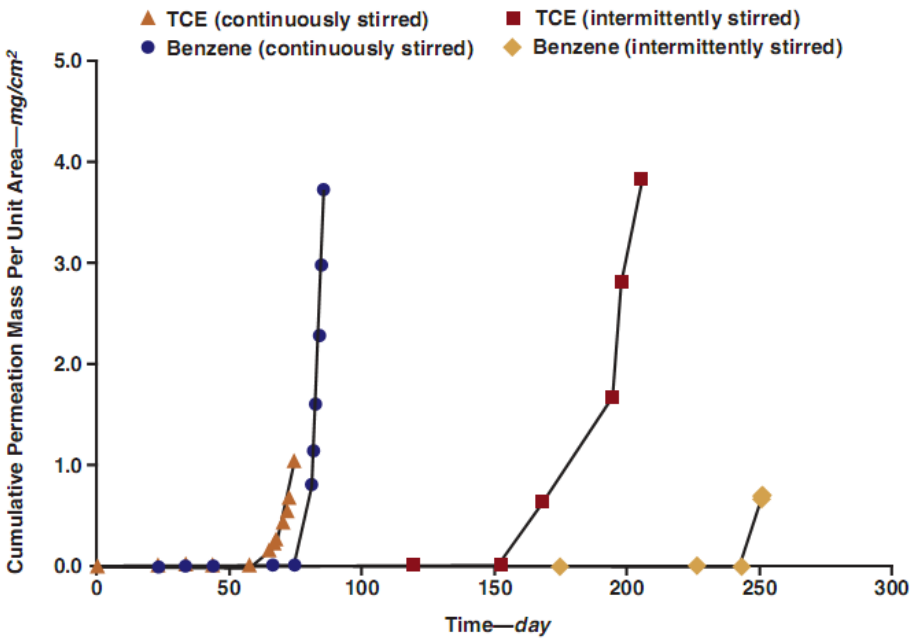

Figure A7: Cumulative mass of benzene and TCE permeated per unit area for 1-in PVC pipe exposed to benzene or TCE aqueous solutions at their solubility limits (Mao et al., 2009).

Mao (2008) also used Gravimetric Sorption Test to evaluate diffusion of contaminants in the form of aqueous solution or vapor at different strength through PVC pipe. The testing procedure consisted of preparing pipe specimens by cutting them across the circumferential axis to form ring-like specimens. Then specimens were exposed to aqueous solutions of contaminants of interest (benzene and Toluene) by immersion of them in a 120 ml glass jar containing such solutions (five concentrations at 100%, 80%, 60%, 40%, and 20% of solubility limits). In the case of vaporized contaminants, the specimen is placed in a one-liter glass jar containing 100 mL of benzene/toluene solvent of different strengths (pure solvent, 80%, 60%, 40%, and 20% v/v benzene or toluene) above the liquid. Then, at various times, the specimens are removed from the glass jar, placed on paper towels, wiped, and allowed to air dry for 30 seconds before weighing. Finally, by measuring weight changes of specimens at different times, sorption coefficients were calculated for each type of contaminants through drawing weight gain against square root of time and obtaining the slope of the fitted straight line (Mao, 2008).

In Figure A8, the sorption rate decreases as the concentration of contaminants reduces. For benzene and toluene, significant sorption could be observed for the 100 and 80% of their solubility limits whereas the percent weight gains for 60, 40, and 20% of solubility limits were below 2% after eight months of exposure. Sorption at the 20% of solubility limit was found to be statistically similar to that of the control experiment (deionized water sorption) (Mao et al., 2009). This implies that sorption can be neglected for contaminant levels below 20% of solubility limit for both toluene

and benzene. In fact, solutions at 20% of solubility limits (toluene, benzene, and TCE at 100, 340, and 220 mg/L, respectively) are considered to be a high level of environmental pollution in contaminated groundwater (Mao et al., 2009). These concentrations are seldom encountered in the field except in close proximity to an NAPL. For water with gasoline at its solubility limit, sorption of benzene, toluene, ethylbenzene, and o-, p-, and m-xylene (BTEX) by pipe materials should be negligible because the concentration of the dissolved BTEX is generally < 150 mg/L (Cline et al., 1991; Mao et al., 2009).

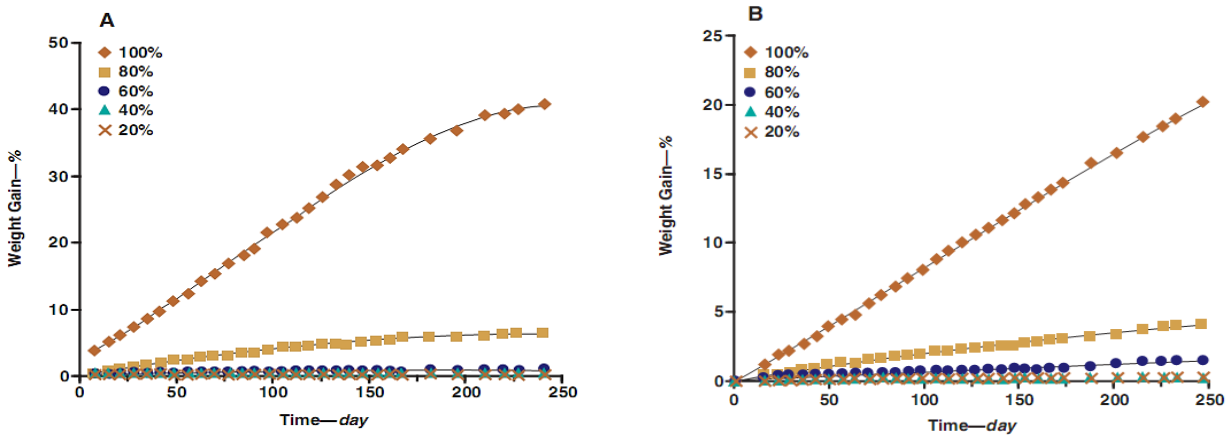

Figure A8: Weight gains of 1-in PVC pipe exposed to various percentages of solubility limit in aqueous solutions of benzene (A) or toluene (B) (Mao et al., 2009).

As shown in Figure A9, the sorption of vapors of benzene or toluene was found to be linear with the square root of time which is a typical characteristic of Fickian kinetics sorption (Mao, 2008; Mao et al., 2009), but with a time lag at the initial period. In addition, as can be seen in Figure A9, weight gain decreased dramatically as the benzene or toluene activity was reduced. When the activity was less than 0.55 for benzene and less than 0.51 for toluene (the corresponding volumetric percent in the reference fuel was ~ 40%), sorption of benzene or toluene vapors by pipe materials was insignificant over a 2.5-day exposure (Mao et al., 2009). Note that in Figure A9 the activities of benzene in organic vapors, a, that were in equilibrium with pure solvent (100%) and 80%, 60%, 40%, and 20% v/v in the reference fuel were estimated as 1.0 and 0.88, 0.73, 0.55, and 0.32, respectively. The corresponding activities of toluene were 1.0 and 0.86, 0.70, 0.51, and 0.28, respectively.

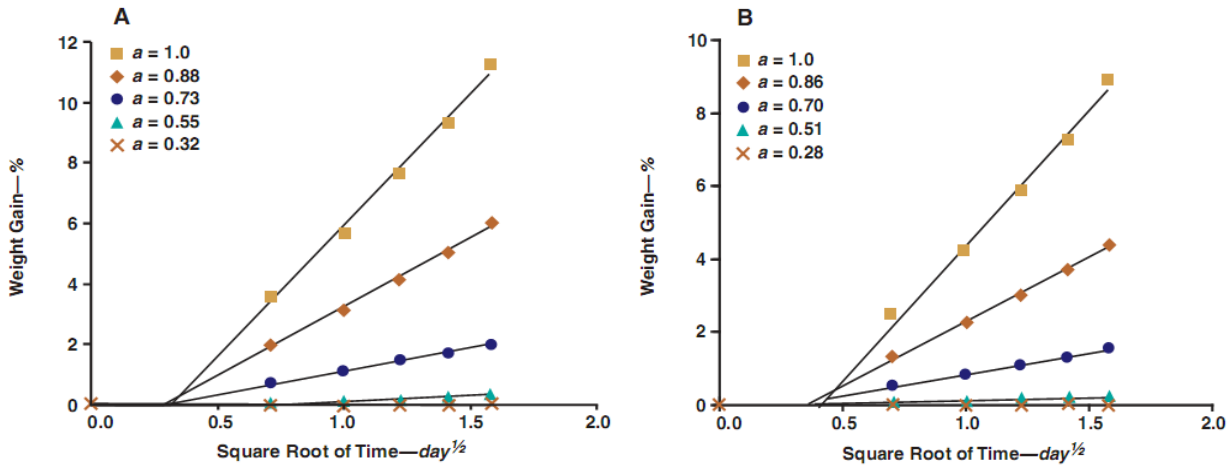

Figure A9: Weight gains for 1-in PVC pipe exposed to benzene (A) or toluene (B) vapor (Mao et al., 2009).

A software program was used to find the regression equations that would describe the three-dimensional data, i.e., weight gain, time, and activity and two empirical equations (A1 and A2) were obtained with an excellent fit (R2 > 0.999) (Mao et al., 2009):

$$\ln(WG) = 6.30 + 0.71\ln(t) - \frac{4.55}{a}\ [for\ benzene] \quad \text{(A1)}$$

$$\ln(WG) = 5.52 + 0.79\ln(t) - \frac{4.07}{a}\ [for\ toluene] \quad \text{(A2)}$$

where WG is the weight gain percentage, t is the exposure time (day), and a is the activity of the target compound in organic vapors.

For commercial gasoline, the total mole fraction of aromatic compounds is approximately 0.25 or lower (Mao et al., 2009). Therefore, the total activity of aromatic compounds in gasoline vapors should be around 0.25 or lower. With a = 0.25, both Equations A1 and A2 predict that a 1% weight gain would require thousands of years. Clearly, sorption of gasoline vapors by PVC pipe is estimated to be low and to have no significant effect during the expected service life of the pipe (Mao et al., 2009).

The last testing procedure used by Mao (2008), to quantify the diffusion of contaminants through PVC pipes during a specific period of time was Microscopic Visualization Test. As swelling of PVC pipe by an organic solvent may result in the formation of a moving (diffusion) front, a sharp interface separating the inner glassy core from the outer swollen layer can represent rate of diffusion of a specific contaminant (Figure A10).

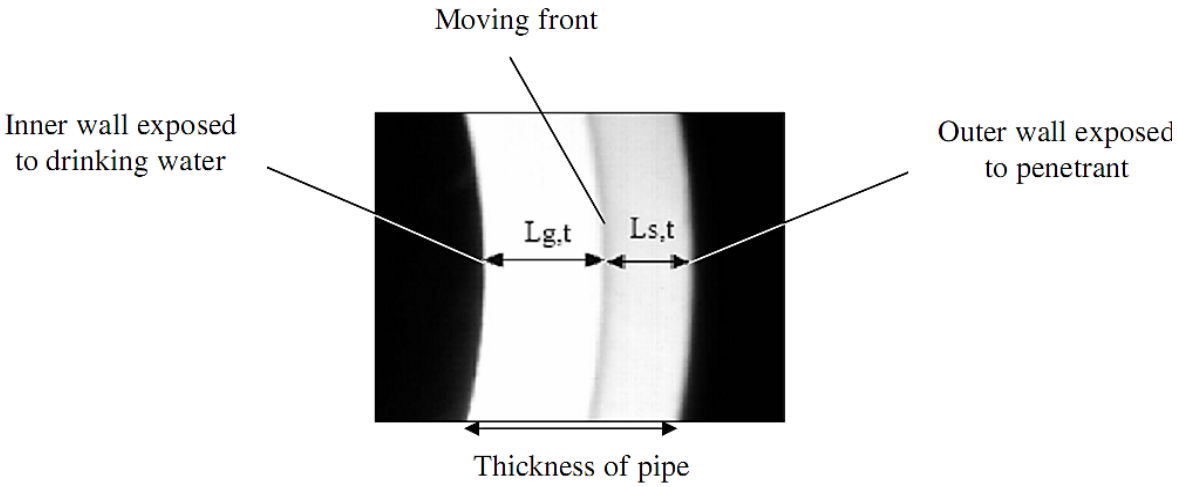

Figure A10: Cross section of pipe showing moving front (Mao, 2008).

The test conditions were identical to those described above in the Gravimetric Sorption experiments. At different exposure times, a pipe specimen was removed from the exposure media (vapors or aqueous solutions) and wiped dry. Each dried specimen was firstly cut parallel to the longitudinal axis and then cut across the longitudinal axis of the pipe specimen. The specimen cross section is observed under a reflected light microscope and its precise image is captured by a camera mounted on the microscope. With PC-Image software package, the penetration distance of the moving front was precisely measured. Finally, similar to Gravimetric Sorption Test, by drawing thickness of swollen layer against square root of time the sorption coefficient was calculated (Mao, 2008; Mao et al., 2009).

Figure A11 shows the results of measurement of moving front for pipe specimens exposed to organic vapors that were in equilibrium with benzene or toluene solvents. The activities of benzene and toluene inorganic vapors were identical to those calculated using the gravimetric tests. Similar to the observations from the gravimetric tests, the penetration data followed Fickian kinetics (linear with square root of time) with a time lag at the initial period (Mao et al., 2009). As observed in gravimetric sorption test results, the growth rates of the thickness of the swollen layer decreased sharply with decreasing benzene or toluene activity. Also, over a 2.5-day exposure, no moving front was detected for benzene at an activity of 0.55 or for toluene at an activity of 0.51 (the corresponding volumetric percent in the reference fuel was 40%).

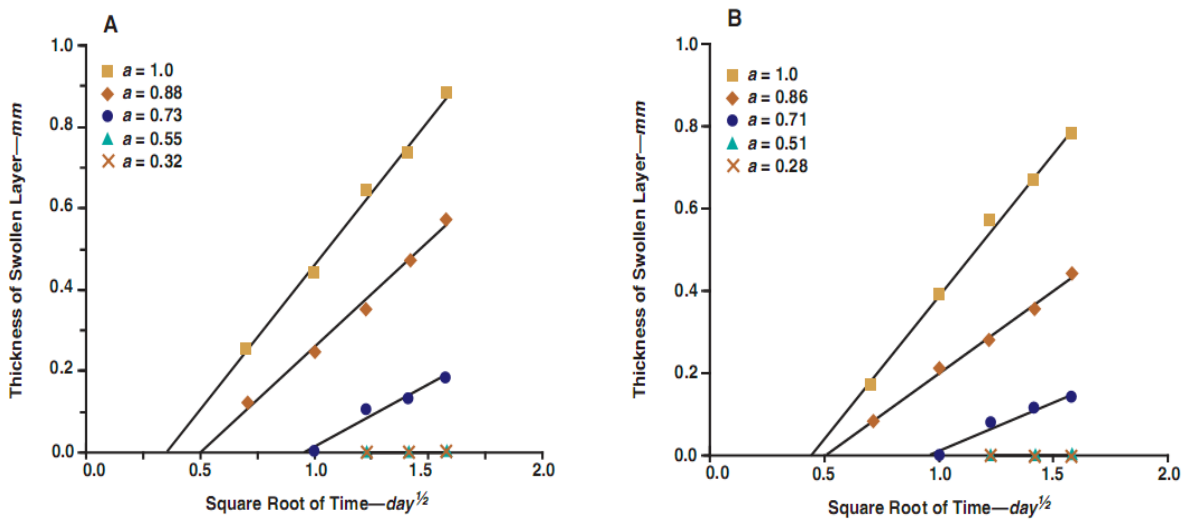

Figure A11: Growth of thickness of swollen layer in 1-in PVC pipe exposed to benzene (A) or toluene (B) vapor (Mao et al., 2009).

A.1.4. Effect of contaminants on PE pipes

Polyethylene (PE) pipes are the second most commonly used polymer pipes in North America and has been installed since the 1950s (Davis et al., 2007; Whelton and Nguyen, 2013). There are many types of PE pipe that differ in chemical composition and operating conditions, but these materials have historically been generically classified as PE (Whelton and Nguyen, 2013). All PE pipes are manufactured from PE resins of different densities, crystallinities, and T_g values and can be classified into three different categories: low-density (LDPE; $0.910 < \rho < 0.925$, Tg = –4 ºF), medium-density (MDPE; 0.926 g/cm3 $< \rho <$ 0.940 g/cm3, T_g = –94 ºF), and high-density (HDPE; $\rho \geq 0.941$, T_g = –220 ºC) (PPI, 2009; Whelton and Nguyen, 2013). In the United States, HDPE pipes with diameter up to 62" have been used for buried water transport (AWWA, 1999; Whelton and Nguyen, 2013). PE pipes are widely used in water service line connections and, to a lesser extent, water mains (CPCCPP, 2003; Mao et al., 2010).

Previous lab and field studies have shown strong evidences that organic contaminants permeate PE pipes of water distribution systems and adversely affect the quality of drinking water in water distribution systems (Holsen et al., 1991a; Mao et al., 2010; Thompson and Jenkins, 1987). As can be observed in Figure A1, PE pipes do not perform well in contaminated areas and 39% of contamination incidents involved PE pipes (EPA, 2002; Holsen et al., 1991a; Thompson and Jenkins, 1987). Moreover, Holsen et al. (1991a), reported that contamination by aromatics and chlorinated solvents in drinking water as a result of permeation through PE pipes were more noticeable especially after a period of water stagnation in the pipe.

The permeability of organic compounds through PE pipes would be connected with the physical characteristics of PE material (Mao et al., 2010). PE is a semi-crystalline polymer, having both crystalline and amorphous regions (Mao et al., 2010). The crystalline zones act as impermeable barriers against diffusion, while the non-crystalline matrix (amorphous regions) is readily permeable since the polymeric chains in the amorphous areas are relatively mobile (Mao et al., 2010; Naylor, 1989; Vonk, 1985).

Mao et al. (2010), performed a research study on quantifying the permeation rate of BTEX compounds that exist in commercial gasoline into HDPE pipes using pipe-bottle test in which three different types of soil were utilized. The tests were conducted in a 1 L glass jar by using three different soils with various amounts of organic matter (two values). The soil types included silica sand (with no organic matter), silica sand-topsoil mixture, and organic topsoil. Soils with different organic matter contents were used since Holsen et al. (1991b), showed that PB pipes buried in high organic soils showed slower permeation than those buried in low organic soils.

In the first testing protocol three diluted aqueous solutions of varying concentrations, 50%, 10%, and 1% of solubility of gasoline in water, were obtained by diluting the gasoline aqueous solution at its solubility limit with deionized water (Mao et al., 2010). The BTEX concentrations in the four aqueous solutions typically reflected the concentration range of BTEX found in groundwater associated with gasoline spills and leaks (Mao et al., 2010). For each experiment, the pipe-bottle apparatuses were filled with silica sand until the bottle was nearly full. Afterwards, aqueous gasoline solution was introduced to the soil through pump and tube from bottom to top until the bottle was full. BTEX concentrations in the soil pore water were periodically measured.

Figure A12 depicts the results of the experiments. In Figure A12, among BTEX compounds, benzene was the first to be detected in the pipe water, mainly because of the high concentration of benzene in the simulated groundwater (aqueous solution) and its relatively smaller molecular diameter (Mao et al., 2010). Moreover, it is worthy of note that the level of benzene in the pipe water quickly exceeded the Maximum Concentration Level (MCL) of 5 μg/L as breakthrough occurred. The breakthrough of toluene was slightly behind that of benzene, whereas ethylbenzene and xylene were detected later and at much lower concentrations. Given the relatively high MCLs for toluene (1,000 μg/L) and ethylbenzene (700 μg/L), it took significant exposure times for the pipe water concentrations of these compounds to exceed the MCLs after breakthrough time (Berens, 1985; Mao et al., 2010). Moreover, owing to the extremely high MCL for xylene (10,000 μg/L), its MCL was not exceeded within an experimental period of 140 days. Also, it can be inferred from Figure A12 that breakthrough time increased with lower BTEX groundwater contamination, implying that higher hydrocarbon concentrations in groundwater would lead to earlier breakthrough time.

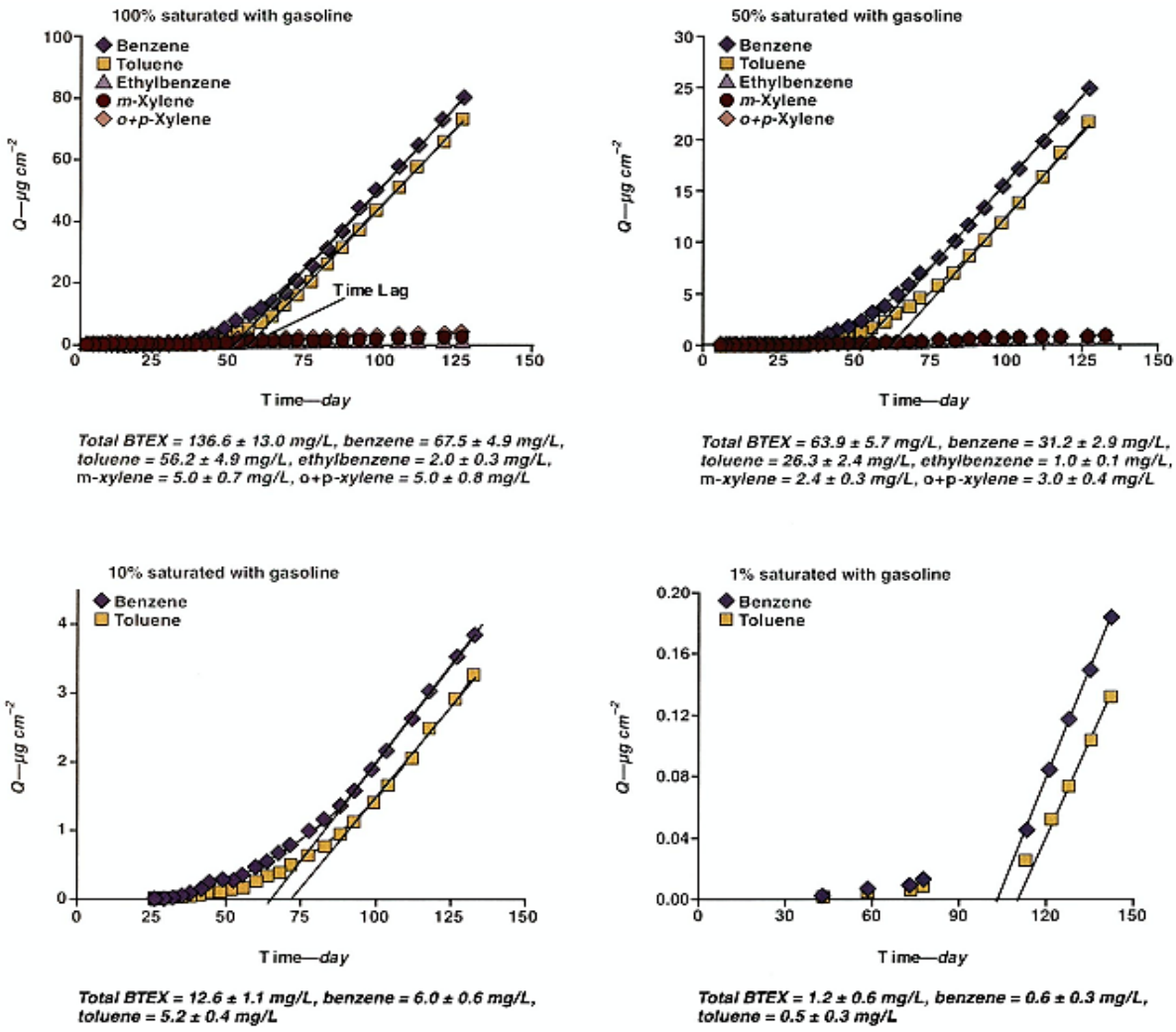

Figure A12: Cumulative mass permeated per unit surface area (Q) for BTEX compounds in 1-in SIDR 9 HDPE pipes exposed to four concentrations of gasoline-contaminated water (Mao et al., 2010).

In the second testing procedure, four levels of gasoline-contaminated soil were prepared by spiking 1 kg sand-topsoil mixture with known amounts of premium gasoline (to reach the total BTEX of 32, 89, 388, and 1,216 mg/kg dry soil) and mixing the soil by rotating the soil container for one week. The volumetric moisture content of the soil was adjusted to approximately 10%. Through this experiment, water inside the pipes was drained for BTEX analysis. The results are shown in Figure A13 where Toluene and Xylenes were the major compounds detected in the pipe water, whereas the permeation of benzene through pipes was insignificant (Mao et al., 2010). One possible reason for the behavior of benzene is its relatively low concentration remaining in the soils. This low concentration in the soils is attributable to benzene's high volatility, which gives it the lowest soil sorption affinity among the BTEX compounds (Mao et al., 2010; Zytner, 1994). In

gasoline-contaminated groundwater, however, a relatively high concentration of benzene is generally detected because of its high solubility in water (Cline, 1991).

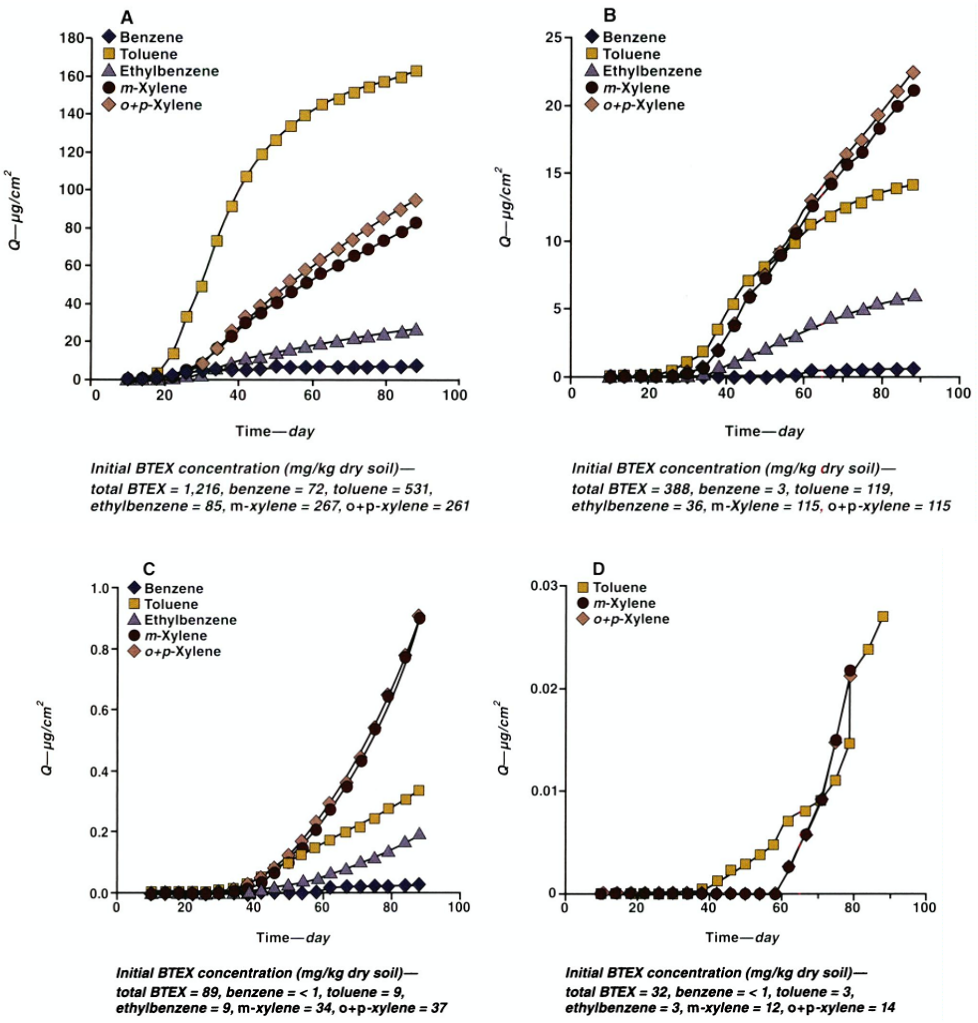

Figure A13: Cumulative mass permeated per unit surface area (Q) for BTEX compounds in 1-in SIDR 9 HDPE pipes exposed to four concentrations of gasoline in unsaturated soils (Mao et al., 2010).

The last test protocol used by Mao et al. (2010), was determining the effect of soil organic matter on the diffusion rate of BTEX into the PE pipes (Figure A14). In addition to the adopted procedure, the changes in concentration of BTEX in the soil-pore water were measured to assess the sorption of BTEX into the soil organic matter (Figure A15). For this protocol pipe-bottle test was considered. The soils were initially soaked with aqueous gasoline solution at its solubility. The experimental procedures were the same as described in simulated groundwater experiments

except that the soils and aqueous solutions were not replenished. Soil-pore water and pipe water were collected periodically, and the BTEX concentrations were quantified.

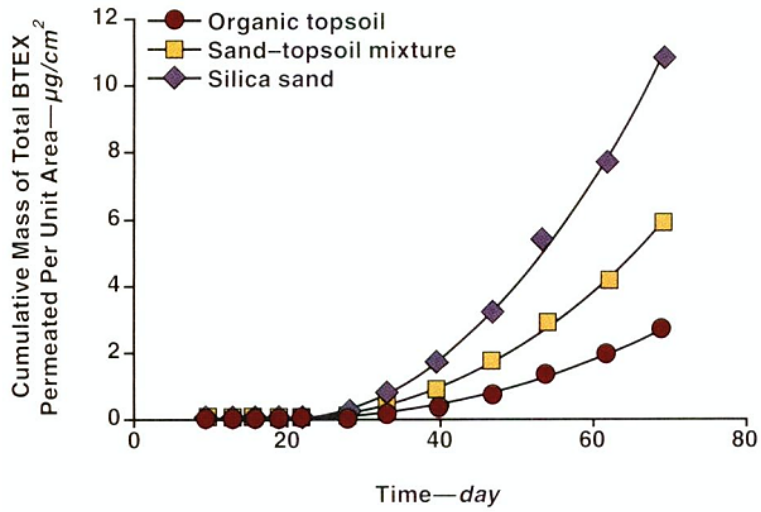

Figure A14: Cumulative mass of total BTEX permeated per unit area versus exposure time (Mao et al., 2010).

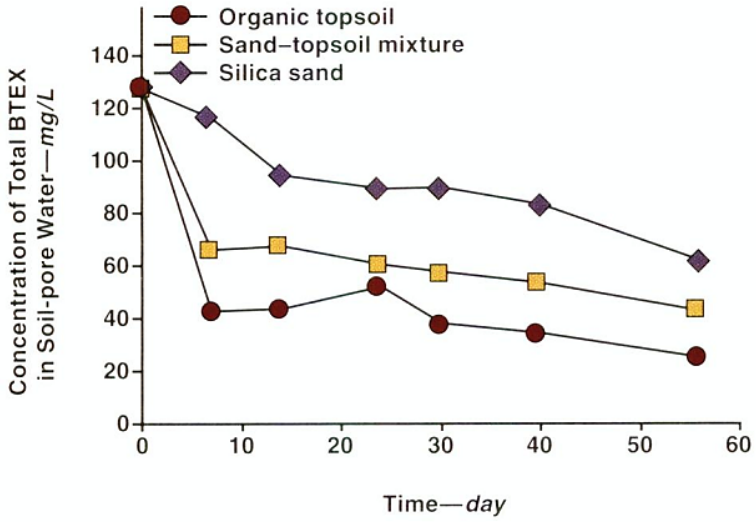

Figure A15: Concentration of total BTEX in soil pore water versus exposure time (Mao et al., 2010).

As seen in Figure A14, the breakthrough times of BTEX (i.e., benzene as it has the fastest diffusion rate among BTEX compounds), for silica sand, sand-topsoil mixture, and organic topsoil

were 13, 16, and, 19 days, respectively. After two months of exposure, the cumulative mass of BTEX permeated per unit area through the pipe buried in silica sand was nearly twice that of the sand-topsoil mixture and four times that of organic topsoil (Mao et al., 2010). However, high soil organic matter cannot be relied on to protect pipes from permeation because such soils eventually will reach their maximum adsorption capacities under field conditions. The effects of soil organic matter on permeation found in this study were consistent with results of research on the permeation of organic contaminants through PB pipes (Holsen et al., 1991b; Mao et al., 2010).

In Figure A15, as the content of organic matter of the soil increases, the sorption of BTEX into the soil organic matter increases. BTEX in the soil pore water, for the soils incorporating organic matter (i.e., organic topsoil and sand-topsoil mixture), decreases dramatically within the first week (mainly because of sorption to the soil) and then decreases slowly (mainly due to sorption/diffusion into the pipe and volatilization losses) (Mao et al., 2010). Therefore, the higher organic matter in the organic topsoil results in a greater soil uptake of BTEX and a significant decrease of BTEX concentrations in the soil-pore water (Kyle, 1981; Mao et al., 2010).

A.1.5. Cement-based pipes

A.1.5.1. Asbestos-cement pipes

As can be seen in Table A1, in general, jointed and unjointed asbestos/cement pipes shows fastest permeation of contaminants (i.e., toluene and TCE) which could be attributed to the high porosity of this type of pipe compared to the others. In other words, this type of pipe exhibited the lowest resistance against permeation of contaminants.

A.1.5.2. Effect of hydrocarbon contamination on concrete properties

There are many brownfield sites that are contaminated with hydrocarbons. The most common types of site and associated contaminants are summarized in Table A2 (Wilson et al., 2001). All these contaminants are complex mixtures of separate organic chemicals.

Table A2: Sources of hydrocarbon contamination in brownfield areas (Wilson et al., 2001).

Use	Typical contaminants
Filling stations	Petrol, diesel
Garages	Petrol, diesel and lubricating oil
Oil storage sites	Petrol, diesel, heavy fuel oil, and lubricating oil
Timber yards and wharves	Creosote, diesel, and fuel oil

With regard to the influence of chemical constituents of mineral oils (hydrocarbons) on the mechanical properties of concrete, Lea (1970), indicated that the effects on hardened concrete were not significant since oils do not contain any constituents that react chemically with hardened concrete. However, Biczok (1964) and Lea (1970), suggested that phenols, creosols and similar acidic compounds in creosote may have some detrimental effect on the mechanical properties of hardened concrete (Wilson et al., 2001). Orchard reported that creosote causes mild deterioration of hardened concrete (Orchard, 1971; Wilson et al., 2001). Other researchers reported that petroleum oils and coal-tar distillates had no or very slight effect on hardened concrete strength and durability (Dobrowolski, 1998; Murdock and Blackledge, 1968; Wilson et al., 2001). Indeed coal-tar paints and pitches are used as protective coatings for concrete to prevent deterioration by other compounds (Wilson et al., 2001). Pye and Harrison (1997), stated that Portland cement concrete surfaces have a good chemical resistance against mineral oil and organic solvents.

Lea (1970) reported severe degradation of the concrete of a garage floor that was exposed to lubricating oils for 20 years and was saturated with oil. Nonetheless, this issue may have been due to mechanical degradation rather than chemical processes (Wilson et al., 2001). Therefore, as mentioned, generally hydrocarbons do not adversely affect the long-term durability of hardened concrete, except for creosote and similar acidic hydrocarbons (Wilson et al., 2001).

Wilson et al. (2001), performed a study investigating the effect of different sources of hydrocarbon-based contamination (creosote, diesel fuel, and lubricating oil) on compressive strength of concrete cubic specimens at 7, 14, 28, and 84 days. Concrete cubes were demolded after 24 hours after casting and then placed into the selected contaminants inside PE bags (as a curing medium) in order to reproduce similar condition to concrete that is cured in the ground in contact with contaminants (Wilson et al., 2001). The solid (mass of concrete specimens) to liquid (contaminant) ratio was considered 1:1 by volume. The PE bags were placed in water bath maintained at a temperature of approximately 68 ^{o}F until specified testing ages. The results of the mentioned study are presented in Figure A16 and Table A3. The results indicate that creosote had the most detrimental effect on concrete strength which caused 20% strength reduction at 84 days as compared to control mixture. This issue may be due to either chemical reactions occurring within the hydrating concrete or because of the presence of hydrocarbons surrounding the cubes preventing adequate curing (Wilson et al., 2001). Furthermore, the diesel had the least negative influence on compressive strength than other hydrocarbons.

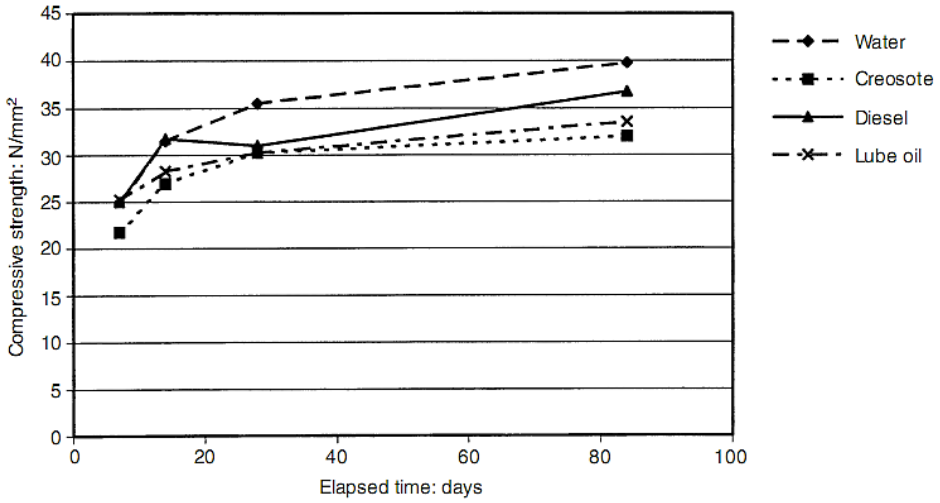

Figure A16: The effect of hydrocarbons on concrete strength gain (Wilson et al., 2001).

Table A3: Reduction in strength gain compared to water cured control specimen (Wilson et al., 2001).

Contaminant	Reduction in strength gain (%)			
	7 days	14 days	28 days	84 days
Water	0	0	0	0
Creosote	13	14	15	20
Diesel	0	0	13	8
Lubricating oil	0	10	15	16

A.1.6. Gasket materials

The most widely used gasket materials in the water distribution system are ethylene propylene diene monomer (EPDM), chloroprene rubber (CR; neoprene), styrene-butadiene rubber (SBR), nitrile rubber (NBR), and fluoroelastomer rubber (FKM) which would be selected depending on the contamination condition of installation sites of piping system (Cheng et al., 2012). SBR and CR gaskets typically are used for water distribution pipes whereas NBR and FKM gaskets are used for pipes conveying hydrocarbons and petroleum products or when hydrocarbon-resistant gaskets are required for water distribution (Cheng et al., 2012). About 90% of the gaskets used in water distribution pipes are SBR gaskets because of its low cost and good durability (Ong et al., 2008, Park et al., 1991).

According to a previous study, organic chemicals are approximately 5 to 100 times more permeable in gasket materials compared to PB pipe (Park et al., 1991). Therefore, considering permeability of gasket materials would be of great importance with regard to evaluating the resistance of pipe system against contamination. However, there are two reasons why most permeation events do not involve gaskets (EPA, 2002). First, the mass transfer area associated with gaskets is considerably smaller than that associated with pipelines (EPA, 2002; DWI0772, 1997). Second, gaskets are usually installed in areas where flow is continuous and flow velocities are high, which increases the dilution effectiveness (EPA, 2002; Holsen et al., 2991a).

Glaza and Park (1992) and Park et al. (1991), tested three gasket materials (SBR, NBR, and special NBR) and concluded that special NBR gaskets performed slightly better than standard NBR gaskets, whereas SBR gaskets were more vulnerable than NBR gaskets to gasoline permeation. Mao et al. (2011b) measured the performance of two types of gaskets utilized in PVC pipe joints (SBR and NBR) using sorption test. The testing procedure was followed by two different exposure mediums. In the first experiment, gasket rings (with nominal 2-in diameter) were immersed in 500 mL of the premium gasoline in a 1-L glass jar. The gaskets were removed at hourly intervals, wiped dry with paper towels, and weighed using an analytical balance. The specimens were returned to the jar immediately after weighing. The specimens were weighed until constant weight was reached (Mao et al., 2011b). In the other experimental procedure, the same measurement procedure was applied except for using gasoline aqueous solution at its solubility limit instead of pure gasoline. Figure A17 shows the results of these experiments. In pure gasoline, sorption equilibrium was rapidly achieved within 24 h for both types of gaskets. The equilibrium weight gains for SBR and NBR gaskets were $102.3 \pm 5.6\%$ and $77.6 \pm 1.1\%$ of their original mass, respectively (Mao et al., 2011b). Sorption of hydrocarbons by the gaskets in gasoline aqueous solution at its solubility limit was extremely slow compared to exposure to commercial gasoline. Moreover, none of the gaskets reached sorption (constant mass) equilibrium for the experimental period of nearly 80 days (Mao et al., 2011b).

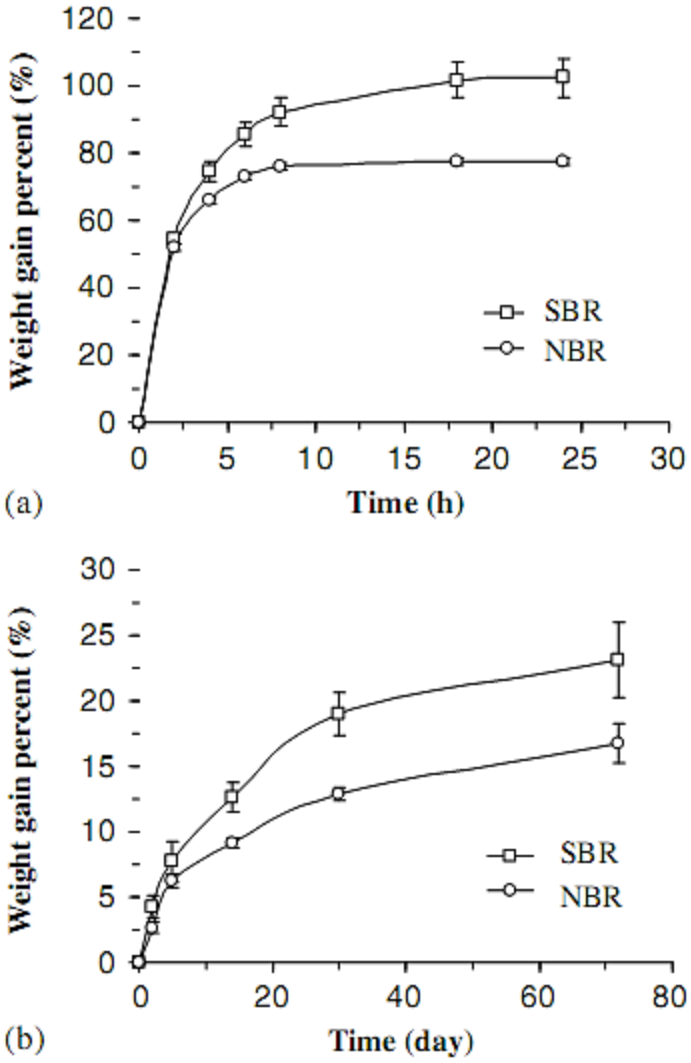

Figure A17: Results of sorption test for 2-in diameter SBR and NBR gaskets exposed to free-product gasoline (a) and gasoline aqueous solution at its solubility limit (b) (Mao et al., 2011b).

Furthermore, Cheng et al. conducted sorption test on five types of push-on gasket materials (including EPDM, CR, SBR, NBR, and FKM) used in Ductile Iron pipe joints (Cheng et al., 2012). To fulfill this issue, equilibrium sorption tests were carried out using the five gasket materials in premium commercial gasoline. The specimens were placed in 120-mL jars filled with gasoline and kept at room temperature. Specimens were periodically removed, wiped dry using a paper towel, weighed using an electronic balance, and then returned to the jars. Based on the attained results, EPDM gaskets had the highest sorption (127% weight gain) of premium gasoline compared to the other four gaskets. Also, FKM gaskets had the lowest sorption (about 0.65%) of gasoline, indicating the material's greater resistance to gasoline permeation than the other four gaskets.

A.1.7. Pipe joints

Gasket materials are installed in pipe connections to provide sealed joints which prevent water leakage. In addition, as described in section A.1.6, joint gaskets have a high intrinsic permeability than piping materials. Accordingly, the permeability characteristic of pipe joints needs to be considered and determined.

Olson et al. (1987), showed that unjointed pipes showed better performance than jointed ones. Mao et al. (2011b) conducted Pipe-Drum test to monitor the ability of gasketed PVC pipes to resist water contaminants permeation. They adopted two types of gasket materials (SBR and NBR) used in Rieber gasket system. In the United States and Canada, the most common PVC pipe joint is the Rieber joint system, in which the gasket is integrated into the pipe bell during the manufacturing and belling process (Figure A18) (Mao et al., 2011b). This gasket system has been fully adopted by the PVC pipe industry in the United States and Canada owing to its many advantages such as high resistance to water infiltration and exfiltration, high internal pressure and vacuum properties, and allowable leakage limits when axial joint deflection takes place (Mao et al., 2011b; Rahman and Alchin, 2005).

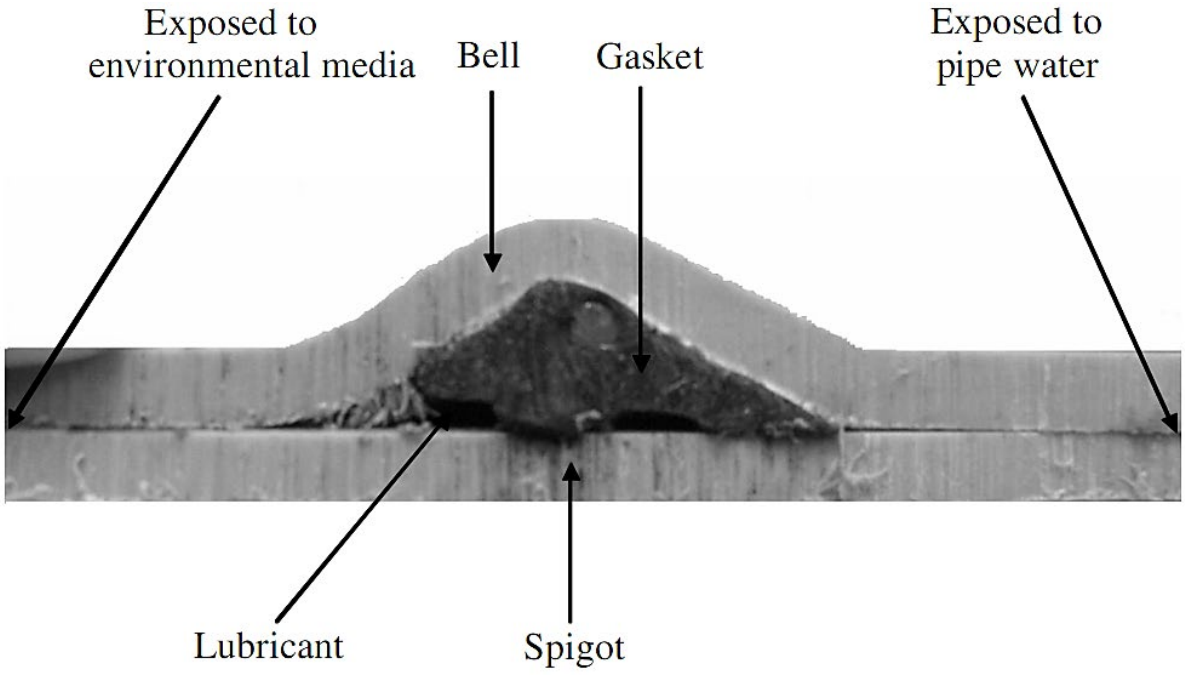

Figure A18: Cross section of PVC pipe joint with SBR Rieber gasket (Mao et al., 2011b).

In Mao et al.'s work (2011b), pipe-drum tests were performed on the nominal 2-in diameter PVC pipes with gasketed joints by SBR and NBR gasket materials. To simulate a buried pipe in contaminated soils, 20-L steel drums with the PVC pipe joints mounted vertically were developed as shown schematically in Figure A19. Pipes were filled with deionized water from bottom to top, and samples were collected by draining under gravitational force. Eight pipe-drum apparatuses with gasoline as the contaminant were setup: three pipe-drum apparatuses with PVC pipes equipped with SBR gaskets (triplicate experiment), three pipe-drum apparatuses with PVC pipes equipped with NBR gaskets (triplicate experiment), and two pipe-drum apparatuses with straight PVC pipes as controls. Two testing procedures were adopted. In the first testing protocol, pure commercial gasoline was added to the drum filled with sand until a visible liquid level of gasoline appeared above the surface of the sand and the exposure of PVC pipes with gasketed joint to pure gasoline was evaluated (Mao et al., 2011b). In the second procedure, jointed PVC pipes were exposed to four different aqueous solutions of varying concentrations (100%, 75%, 50%, and 10%) in the pipe-drum test.

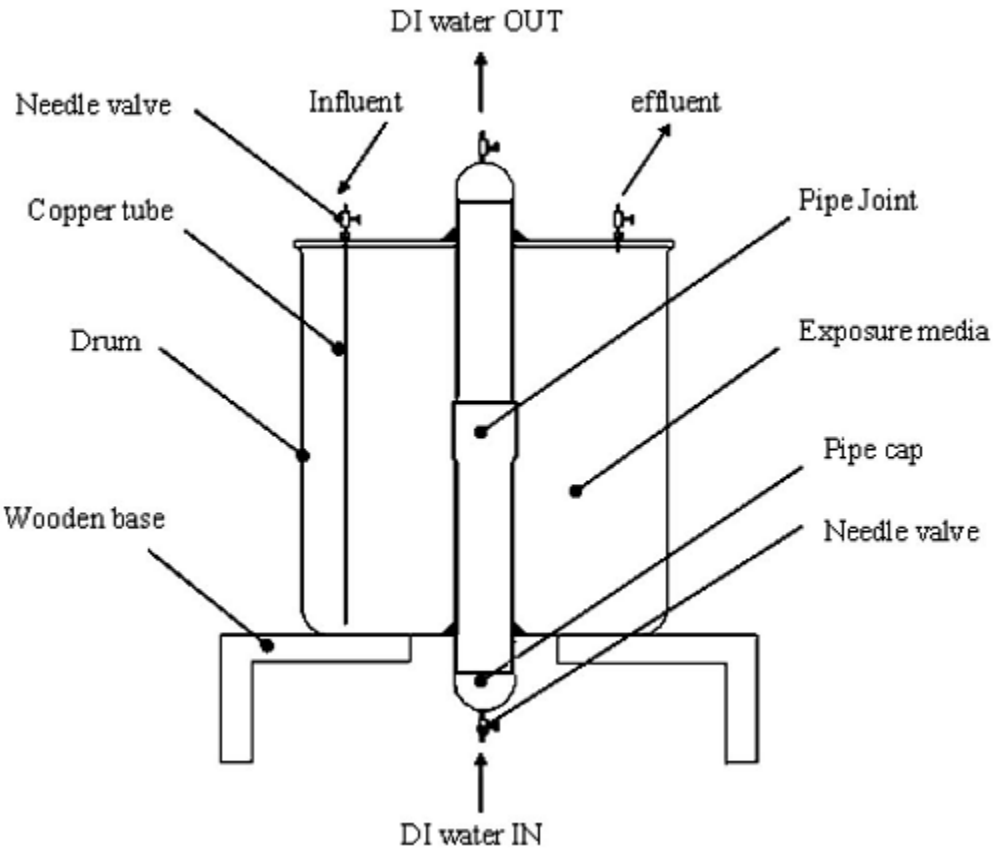

Figure A19: Pipe-drum apparatus (Mao et al., 2011b).

Figures A20 and A21 show the results of pipe-drum test conducted on gasketed PVC pipes equipped with SBR and NBR gaskets, respectively (Mao et al., 2011b). According to Figures A20 and A21, no BTEX compounds were detected in the pipe water of the straight (ungasketed) PVC pipe after nearly 4 months of exposure (Figure A20a). This is mainly because BTEX concentrations in the commercial gasoline were not sufficiently high to soften the glassy PVC materials and thus inhibit the permeation of BTEX compounds (Mao et al., 2011a; Mao et al., 2011b). In contrast, PVC pipes with SBR and NBR gaskets were rapidly and significantly permeated by BTEX compounds when exposed to premium gasoline. This observation generally indicates that gasoline permeation incidents related to PVC pipelines were mainly attributed to the permeation of gasoline through gasket materials or inflow through broken pipes, rather than permeation through the intact pipe materials (Mao et al., 2011b). For SBR gasketed PVC pipes, the steady-state permeation rates for benzene, toluene, ethylbenzene, m-xylene, and o+p-xylene were found to be 0.73 ± 0.29, 0.95 ± 0.44, 0.04 ± 0.02, 0.1 ± 0.05, and 0.1 ± 0.05 mg/joint/day, respectively.

Based on the gathered data for PVC jointed with SBR gaskets (Figure A20), when breakthrough occurred, the concentration of benzene in the pipe water immediately exceeded the MCL of 5 µg/L. Toluene breakthrough lagged slightly behind that of benzene, whereas ethylbenzene and xylene were detected later at approximately 50 days and at much lower concentrations. benzene and toluene accounted for 85-90% of the total BTEX that permeated into the pipe water. It should be noted that similar permeation behavior for BTEX (i.e., the order of breakthrough time and the relative permeation rate) was found for the permeation of premium gasoline in PE and ductile iron pipes joints (Glaza and Park, 1992; Mao et al., 2010; Mao et al., 2011b; Ong et al., 2008).

The permeation rates for NBR gaskets were relatively lower than that for SBR gaskets. It is worth mentioning that these NBR results were different from the results for ductile iron (DI) pipes with NBR gaskets where the NBR gaskets were found to be much more resistant to gasoline permeation than SBR gaskets (Mao et al., 2011b; Ong et al., 2008). This issue may be because NBR materials for PVC pipes and ductile iron pipes were not identical in their composition or their permeation properties (Mao et al., 2011b).

Finally, according to the results obtained for exposure of gasketed PVC pipes to aqueous solutions of gasoline with four different concentrations, no significant amounts of BTEX compounds were detected in the pipe water for pipes using either SBR or NBR Rieber gaskets after 9 months of exposure to any level of gasoline contamination in water, even at its solubility limit (Mao et al., 2011b).

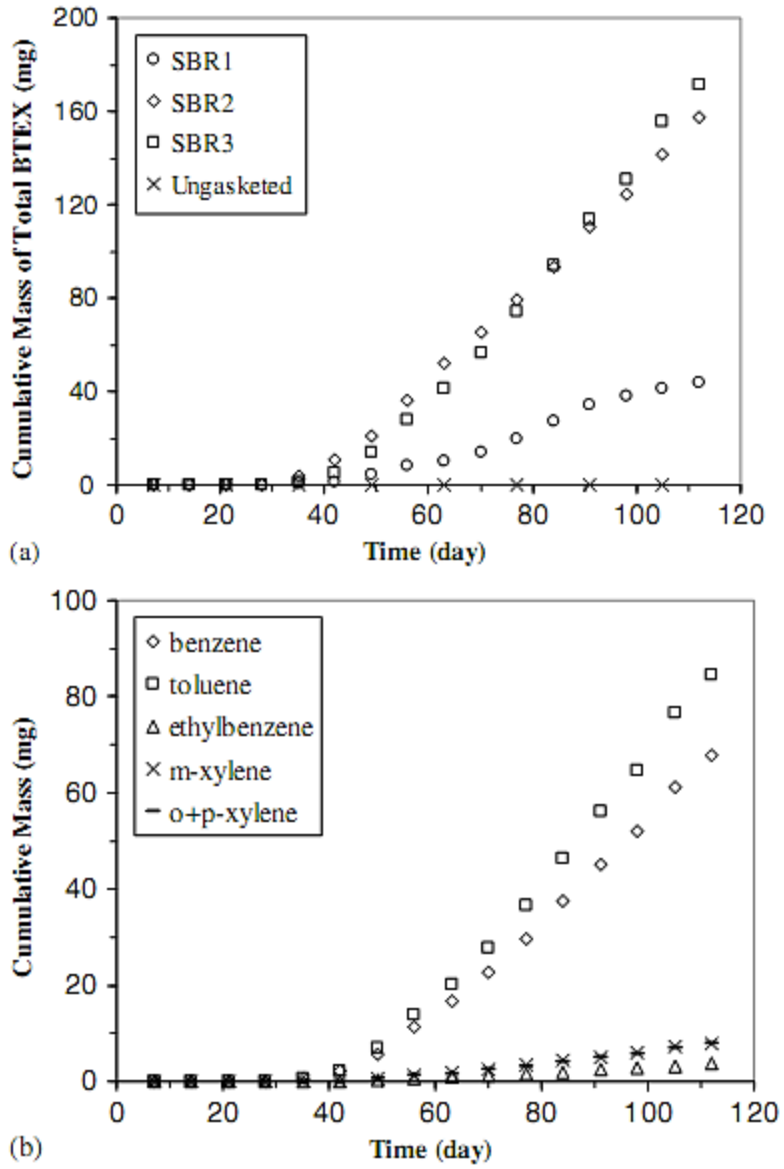

Figure A20: Cumulative mass of BTEX compounds permeated per joint in PVC pipes with SBR gaskets exposed to premium gasoline (Mao et al., 2011b).

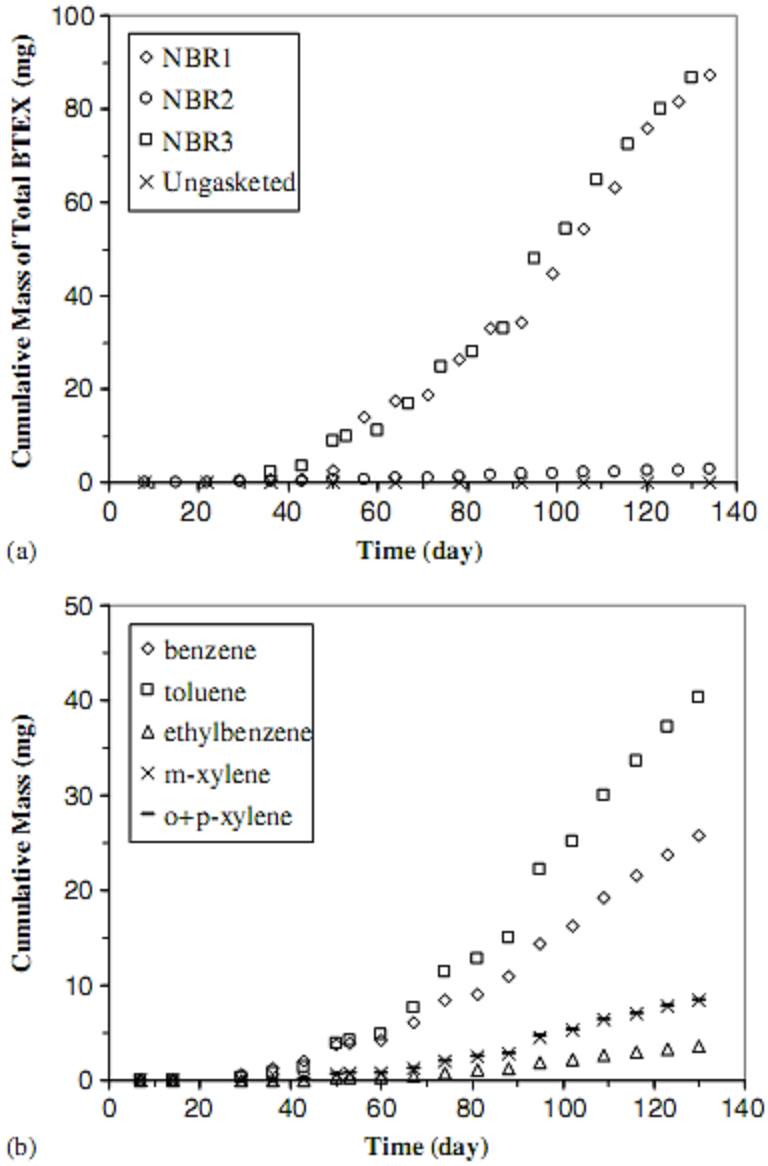

Figure A21: Cumulative mass of BTEX compounds permeated per joint in PVC pipes with NBR gaskets exposed to premium gasoline (Mao et al., 2011b).

A.2. Soil contamination in the saturated condition

The numerical groundwater flow model MODFLOW and associated contaminant transport module MT3D are commonly used for modeling subsurface hydraulic head distribution and movement of contamination plumes. MODFLOW is a three-dimensional model, initially developed by the United States Geological Survey (USGS) (McDonald and Harbaugh, 1988). The program utilizes the finite difference approach for simulating and predicting groundwater flow and the impact of various source/sink configurations on the head distribution.

The modular three-dimensional transport model (MT3D) was initially developed by Zheng (1990). Mass-Transport 3D Multi-species (MT3DMS) is a most recent version of the MT3D model and has a broad set of options and abilities to simulate dispersion/ diffusion, advection, and chemical reactions of contaminants in groundwater flow systems under general hydrogeological conditions. Visual MODFLOW Flex is a graphical interface for MODFLOW, and it is used to simulate groundwater flow and contaminant transport, whereby combining MODFLOW-2000-2005 with MT3DMS.

Saghravani et al. (2011) modeled the groundwater flow and the migration of phosphorus in groundwater by using Visual MODFLOW for 10 and 50 years in Malaysia. Their study was focused on the determination of phosphorus contaminants in different zones of groundwater as well as a demonstration of contaminant transport in the aquifer. Islam et al. (1998) developed a 3-D numerical model for groundwater flow and contaminant transport for the town of Ogallala, Nebraska, by using MODFLOW coupled with MT3D. They simulated an aquifer that was contaminated with Perchloroethylene (PCE), trichloroethylene (TCE) and carbon tetrachloride (CCl4) and the simulation findings suggested that clean up time via using the pump and treat technology for TCE, PCE, and CCl4 was 15, 10, and 10 years, respectively.

He et al. (2009) conducted a 3-D MODFLOW model coupled with MT3D to predict groundwater contamination caused by oil pipe leakage that started from Rizhao to Chuzhou in China. The results showed that the generated contaminant from oil pipeline leakage is transported mainly along the direction of the groundwater flow (i.e., advection process). Dhaka et al. (2016) studied groundwater contamination of area located in Delhi, India, via using Visual MODFLOW Flex interface. Similar to He et al. (2009) findings, the results of the model showed that the groundwater contamination movement is dominated by the advection mechanism, and the direction of the plume transport depends on the differential hydraulic head conditions.

Lautz and Siegel (2006) modeled mixing surface and groundwater and solute transport by using a 3-D MODFLOW paired with MT3D, to simulate hydro-chemically active hyporheic zone (beneath and alongside a streambed) around debris dams for Red Canyon Creek, Wyoming, US. The findings of the study indicated that the movement of surface water into the hyporheic zone is predominantly an advective process. Ghoraba et al. (2013) modeled groundwater flow and

contaminant transport movement for quaternary aquifer in the central part of the Nile Delta, Egypt. The results showed that the Ammonium concentration of groundwater exceeded the drinking water standard. The results from the study suggested a cleanup approach whereby a dewatering system through eight extraction wells is used to pump the contaminated groundwater out of the aquifer. The eight extraction wells' locations were chosen to be toward the flow direction since the movement of contamination was governed by the advection mechanism for this area.

A.3. Soil contamination in unsaturated condition

Leakage from permanently closed or, in service, underground storage tanks (UST), leakage from pipelines or disposal by factories in US and other countries poses serious contamination threat to the vadose zone and subsurface utilities. The volatile organic compounds (VOCs) such as hydrocarbon fuels (gasoline, diesel, BTEX), or Trichloroethene (TCE) can migrate through unsaturated profile break through subsurface utilities such as culvert and water/drainage pipes, and therefore contaminate surface and groundwater. In the unsaturated zone, transport of the contaminant can occur as solutes in the water (or aqueous phase), vapors in the air phase, and as unaltered constituents in the oil (immiscible phase or NAPL phase). Work presented herein is focused on the potential transport of benzene as VOC with high vapor pressure through unsaturated zone into the subsurface concrete utility pipes with polymeric gaskets.

To allow robust prediction of VOC effects on utilities, also suggest an appropriate technique to face the problem and attenuate the contamination, an integrated understanding of governing processes is required.

Mechanisms of interphase mass transfer include evaporation of the NAPL and dissolution into the liquid water phase, and equilibrium partitioning of the organic chemical between the gas, water, and solid phases (Falta et al., 1992). In some scenarios, it is possible for vapor transport, rather than the slowly percolating dissolved-phase plume, to be largely responsible for VOC transport to the underlying layers (Wealthall, Rivett and Dearden, 2010).

The transport of contaminants in the gas phase may occur due to both advection and diffusion and is influenced by phase partitioning into the water and solid phases. In a field investigation by Hinchee and Reisinger (1985), lateral diffusive transport in unsaturated zone was suggested as a main mechanism for hydrocarbon contamination of soil and groundwater some distance away from a leaking gasoline storage tank (Baehr, 1987). Through partition into water and air phases, the vapors can migrate into the subsurface utilities and to aquifer with the potential of transport over large horizontal distances. Small concentrations of petroleum products render groundwater unfit for domestic use (Baehr, 1987).

The past studies can be categorized into two groups;

i) Literature on governing equations and parameters and ii) Literature on different scenarios of contaminant migration in real life.

i) Several studies have been done to develop the models describing simultaneous transport of a chemical contaminant in three physical forms; as a nonaqueous phase, as an aqueous phase, and a gas phase. (Jury et al., 1983; Abriola and Pinder, 1985; Corapcioglu and Baehr, 1987; Sleep and Skyes 1989; Falta et al., 1989). Equations which describe this complex system are derived from basic conservation of mass principles by the incorporation of various constitutive relations and approximations. Effects of matrix and fluid compressibilities, gravity, phase composition, interphase mass exchange, capillarity, diffusion, and dispersion are all considered. One of the

necessary equations describing the three-phase flow in system is relative permeability-saturation-pressure (K-S-P) functional relationships. Parker et al. (1987) developed a parametric model to demonstrate K-S-P relationships in two- or three-fluid phase flow in porous media systems subject to monotonic saturation paths. Due to complexity in the manner in which three fluids may interact in a porous medium and the difficulty of directly measuring fluid pressures and saturations simultaneously in three-phase systems, so in practice, three-phase behavior is commonly estimated from two-phase measurements. The two-phase system is described by three porous medium-specific parameters (α, n, S_r) and a fluid pair-dependent scaling factor (β) and for three-phase saturation-pressure relations involve five parameters (α_{aw}, α_{ao}, α_{ow}, n, S_m). In another work they obtained scaling factors for four organic liquids (benzene, o-xylene, p-cymene, benzyl alcohol) in a sandy porous medium (Parker et al. 1987). Oostrom and Lenhard (1996) evaluated the predictions from commonly used constitutive relations for multi fluid flow by comparing the results of numerical simulations by STOMP and experimental data on a uniform sand. The results show LNAPL moves faster downward when predicted by the Van Genuchten models compared to the Brooks-Corey/Burdine (BCB) model. Mathematical models of NAPL movement in three-phase porous media consisting of water-oil-air, commonly assume nonhysteretic permeability-saturation-capillary pressure (k-S-P) relationships. Some studies described hysteresis including air and oil phase occlusion or "entrapment" during imbibition and considered effects of pore blockage by air trapped in water and oil phases and oil trapped in the water phase and has shown significant effects on predictions of flow in two- or three-phase systems. (Parker and Lenhard, 1987; Kaluarachchi and Parker, 1992; Van Geel et al, 1994).

ii) The other group have addressed different scenarios related to contaminant migration in real life.

Dafny (2017) studied migration and longevity of Trichloroethene (TCE) through a sandy unsaturated zone under episodic NAPL releases from a metal planting factory sewer system by using Petrasim2016 graphical user interface and assessed the effect of episodic NAPL releases, vadose zone depth and surface condition (land cover) on NAPL partitioning in the domain and loading to the groundwater. The results show the NAPL was depleted within a few years while partitioning into the aqueous and gaseous phases and in total, 1-3% of released TCE reached the groundwater. Considering land cover TCE reached groundwater in higher mass for bare case compared to the sealed and roofed cases (bare (recharge and emission to atm)>sealed>roofed (just atm)) and so it was shown the atmosphere layer has the most important impact on the VOC evolution in the subsurface so that in case of roofed conditions maximal TCE (Aq) loads to the groundwater are lower by an order of magnitude in compared to those simulated for the respective sealed cases. Interception of recharge seems to have minor impact on the pollution partitioning but it has significant effect on the TCE loading to groundwater during the disposal period. The vadose zone thickness has secondary effect on dissolved loading to the groundwater and the thinner the vadose zone is, the higher total mass of pollution transports to the water table. The fluctuation of the source load or pulses are completely attenuated in the unsaturated zone and the only observed fluctuations in TCE load to the groundwater occurs when recharge is applied.

Yang et al. (2012) made numerical simulations using "NAPL" simulator to study benzene migration in an air-NAPL-water three phase system containing three soil layers; sand, sandy clay and sand layers under water table fluctuation. The laboratory column tests were used to extend saturation-Capillary pressure (S-P) relationships for field scale. To simulate water table fluctuation, the modeling process was divided into the steps and dynamic boundary conditions at left and right were used. The results showed benzene is trapped as a residual phase behind the flow path when falling and rising water table.

Rasmusson (2009) simulated a NAPL spill in a specific site in Israel and following pumping remediation using TMVOC code. The results from simulations of pumping with a static groundwater level and a fluctuating groundwater level showed great differences. The fluctuating groundwater level simulation resulted in a much smaller accumulated NAPL recovery volume than the static groundwater level simulation because of enhanced spreading of the NAPL over a larger region in case of fluctuation.

Joun W. et al. (2016) performed sand tank experiments and 2-D numerical modeling by STOMP to measure borehole TCE gas concentrations with different source distributions under water table fluctuation. The sources of the borehole TCE gases could be the residual TCE in the unsaturated zone or the dissolved TCE in the groundwater. The results showed when water table fell below a residual NAPL-phase TCE source or groundwater contaminated with dissolved TCE fell to form a lower water table, increases in borehole TCE gas were observed. When the water table was lowered, the NAPL-phase TCE source produced relatively higher and longer lasting borehole gas concentrations.

The influence of two factors; geological heterogeneity (variable log permeability standard deviations) and variability in water infiltration on LNAPL (TCE and toluene) migration in the unsaturated zone is investigated by Yang et al. (2013). Rainfall events can lead to considerable increase in water saturations in the soil near the ground surface over a short period. When water saturations are high in the upper part of the model domain at the time of the spill, a considerably smaller amount of NAPL infiltrates into the model. For example, an 8-h rainfall (15 mm/h) leads to 50 % reduction in total infiltrated mass, in comparison to the case with no preceding rainfall.

Sookhak-Lari et al. (2016), compared partitioning and fate of different gasoline components considering the effects of release depth and release duration.

So far, the contaminant migration in a vadose zone with subsurface utilities and different types of porous media have received rare attention in literature.

A.3.1. Governing equations

(Falta et al. 1992) developed a finite difference code for modeling of steam displacement of nonaqueous phase liquid (NAPL) contaminants in shallow subsurface systems. The code considers three flowing phases, gas, aqueous, and NAPL; and three mass components, air, water, and an organic chemical. Interphase mass transfer of the components between any of the phases is calculated by assuming local chemical equilibrium between the phases, and adsorption of the

chemical to the soil is included. Here is a summary of governing equations employed in T2VOC code developed by (Falta et al. 1995) that we are using for our simulations.

In a nonisothermal system containing three mass components, three mass balance equations and an energy balance equation are needed to fully describe the system as equation (A3):

$$\frac{d}{dt}\int_{V_l} M^K \, dV_l = \int_{T_l} F^K . \; n \, dT_l + \int_{V_l} q^K \, dV_l \quad \text{(A3)}$$

K: a: air; w: water; c: chemical; h: heat

Where M^K is the mass of component K per unit porous medium volume (for K=h, M^K is the amount of energy or heat) , F^K is the mass flux of component K into V_l (net flux), n is outward unit normal vector, q^K is rate of mass generation of component K per unit volume (source)

Mass accumulation terms:

The mass accumulation terms for air and water (K= a, w) are defined as follows:

$$M^K = \varphi \sum_\beta S_\beta \, \rho_\beta \, \omega_\beta^K, \beta\text{=gas, aqueous, NAPL} \quad \text{(A4)}$$

Where φ is porosity, S_β is the β phase saturation, ρ_β is the β phase density, and ω_β^K is the mass fraction of component K in phase β.

For NAPL (K= c) it includes linear equilibrium adsorption as equation (A5):

$$M^c = \varphi \sum_\beta S_\beta \, \rho_\beta \, \omega_\beta^C + \rho_b \rho_w \omega_w^C K_D \quad \text{(A5)}$$

Where ρ_b is the dry bulk density of the soil, ω_β^c is the mass fraction of the chemical in the aqueous phase, and K_D is the soil water distribution coefficient for the organic chemical (Freeze and Cherry, 1979).

$$C_s^c = \rho_b K_D \, C_w^c \;\; (kg/m^3) \;\; C_w^c = \rho_w \omega_w^C \quad \text{(A6)}$$

Where C_s^c is the adsorbed mass of chemical per unit volume of soil, and C_w^c is the chemical mass concentration in aqueous phase, and. Degree of adsorption of organic chemicals (C_s^c) depends largely on the amount of organic carbon present in the soil (foc), Koc is the Organic carbon partition coefficient.

$$K_D = K_{oc} \, f_{oc} \quad \text{(A7)}$$

Flux terms:

The three mass flux terms (air, water, chemical) sum over the three phases (gas, aqueous, NAPL) as equation (A8):

$$F^K = \sum_\beta F_\beta^K \quad \text{(kg/ (m}^2\text{.s))} \quad \text{(A8)}$$

The mass flux of each component in the water and NAPL phases are calculated by considering only advection as equation (A9) and (A10):

$$F_w^K = \frac{-k \, k_{rw} \rho_w}{\mu_w} \, \omega_w^K \, (\nabla P_w - \rho_w g) \quad \text{(A9)}$$

$$F_n^K = \frac{-k \, k_{rn} \rho_n}{\mu_n} \, \omega_n^K \, (\nabla P_n - \rho_n g) \quad \text{(A10)}$$

The mass flux of each component in the gas phase considers advection and diffusion:

$$F_g^K = \frac{-k \, k_{rg} \rho_g}{\mu_g} \, \omega_g^K \left(\nabla P_g - \rho_g g\right) + J_g^K \quad \text{(A11)}$$

Where k is the absolute permeability tensor, $k_{r\beta}$ is the β phase relative permeability, μ_β is the β phase dynamic viscosity, P_β is β phase pressure, g is the gravitational acceleration vector, and J_g^K is the diffusive mass flux of component K in the gas phase.

The diffusive Mass fluxes of water and organic chemical vapor J_g^w & J_g^C are calculated as follows:

$$J_g^K = -\varphi S_g \tau_g D_g^K \rho_g \nabla \omega_g^K \quad \left(\frac{kg}{m^2.s}\right) \quad , K = C, W \tag{A12}$$

Where Sg is gas saturation, ϕ is porosity, ρg is gas phase density and ω_g^K is the mass fraction of component K in gas phase, D_g^K is the molecular diffusion coefficient of component K in the gas phase and τ_g is the gas phase tortuosity calculated from equation (A13) as follows:

$$\tau_g = \varphi^{1/3} S_g^{7/3} \quad \text{(Millington and Quirk 1961)} \tag{A13}$$

With the water and chemical diffusive mass fluxes, the air diffusive mass flux, J_g^a is determined from equation (A14):

$$J_g^a + J_g^w + J_g^c = 0 \tag{A14}$$

The above equation ensures that the total gas phase diffusive mass flux summed over VOC, air and water is zero. Therefore, the total gas phase mass flux is the product of the gas phase Darcy velocity and the gas phase density.

The phase pressures are related to each other by capillary pressures as:

$$P_w = P_g - P_{cgw} \tag{A15}$$

$$P_n = P_g - P_{cgn} \tag{A16}$$

$$P_{cnw} = P_{cgw} - P_{cgn} = P_n - P_w \tag{A17}$$

Note, as our model works in isothermal condition, we didn't mention the formulation of heat transfer, for more details refer to (Falta et al. 1992).

In order to determine the thermodynamic state of four components (air, water, chemical and heat) so that the local thermal and chemical phase equilibrium is established, it is needed to choose four primary variables and in addition to four primary variables, a complete set of secondary variables is needed to solve four coupled balance equations. The secondary variables include thermodynamic and transport properties such as concentration, mole or mass fractions, relative permeabilities, capillary pressure, viscosities, densities, water and chemical molecular diffusivity, tortuosity and enthalpies. The four primary variables must be chosen so that the entire set of secondary variables may be calculated as functions of the primary variables (Falta et al. 1992)

Primary variables and variable substitution:

Primary variables applied as input for simulation are defined as follows; (S_w, S_g, P, T) for three-phase gas-water-NAPL, (S_w, X_g^c, P, T) for two-phase water-gas, (S_w,X_{aw} , P, T) for two-phase water-NAPL, (P, T, X_w^a, X_w^c) for single phase water.

X_{aw} is mass fraction of air in water, X_w^c is mole fraction of VOC (or chemical) in water and X_g^c is mole fraction of VOC in gas phase. The code uses the technique of primary variable substitution during phase transitions. For example in a three-phase system, when Sg+Sw≥1 NAPL

phase disappears the system alters to two-phase water-gas and primary variables are switched from (S_w, S_g, P, T) to (S_w, X_g^c, P, T). In such fashion, three-phase transforms to two-phase NAPL-water if Sg < 0, two-phase water-gas transforms to single-phase water when Sw>1, single-phase water to two-phase water-NAPL (or two-phase water-gas to three-phase) if $X_w^c > \bar{X}_w^c$ solubility limit at prevailing temperature, single-phase water to two-phase water-gas (or two-phase water-NAPL to three-phase) if Pg> P (hydrostatic+atm), (Falta et al. 1995).

Secondary Variables

The NAPL or VOC concentration as gas phase is a secondary variable that defined as a function of primary variables as follows:

$$C_g^C = \frac{P_g^C M_{wt}^C}{RT} \quad (\text{kg/m}^3) \qquad (C_g^C = \frac{m_g^c}{V_g}) \tag{A18}$$

Where M_{wt}^C is the molecular weight of chemical (g/mol), R is universal gas constant, T is temperature and P_g^C is partial pressure of chemical or VOC that is defined as below:

If NAPL phase is not present (two-phase water-gas):

$P_g^C = X_g^c P_g \quad P_g: gas\ phase\ pressure \quad X_g^c: chemical\ mole\ fraction\ in\ gas\ phase$

If NAPL is present the equation (A17) is used:

$$P_g^C = P_{sat}^C = P_{crit}\, exp\left(\frac{ax+bx^{1.5}+cx^3+dx^6}{1-x}\right) \quad , x = 1 - \frac{T}{T_{crit}} \tag{A19}$$

Where P_{sat}^C is saturated vapor pressure at given temperature, P_{crit} , T_{crit} are the critical pressure and critical temperature of organic compound that are constant values and a, b, c and d are empirically determined constants.

Also, concentration of other components water and air in gas phase are defined as follows:

$$C_g^w = \frac{P_g^w M_{wt}^w}{RT} , C_g^a = \frac{P_g^a M_{wt}^a}{RT} \tag{A20}$$

P_g^w: saturated vapor pressure of water at the local temperature (P_{sat}^w)

$$P_g^a = P_g - P_g^C - P_g^w \tag{A21}$$

$$\rho_g = C_g^a + C_g^w + C_g^C , \omega_g^c = \frac{C_g^c}{\rho_g} , \omega_g^a = \frac{C_g^a}{\rho_g} , \omega_g^w = \frac{C_g^w}{\rho_g} \tag{A22}$$

Under conditions of local chemical equilibrium, the concentration of a compound in a phase is related to the concentration in another phase by a constant. The code calculates the concentration of NAPL in gas phase at first and then determines the concentration of NAPL in aqueous phase by using local chemical equilibrium law. The equilibrium expression for the gas-liquid distribution of a dilute compound is known as Henry's law as:

$$P_g^K = H_{gw}^K X_W^K \quad K = a, c \tag{A23}$$

Where P_g^K is partial pressure of component K in the gas phase, X_W^K is the mole fraction of component in aqueous phase and H_{gw}^K is Henry's constant that may be determined by:

$$H_{gw}^C = \frac{P_{sat}^C}{\bar{X}_W^C} \ (pressure\ unit), : solubility\ (mole\ fraction) \tag{A24}$$

$\bar{X}_W^C$ is the solubility of chemical in water (mole fraction) and P_{sat}^C is the saturated vapor pressure of the chemical as a function of temperature.

Also, the Henry's law is defined in some literature (Baehr 1987) as equation (A25):

$$C_g = H\, C_w \ , H = \frac{C_g^0}{C_w^0} \quad \text{(A25)}$$

Where C_g^0 is saturated vapor concentration of chemical and C_w^0 is solubility of the chemical in water. If liquid VOC phase is present local equilibrium requires that $C_g = C_g^0$, $C_w = C_w^0$

Solubility and henry's constant are function of temperature.

The multicomponent diffusivities for water and chemical vapor in the gas phase are defined by equations (A24) and (A25).

$$D_g^w = (1 - X_g^w)/(\frac{X_g^a}{D_g^{aw}} + \frac{X_g^c}{D_g^{cw}}) \text{ and } D_g^c = (1 - X_g^c)/(\frac{X_g^w}{D_g^{cw}} + \frac{X_g^a}{D_g^{ac}}) \quad \text{(A26)}$$

D_g^K is the multicomponent molecular diffusion coefficient of component K in the gas phase and calculated by using binary diffusivity (air-water and air-chemical diffusivities) as below:

$$D_g^{ij} = D_g^{ijR}\ (P_R/P_g)\ (T/T_R\ )^{\theta_{ij}} \quad \text{(A27)}$$

D_g^{ijR} is the experimentally determined i-j binary diffusivity at a temperature T_R and a pressure of P_R (Reference binary diffusivity), and θ_{ij} is an experimentally determined constant. D_g^{cw} or water-chemical diffusivity is calculated using Wilke and Lee empirical correlation, (Reid et al. 1987).

Capillary pressures and Relative permeabilities

The code uses the relationships from Parker et al. (1987) for three-phase capillary functions,

In this work water retention curves are described by the Van Genuchten (1980) capillary pressure-saturation function extended by Parker et al. (1987) for three phases.

$$P_{cgn} = -\frac{\rho_w g}{\alpha_{gn}}\left((\bar{S}_l)^{-\frac{1}{m}} - 1\right)^{\frac{1}{n}} , P_{cnw} = -\frac{\rho_w g}{\alpha_{nw}}\left((\bar{S}_l)^{-\frac{1}{m}} - 1\right)^{\frac{1}{n}} \quad \text{(A28)}$$

$$P_{cgw} = -\frac{\rho_w g}{\alpha_{nw}}\left((\bar{S}_w)^{-\frac{1}{m}} - 1\right)^{\frac{1}{n}} - \frac{\rho_w g}{\alpha_{gn}}\left((\bar{S}_l)^{-\frac{1}{m}} - 1\right)^{\frac{1}{n}} \quad \text{(A29)}$$

$$\bar{S}_w = \frac{S_w - S_m}{1 - S_m} \ , \ \ \bar{S}_l = \frac{S_w + S_n - S_m}{1 - S_m} \ , m = 1 - {}^1\!/_n \quad \text{(A30)}$$

where P_{cgn} is gas-NAPL capillary pressure, P_{cnw} is NAPL-water capillary pressure and P_{cgw} is gas-water capillary pressure, $\bar{S}_w$ is effective water saturation, $\bar{S}_l$ is effective total liquid saturation where effective means that residual water saturation (Sm) is excluded when calculating the relative saturation, ρ_w is water density, g is acceleration of gravity, and the α_{gn}, α_{nw}, m and n are fitting curves parameters. The parameters needed to be defined are S_m, n, α_{gn}, α_{nw}. The α_{gn} and α_{nw} are defined by using scaling factor β.

The scaling factor enables extending the capillary pressure–saturation functions for two-phase system to a three-phase system. Because of the difficulty of directly measuring fluid pressures and saturations simultaneously in three-phase systems, so in practice, three-phase behavior is commonly estimated from two-phase measurements. This can be accomplished under

the assumption of the following wetting order, water>NAPL>air, a rigid media, negligible fluid solid interference and a monotonic saturation path, i.e. no hysteresis (Parker et al., 1987).

Table A4: Scaling factors for benzene in a sandy porous medium, (Paker et al., 1987)

Fluid system (benzene)	βij from regression		βij from measured interfacial tensions	βij from handbook interfacial tensions
	Van Genuchten	Brooks-Corey		
βgn	2.18±0.18	2.05±0.33	1.94±0.28	2.52
βnw	1.85±0.19	1.96±0.33	2.12±0.1	2.08

The scaling procedure presented by Fagerlund et al. (2006) is used. The scaling factors are determined by the interfacial tension (σ). Ref stands for reference fluids, i.e. the two-phase system fluids, usually air and water.

$$\beta_{gn} = \frac{\sigma_{ref}}{\sigma_{gn}} \quad , \ \alpha_{gn} = \ \beta_{gn} \ \alpha \tag{A31}$$

$$\beta_{nw} = \frac{\sigma_{ref}}{\sigma_{nw}} \quad , \ \alpha_{nw} = \ \beta_{nw} \ \alpha \tag{A32}$$

$$\beta_{gw} = \frac{\sigma_{ref}}{\sigma_{nw}+\sigma_{gn}} \ , \alpha_{gw} = \ \beta_{gw} \ \alpha \tag{A33}$$

$$\frac{1}{\alpha_{gw}} = \frac{1}{\alpha_{nw}} + \frac{1}{\alpha_{gn}} \tag{A34}$$

The relative hydraulic conductivity (kr) is the ratio of unsaturated hydraulic conductivity to the saturated one. Modified version of stone's three-phase method (Stone, 1970) used by the code to define the hydraulic conductivities is expressed as:

$$k_{rg} = \left[\frac{S_g - S_{gr}}{1 - S_{wr}}\right]^n \tag{A35}$$

$$k_{rw} = \left[\frac{S_w - S_{wr}}{1 - S_{wr}}\right]^n \tag{A36}$$

$$k_{rn} = \left[\frac{1 - S_g - S_w - S_{nr}}{1 - S_g - S_{wr} - S_{nr}}\right]\left[\frac{1 - S_{wr} - S_{nr}}{1 - S_w - S_{nr}}\right]\left[\frac{(1 - S_g - S_{wr} - S_{nr})(1 - S_w)}{(1 - S_{wr})}\right]^n \tag{A37}$$

The parameters needed to be defined are S_{wr}, S_{nr}, S_{gr}, n.

The other secondary variables are gas viscosity (μg) as a function of temperature, pressure and composition, aqueous and NAPL viscosity (μw, μn) as function of temperature, NAPL density as function of temperature and pressure, and the specific enthalpies of water and NAPL as function of temperature and pressure and porous medium porosity changes due to pressure and temperature

variations. The density and viscosity of liquid water are calculated from steam table equations given by the (International Formulation Committee 1967).

Appendix B: Experimental part

B.1. General

In this section, first, the properties and specifications of the materials used in the experimental part are mentioned. Then, the experimental methods adopted to assess the performance of plastic and concrete pipe specimens and rubber gaskets exposed to contaminated water. Finally, the results obtained in the experimental part will be presented and related discussion will be provided.

B.2. Materials and methods

B.2.1. Materials

B.2.1.1. Plastic pipe and gasket materials

Green PVC pressure pipe with a diameter of 8" conforming to ANSI/AWWA C900 with a dimension ratio (DR) of 18 which is equivalent to the pressure class of 235 psi was used. As the thickness of the pipe wall was 0.55", based on ASTM D638, type III specimen was considered which specifies the dimensions for a specimen with a thickness between 0.28" to 0.55". The specimens were directly prepared from a PVC pipe with the specifications mentioned above.

For the rubber gaskets, three commercially available types of rubber sheets i.e. neoprene (CR), nitrile (NBR), and Viton® (FKM) were purchased and the specimens were prepared manually using a die with the dimensions specified for type C dumbbell specimens according to ASTM D412. The thickness of sheets was 0.125" as stated in ASTM D412. The mechanical properties of PVC and gasket specimens either provided by the manufacturers or tested in the current project are presented in Table B1. Figures B1 and B2 show the die used for the preparation of rubber specimens and dimensions of rubber gasket dumbbell and PVC dog bone shaped specimens used in this study, respectively.

Table B1: Mechanical properties of PVC and rubber gasket materials.

Property	ASTM - PVC	ASTM - Rubber	PVC	CR	NBR	FKM
Tensile strength (psi)	D638	D412	7100 ± 170	412 ± 19	918 ± 76	1033 ± 57
Elongation @ maximum load (%)	D638	D412	13	114 ± 17	223 ± 11	103 ± 8
Hardness	D785 (Rockwell R)	D2240 (Shore A)	115 ± 10	60 ± 7	60 ± 5	75 ± 5

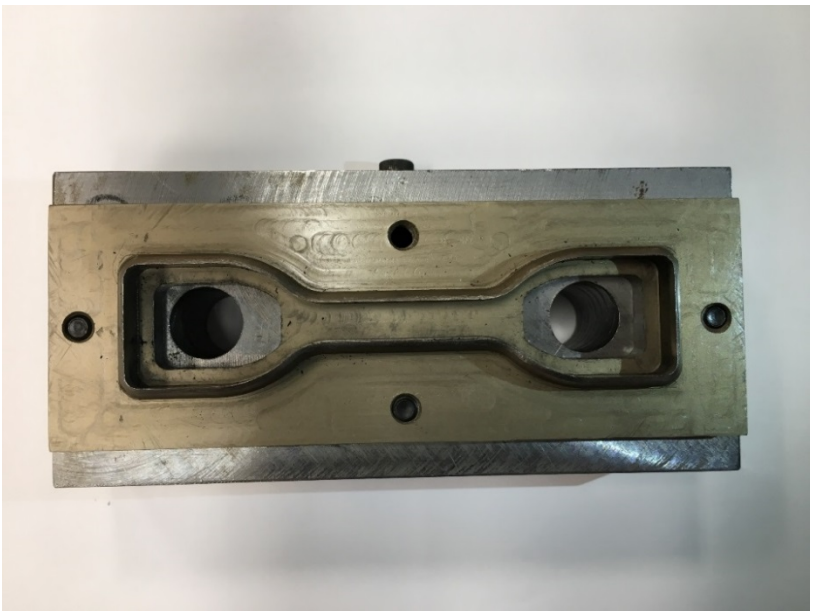

Figure B1: Die prepared for cutting rubber specimens.

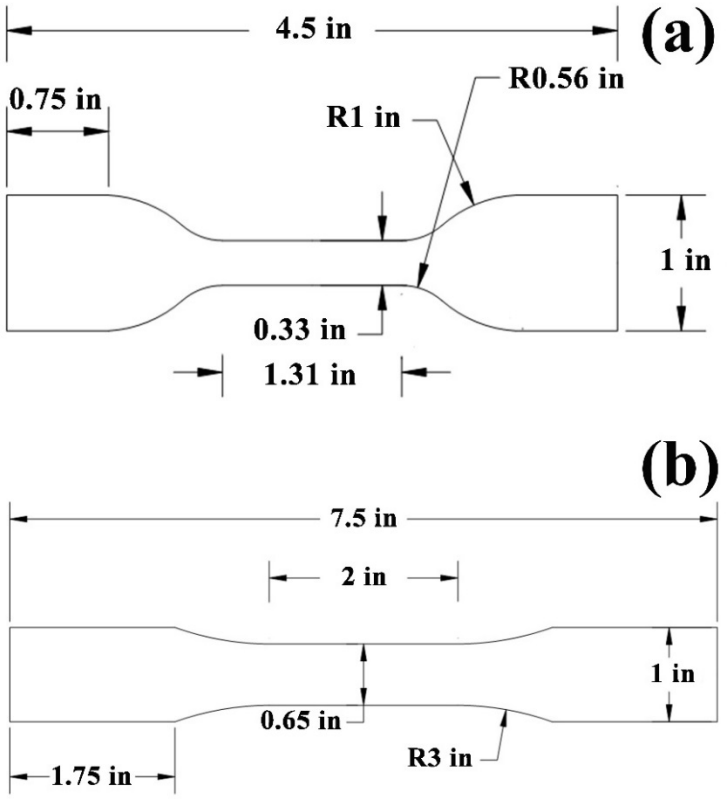

Figure B2: Dimensions of rubber gasket and PVC specimens (not to scale).

B.2.1.2. Concrete pipe

To perform unsaturated sorption and diffusion tests, cores from concrete pipes were provided by NCDOT. Mortar specimens were also prepared to investigate the effect of contaminated water on the compressive strength of cement-based materials. In addition, to quantify the effect of Xypex® on inhibiting VOCs transport through concrete pipe, a specimen of such chemicals compatible with the mix design used in concrete pipe proportioning was obtained from Xypex® company, Canada. Since the mix design of concrete pipe is composed of fly ash, a special type of Xypex® admixture (Admix C-500 NF) was used. The corresponding mortar specimens with and without Xypex® was produced for sorption and diffusion tests.

B.2.2. Methods

B.2.2.1. Plastic pipe and gasket materials

B.2.2.1.1. Accelerated aging

As aging plastic and elastomers at ambient temperature is a prolonged process, accelerated aging is considered to reduce testing and product development durations (Le Saux et al., 2014). Accelerated aging is usually taken place by elevating the aging temperatures which in turn requires proper models to translate it into ambient temperature.

Three different aging temperatures were considered i.e. 68 ºF, 104 ºF, and 140 ºF. Specimens were placed in bottles and aged up to 7 months (Figure B3). Aqueous solutions of benzene and PCE at their solubility limits i.e. 1790 mg/L and 206 mg/L, respectively, were prepared by adding 10-20 times more than the solubility limits of corresponding chemical to maintain the saturation level during the aging. Bottles were monitored to check the availability of contaminants (benzene or PCE) every other week and more chemicals were added if needed. To prepare the benzene or PCE aqueous solutions at their solubility limits, deionized water and ACS analytical grade of benzene and PCE were utilized to avoid the existence of other chemicals and substances which may affect the performance of chemicals of interest. After preparing headspace free bottles and sealing them using a commercial chemical- and heat-resistant glue, the bottles were then put in water tanks with controlled temperatures (104 ºF and 140 ºF) until the specified testing times. At each testing time, the specimens were removed from the bottles and then placed in a laboratory oven set at 104 ºF to become dry. Depending on the specimen type and aging duration, drying in an oven took one or two days and defined as less than 0.1% changes in the weight of specimen within an hour.

Figure B3: Insulated water bath with a control temperature system used for aging PVC pipe and rubber gasket specimens.

B.2.2.1.2. Tensile strength test

Tensile strength is the most important mechanical properties of plastics and rubbers. Tensile strength of the aged and unaged PVC and rubber gasket specimens were measured according to ASTM D638 and ASTM D412, respectively. The loading rate for all specimens was set at 2 in/min (50 mm/min). Also, note that three replicates of PVC or rubber materials were tested at each age and the average results were reported. Figure B4 shows the set-up of tension test on plastic and rubber specimens.

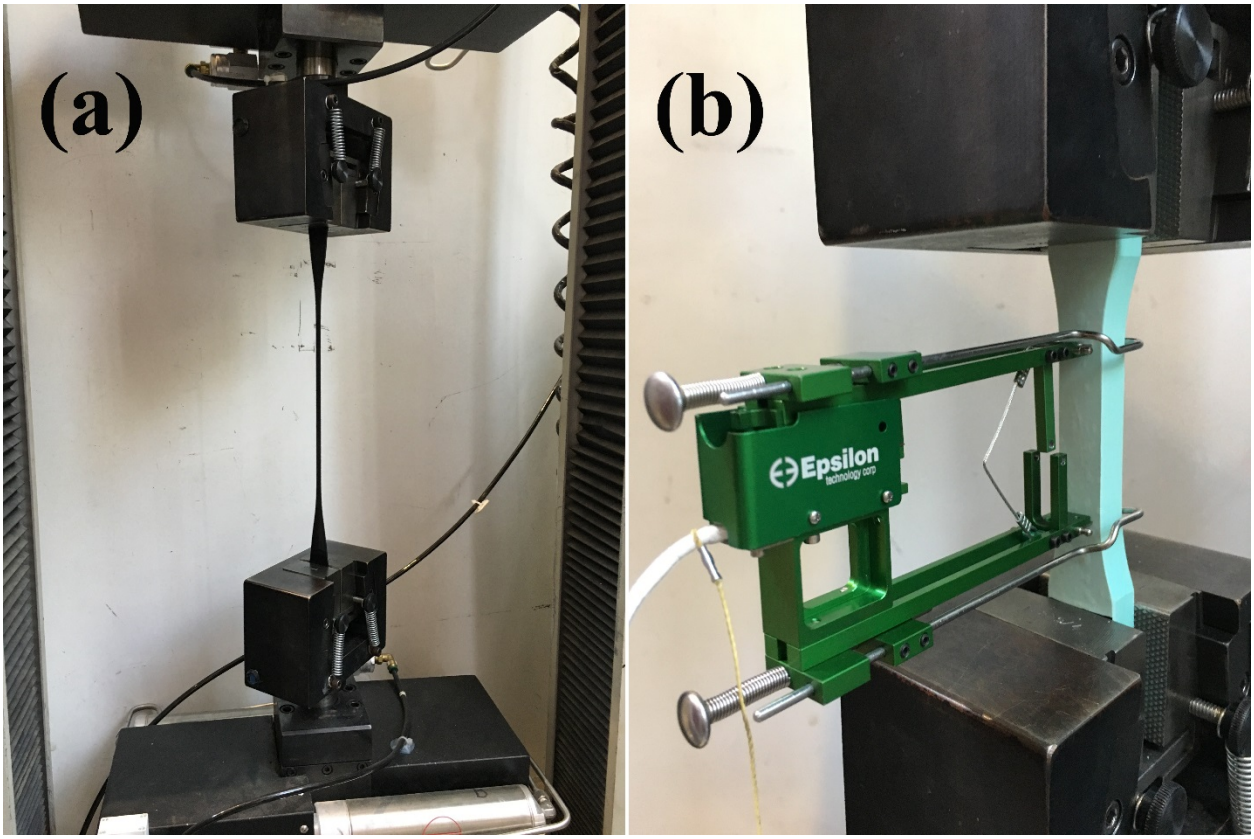

Figure B4: Tensile strength measurements: (a) rubber specimens (b) PVC pipe specimen.

B.2.2.1.3. Tensile strength degradation modeling

In this project, mechanical strength degradation modeling of plastic and rubber specimens is performed by obtaining models for their tensile strength change due to the exposure to contaminated water and undergoing accelerated aging. Williams-Landel-Ferry (WLF) methodology was adopted to convert the tensile strength measured at elevated temperatures used in accelerated aging to those quantified at ambient temperature (68 ^{o}F) using Equation B1. Then, relationships for the tensile strength loss/gain vs. aging duration at ambient temperature are developed (Brown, 2001).

$$\log(a_T) = \frac{c_1\,(T - T_o)}{c_2 + (T - T_o)} \tag{B1}$$

where a_T is the shift factor of the curve of the measured tensile strength at each specific temperature (T) over time, T_o is reference temperature (taken as fixed at 68 ^{o}F in this study), and c_1 and c_2 are two coefficients dependent upon the material type.

By employing shift factors, all data measured at temperatures higher than reference temperature (T_o = 68 ^oF) over time, is shifted in time. The master curve at the reference temperature is then constructed by fitting a curve on all shifted and at reference temperature data. Using the obtained master curve, one can predict how long it will take to reach a specified tensile strength loss limit which in turn can be translated into the service life of the material aging naturally under the exposure media.

The procedure of developing tensile strength degradation models for PVC and rubber gaskets is summarized in Figure B5. As can be seen in Figure B5, the first step is to plot the degradation of tensile strength at each aging temperature over exposure duration. Then, the curves for the temperatures other than the reference are shifted forwards considering their shift factor calculated using the least squares method. Afterwards, the exponential model is fitted to the shifted data to obtain the degradation curve. Note that the exponential model was considered as it is the best fit model for the degradation of polymeric materials (Brown, 2001).

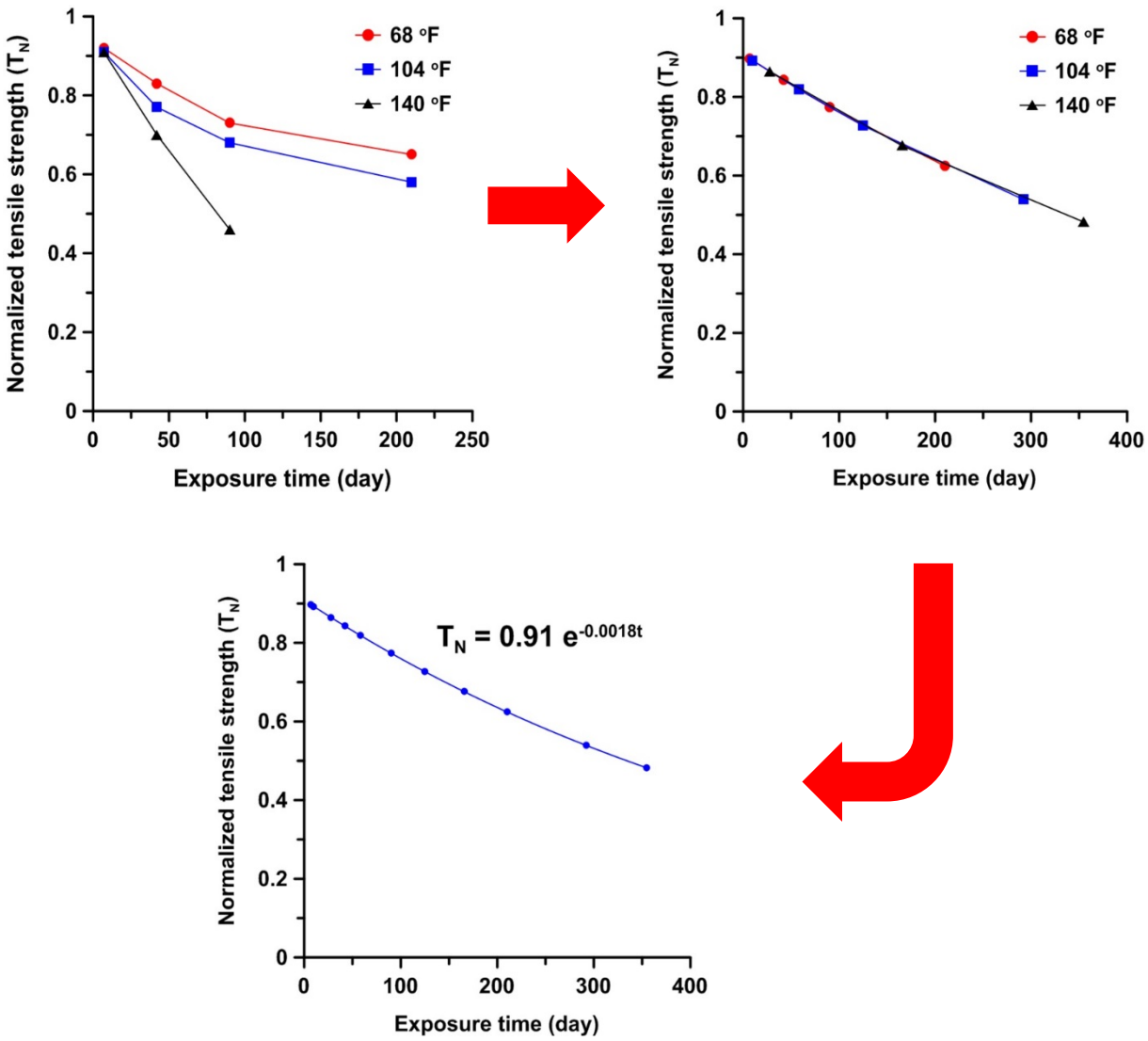

Figure B5: The process of obtaining the degradation models.

It should be noted that tensile strength of aged specimens for each material of interest was normalized to its unaged tensile strength mentioned in Table B1. The normalized tensile strength (T_N) at each aging time and temperature was then used for modeling purposes.

B.2.2.2. Concrete pipe

B.2.2.2.1. Mix designs

Table B2 shows the mix proportions of concrete mixture of concrete pipe of which cores were used for sorption and diffusion quantification. Also, mortar specimens with the same water to cement and fly ash to cement ratios were prepared to assess the effect of contaminated water on compressive strength of cement-based materials. The mix proportions of the mortars with and without Xypex® are the same as the one produced for compressive strength test. The only difference compared to control mixture (without Xypex®) is the addition of 1.5% Xypex® by weight of cementitious materials (i.e. cement and fly ash) as recommended by the manufacturer. Also, note that according to the manufacturer Xypex® should be replaced with aggregates not cementitious materials. Additionally, as the control specimens were sealed cured, the same curing method (i.e. self-curing) was adopted for the mixture made with Xypex®.

Table B2: Mix design of concrete used for pipe production (all amounts are in lbs)

Water to cement ratio	Cement	Fly ash	Water	Coarse aggregate	Fine aggregate
0.44	500.0	95.0	217.1	1600.0	1684.0

B.2.2.2.2. Compressive strength test

Compressive strength test was performed on mortar specimens exposed to deionized (clean) and contaminated water in accordance with ASTM C109. Contaminated water here is an aqueous solution of benzene and PCE at their solubility limits i.e. 1790 mg/L and 206 mg/L, respectively, to evaluate the effect of polluted water with both aromatic and chlorinated hydrocarbons. Mortar specimens were sealed cured at room temperature for three months. Then, specimens were placed in deionized or contaminated water for 6 and 12 months at which five specimens were tested and the average results were reported.

B.2.2.2.3. Unsaturated sorption test

Capillary suction as a durability factor of concrete materials was performed on the specimens prepared from the concrete pipe cores provided by NCDOT. This test will provide an

understanding of the effect of water contaminants on the rate of sorption of concrete. Equation B2 shows that the depth of fluid penetration is proportional to the square root of surface tension and inversely proportional to the square root of viscosity (Kelham, 1988; Spragg et al., 2011).

$$x(\tau) = \sqrt{\frac{4k\gamma\cos(\theta)\tau}{p\eta r}} \quad \text{(B2)}$$

where x(τ) (mm) is the penetration depth, γ (N/mm) is the surface tension, θ (rad) is the liquid–solid contact angle, p (dimensionless) is the porosity of the medium, r (mm) is the pore radius, k (mm^2) is the intrinsic permeability of the material, and η (Pa.s) is the viscosity of fluid.

Since the solubility of benzene and PCE in water at ambient temperature is very small (1.79 g/L and 206 g/L, respectively) it is hypothesized that there should not be a significant effect on surface tension and viscosity of water due to the application of aromatic hydrocarbons or chlorinated solvents up to their solubility limit. To validate the hypothesis, surface tension measurements were carried out on the contaminated water at different concentrations of benzene and PCE. The results of surface tension measurements are shown in Figure C1 (Appendix C, section C.1). As can be seen in Figure C1, the surface tension of water is negligibly affected by the presence of VOCs up to their solubility limits. Also, since the coefficient of variation of the surface tension results for all solutions compared to pure water is 0.83% which is even below 1%, it can be stated that water contamination due to aromatic or chlorinated hydrocarbons up to their solubility limits does not have significant effect on the surface tension of water.

Moreover, according to the mixture rules (Viswanath et al., 2007), since the concentration of the VOCs even at their solubility limits is very low (2.04 mL benzene, and 0.13 mL PCE per one-liter aqueous solution), changing in viscosity of water would not be anticipated. As a result, based on the above-mentioned discussion on properties of contaminated solutions, it is hypothesized that the penetration depth of such solutions would be the same as that of water.

Sorption test was conducted according to ASTM C1585 on specimens prepared from concrete pipe cores provided by NCDOT to measure the initial and secondary sorption rates of concrete specimens in contact with pure water and aqueous solution of PCE at its solubility limit (i.e. 206 mg/L) to check the validity of the hypothesis (Figure B6).

To quantify the effect of Xypex® on sorption rates of clean and contaminated water (with PCE at its solubility limit), unsaturated sorption test was carried out on mortar specimens with and without Xypex® admixture. The mix proportions of mortar specimens were mentioned in section B.2.2.2.1.

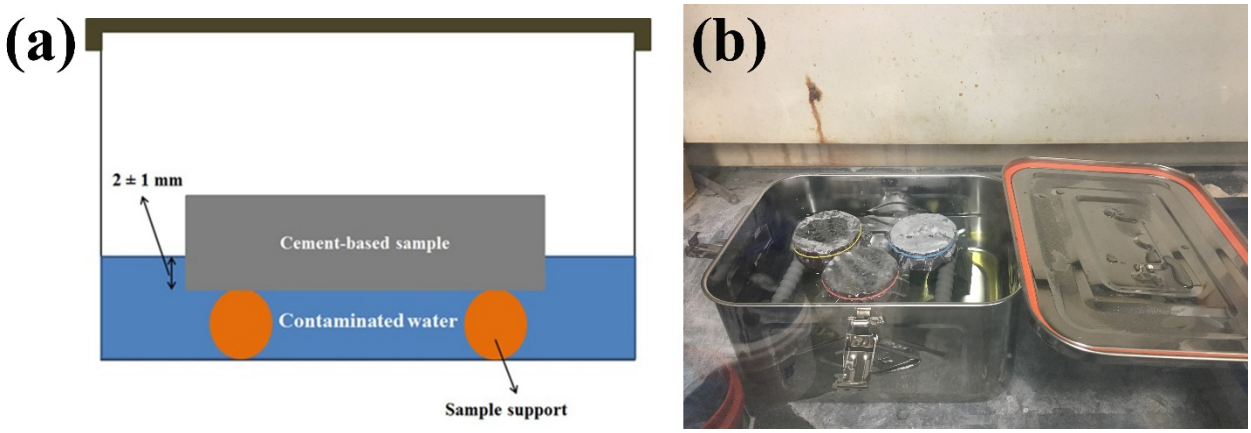

Figure B6: Sorption test setup.

To measure the surface tension of the contaminated water at different concentrations of the contaminant of interest (benzene and PCE), first, aqueous solutions of benzene and PCE at their solubility limits i.e. 1790 mg/L and 206 mg/L, respectively, were prepared by utilizing deionized water and VOCs five times higher than their solubility limit at room temperature. Then, the solutions were mixed continuously by magnetic stirrer for two days. Note that for preparing aqueous solutions containing VOCs below their solubility limits, a specified portion of the prepared solutions was diluted in deionized water. To measure the surface tension of the solutions of interest, a tensiometer (Attension, Biolin Scientific, Stockholm, Sweden - Figure B7) equipped with a Wilhelmy platinum plate (19 × 10 × 0.1 mm) was used. The surface tension calculation is based on measuring the force resulted from the tension phenomenon between the bottom edge of the platinum plate and the surface of solution (Li et al., 2016).

Figure B7: Liquid surface tension measurement test setup.

B.2.2.2.4. Diffusion measurements

To measure coefficient of diffusion of VOCs vapors through saturated concrete, an in-house diffusion cell was developed by the researchers (Figure B8). The diffused mass of benzene and PCE vapors through the concrete specimens was measured using a Gas Chromatography (GC) equipment. The diameter of the exposed surface to the VOCs vapors was set to 2". The specimen was sandwiched between two stainless steel plates which were later connected to the bottles. The procedure followed for obtaining the samples from the diffusion setup is as follows:

Using gastight syringes, at each specified sampling time, two samples of 500 µL from the downstream bottle were taken and diluted in a ratio of 1/100 with deionized distilled water previously acidified with ascorbic and maleic acids for preserving the samples. Afterwards, second dilution was performed using 300 µL of the samples prepared during the initial sampling in a ratio of 1/150 with deionized distilled water. The samples were then kept in a refrigerator at a temperature of 40 ºF until the testing date for measuring the concentration of hydrocarbon of

interest in the second set of samples prepared using a GC. The results over a period of three weeks were then combined and the diffusion coefficient was calculated using Fick's second law.

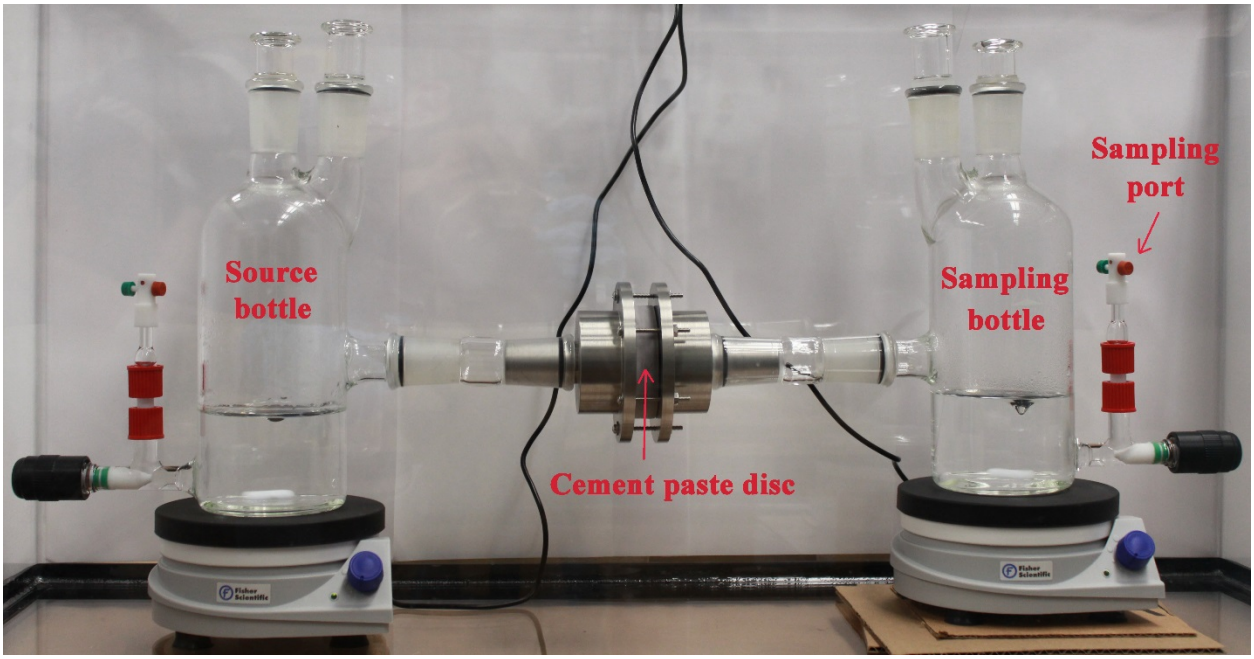

Figure B8: Set-up developed for measuring diffusion of VOCs through concrete specimens.

Appendix C: Concrete pipe

C.1. Water surface tension measurements

The changes in the surface tension of water due to its contamination with aromatic (benzene) and chlorinated (PCE) hydrocarbons at their different percentages of their solubility limits i.e. 1790 mg/L and 206 mg/L, respectively, are presented in Figure C1.

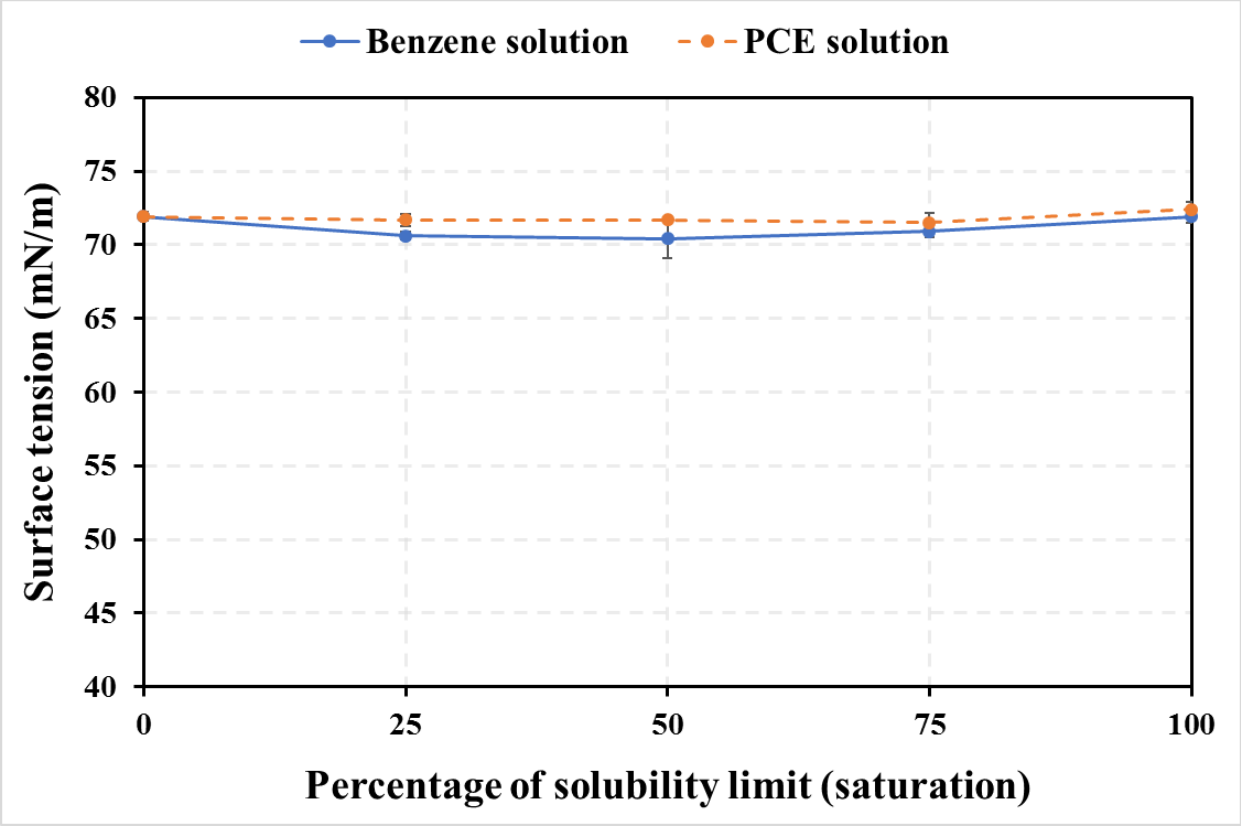

Figure C1: Surface tension of aqueous solutions of benzene and PCE at different percentages of their solubility limits

C.2. Unsaturated sorption test

C.2.1. Concrete pipe specimens

The results of sorption of clean and contaminated water by concrete pipe specimens are shown in Figures C2 to C4. Total liquid absorption for the specimens is shown in Figure C2.

Figures C3 and C4 exhibit the calculation of initial and secondary liquid absorption rates, respectively.

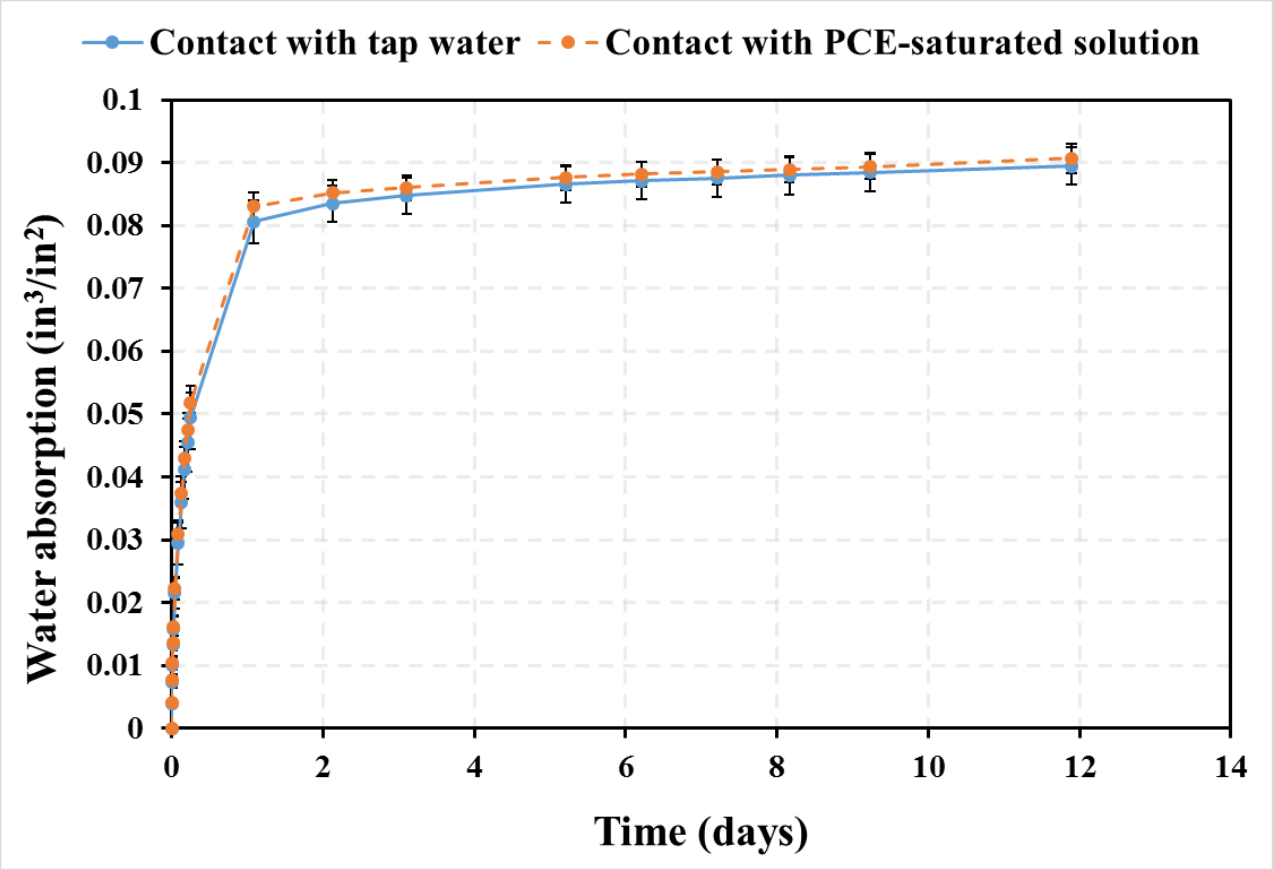

Figure C2: Absorbed liquid by concrete specimens up to 12 days of exposure.

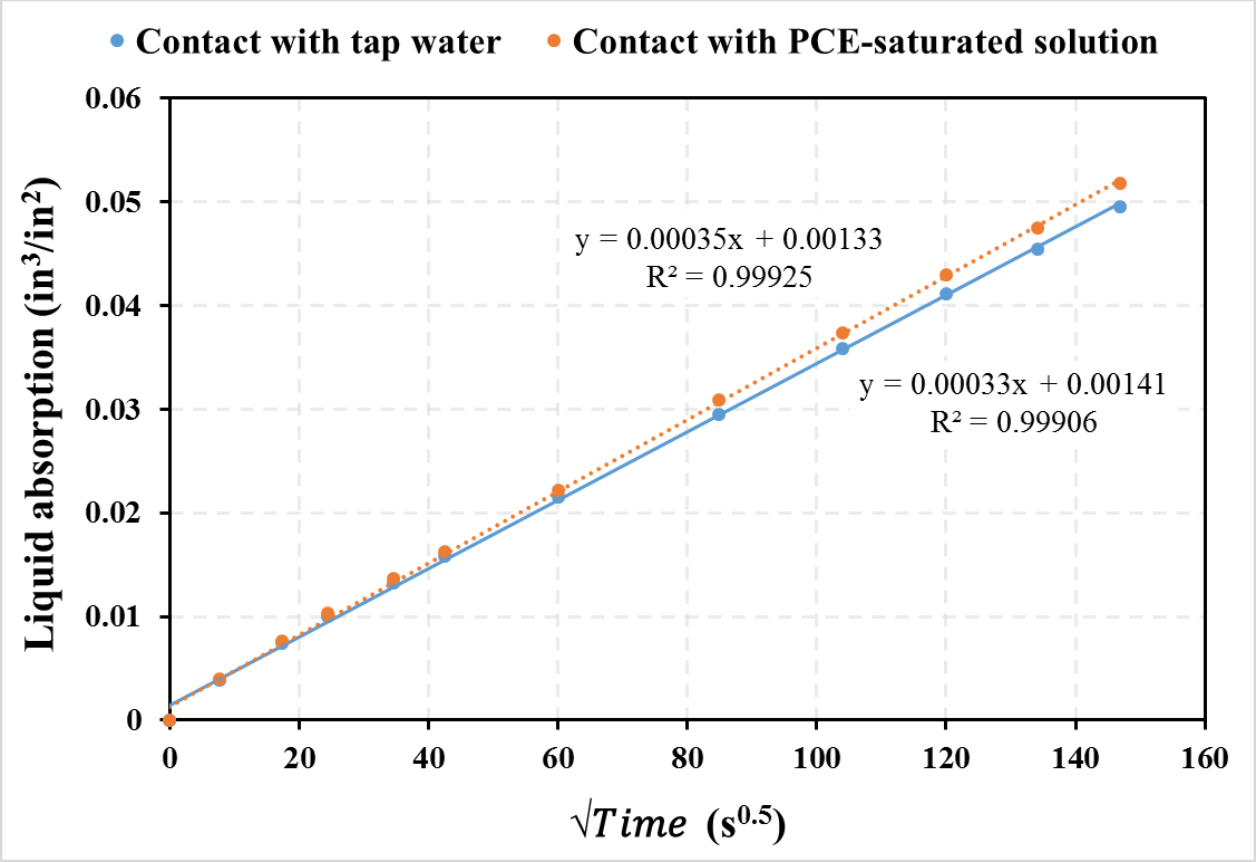

Figure C3: Fitted linear model to obtain initial sorption rate of concrete specimens.

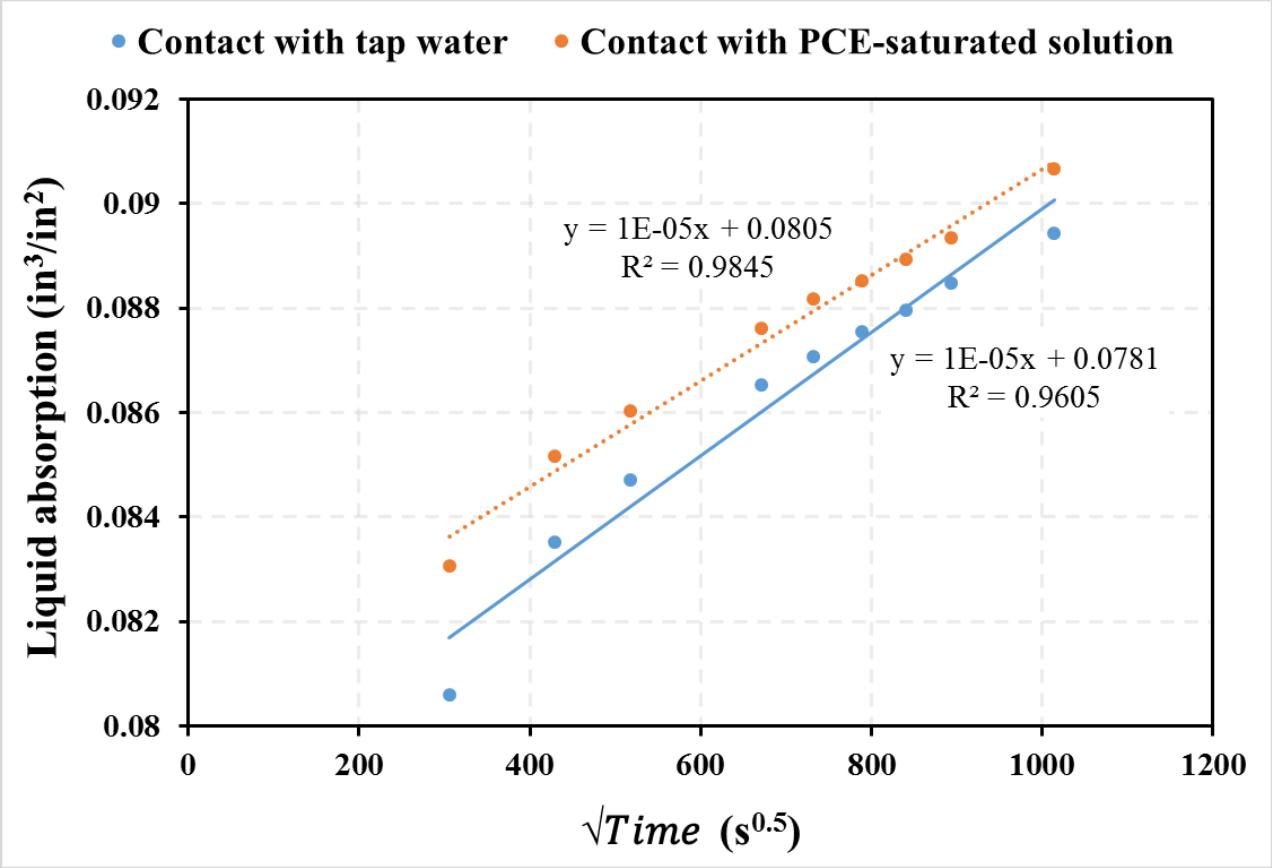

Figure C4: Fitted linear line to obtain secondary sorption rate of concrete specimens.

C.2.2. Xypex® effect

The effect of Xypex® on the sorptivity of mortar specimens was investigated. The results of measuring total liquid absorption are plotted in Figures C5 and C6. Figures C7 and C8 show the calculation of initial liquid absorption rates for pure water and PCE aqueous solution (at 206 mg/L PCE) as exposure media. Figures C9 and C10 depict the calculation of secondary liquid absorption rates for pure water and PCE aqueous solution (at 206 mg/L PCE) as exposure media.

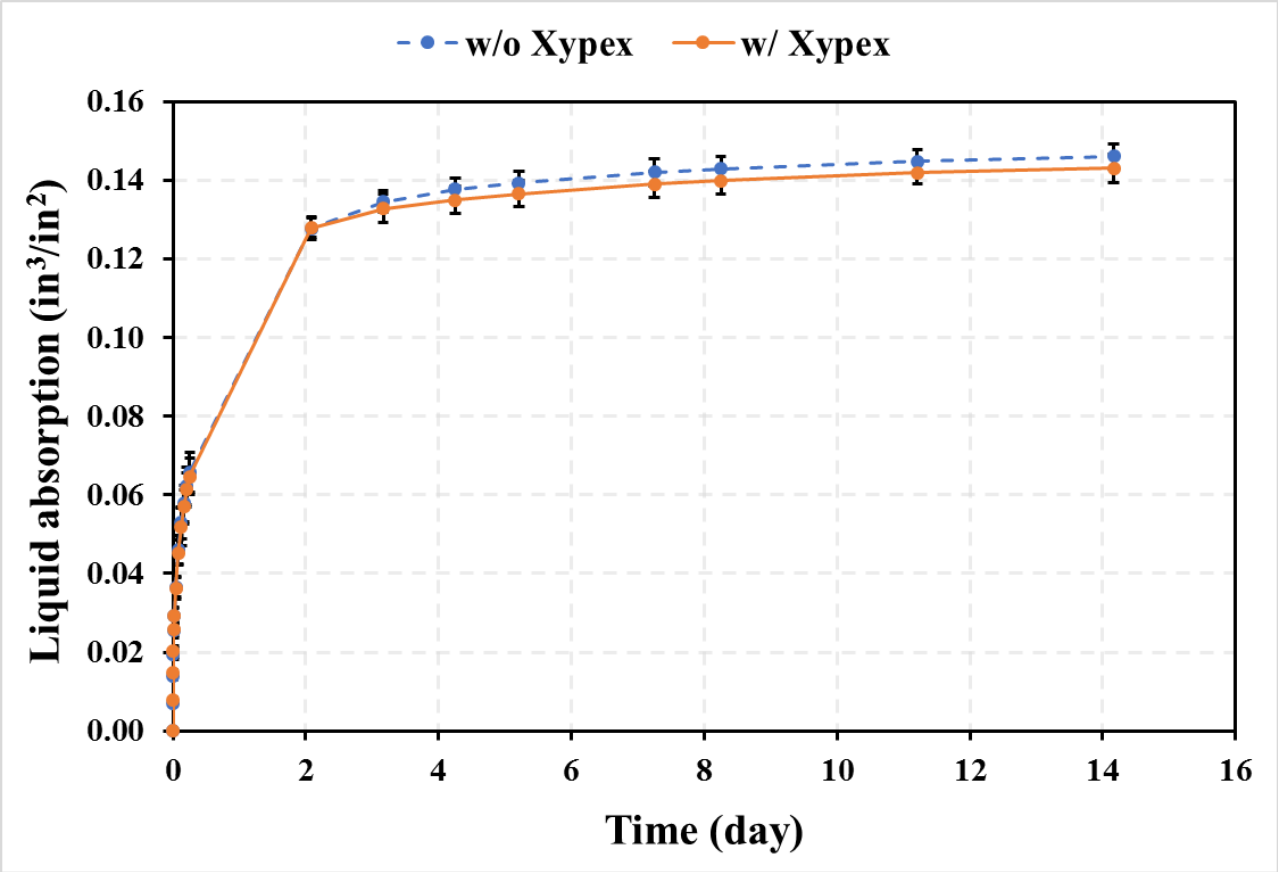

Figure C5: Absorbed liquid by mortar specimens up to 14 days of exposure to pure water.

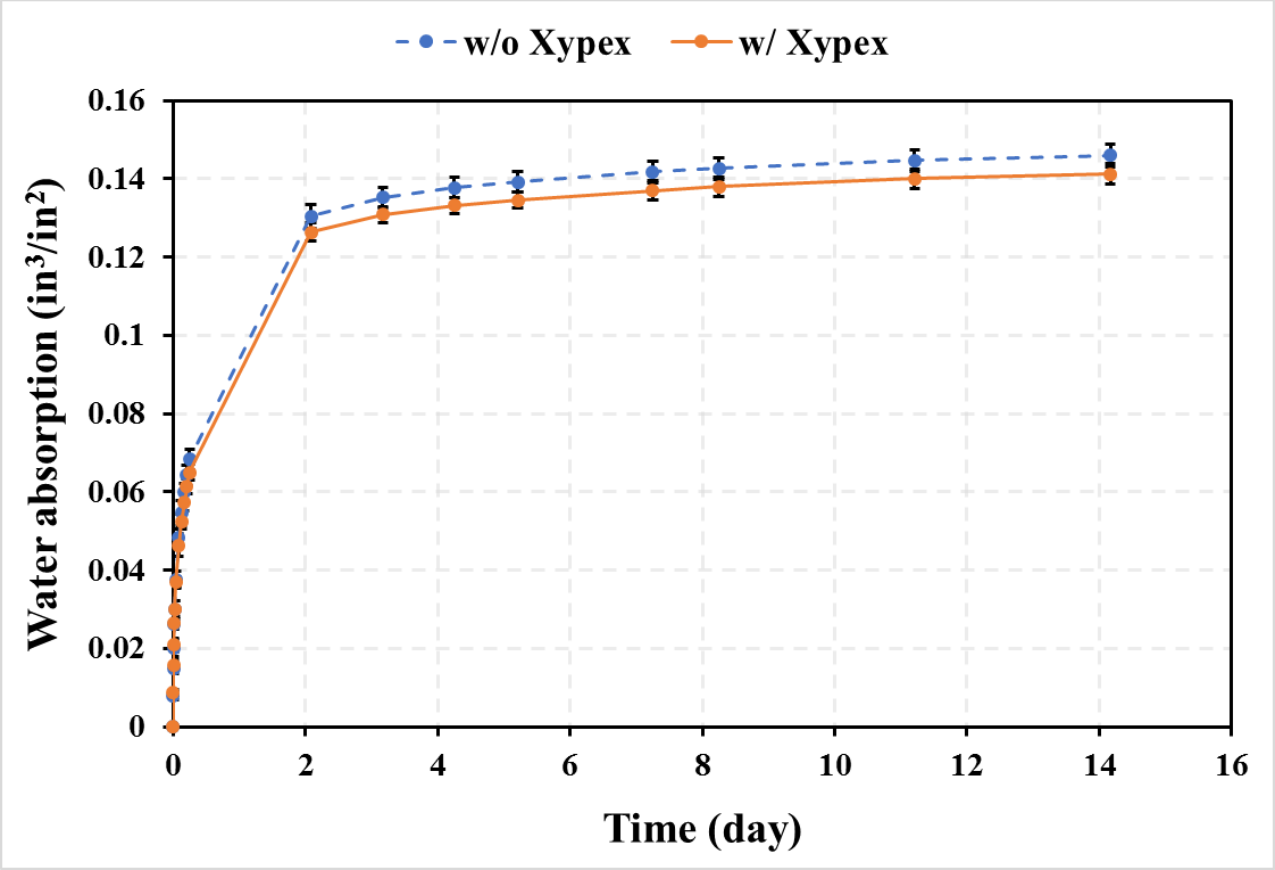

Figure C6: Absorbed liquid by mortar specimens up to 14 days of exposure to PCE solution (206 mg/L PCE).

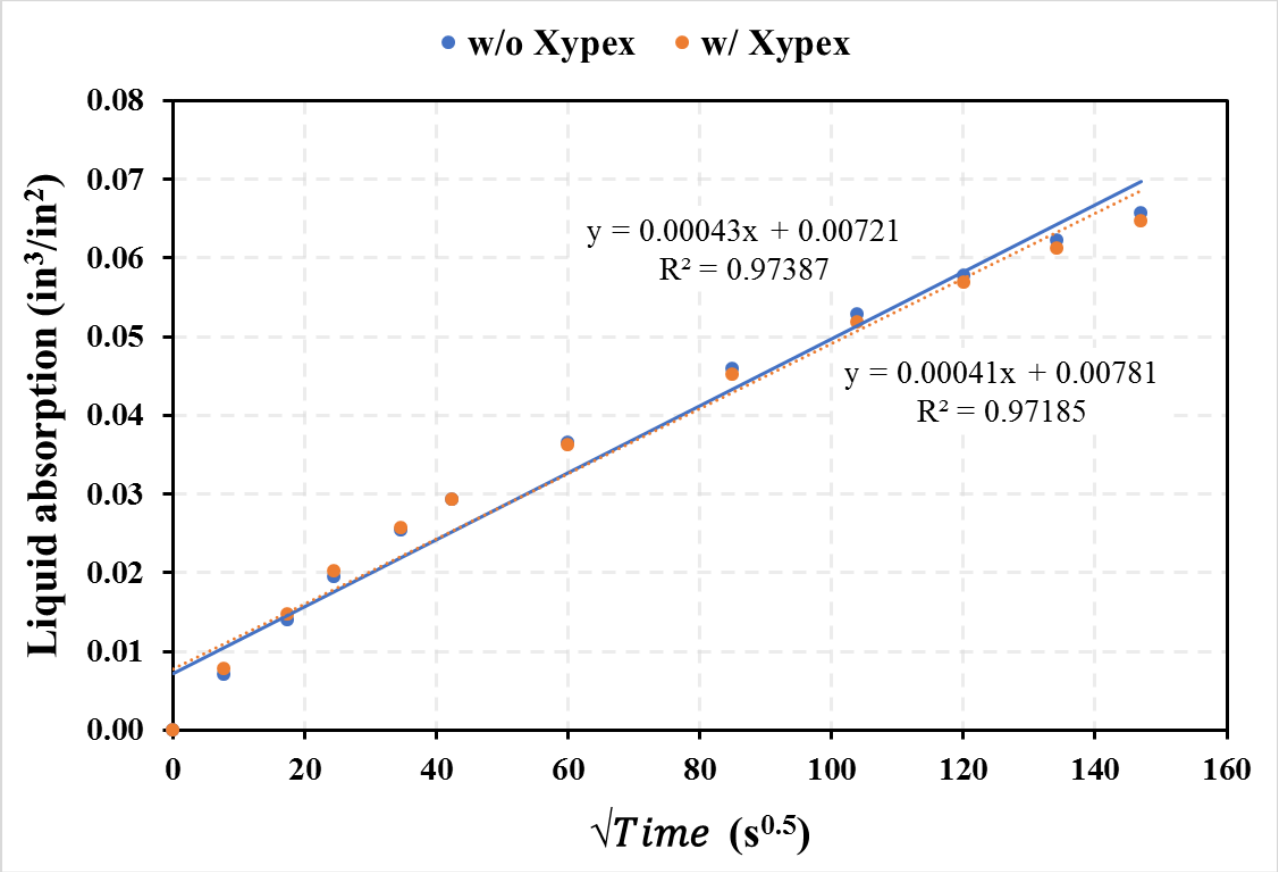

Figure C7: Fitted linear model to obtain initial sorption rate of mortar specimens in contact with pure water.

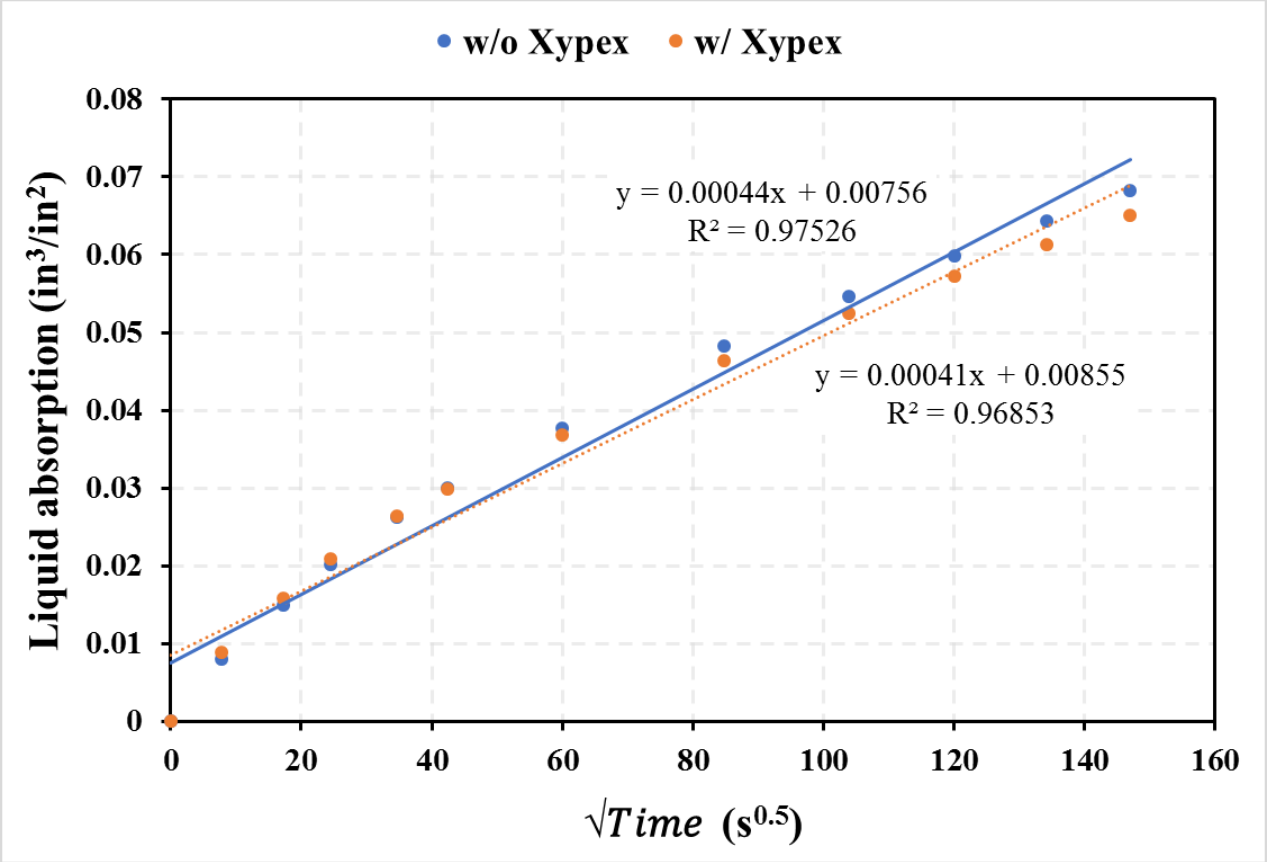

Figure C8: Fitted linear model to obtain initial sorption rate of mortar specimens in contact with PCE solution (206 mg/L PCE).

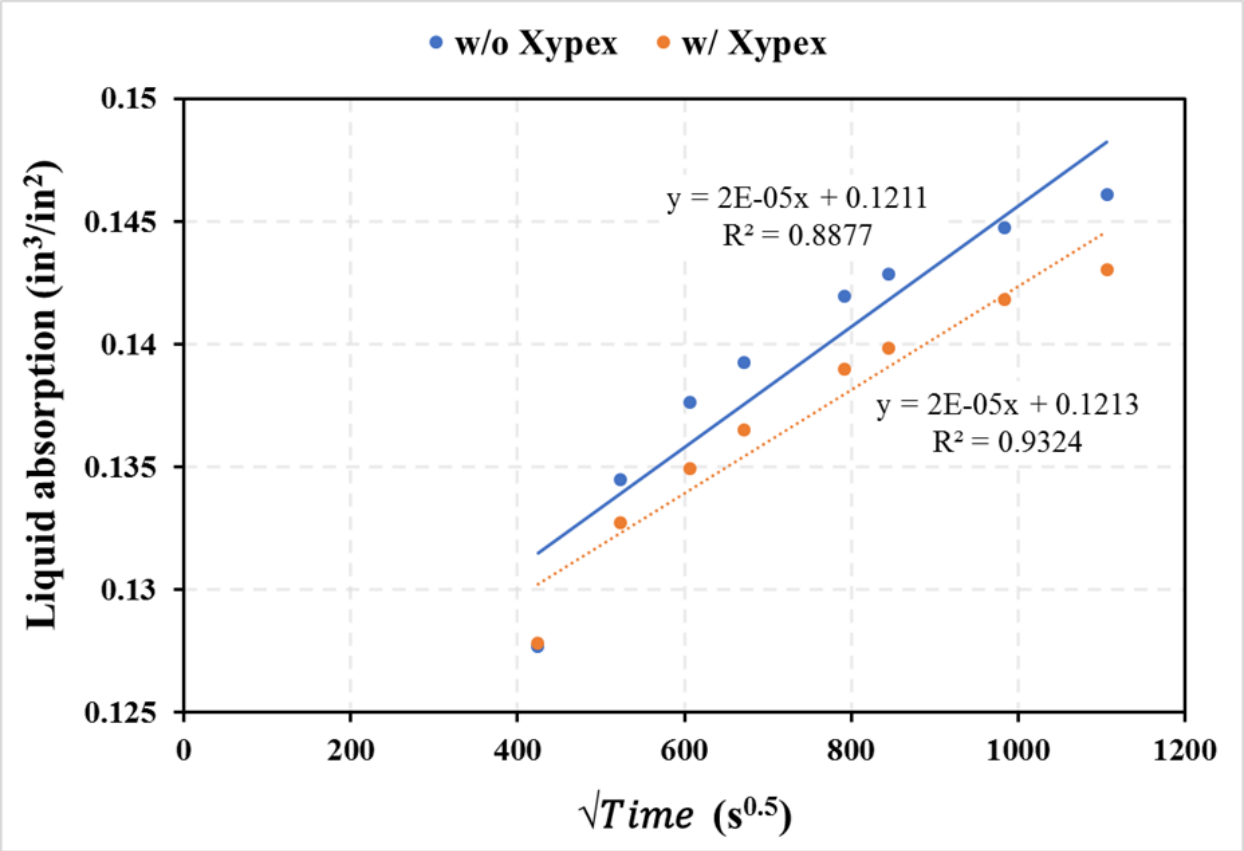

Figure C9: Fitted linear model to obtain secondary sorption rate of mortar specimens in contact with pure water.

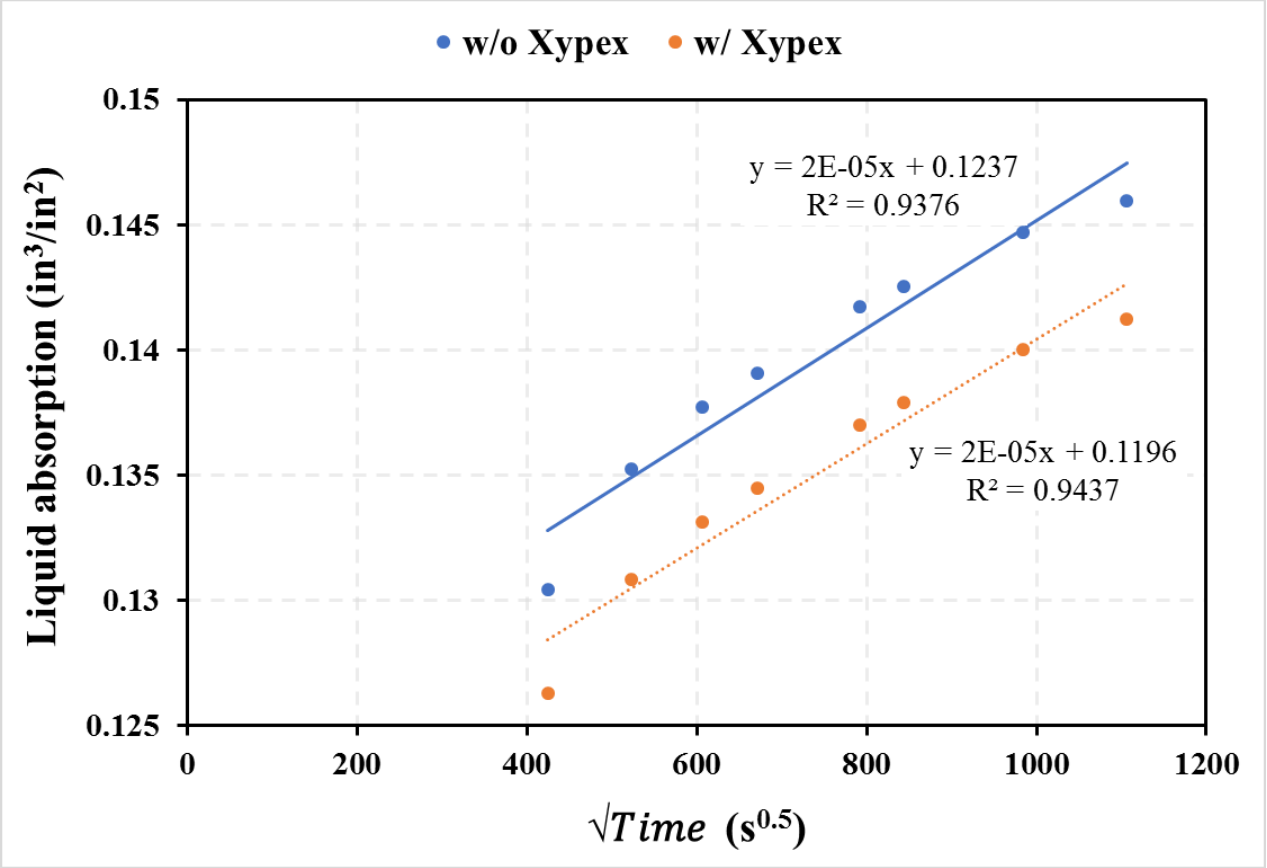

Figure C10: Fitted linear model to obtain secondary sorption rate of mortar specimens in contact with PCE aqueous solution (206 mg/L PCE).

Appendix D: Unsaturated model

D.1. Model parametrization

The specific properties used in the numerical model are presented in Tables D2 and D3. The native soil in subsurface is mostly sandy clay with intrinsic permeability of 6.4×10^{-14} m^2 (6.24×10^{-5} cm/s, Delta 2000). The hydraulic conductivity in vertical direction is assumed to be half of the value in the horizontal direction. To define capillary pressure and relative permeability of materials, the governing equations from Parker's three-phase functions (Parker et al., 1987) and Stone's three phase equations (Stone, 1970), are used respectively.

To simulate the conditions representative of atmosphere layer, the uppermost layer is assigned as a zero concentration boundary at fixed atmospheric pressure and temperature. Also, capillary pressure is taken as zero in this layer. Applied gas relative permeability as high as 100%, a water saturation smaller than residual water saturation and liquid relative permeability as zero allow for gaseous emission to the atmosphere.

The water table gradient is established by fixed total heads at right and left side boundaries. Two fixed boundary conditions with near atmospheric pressure are applied at two ends of pipe while half full flow is assumed inside it from back to the front face. No flow boundary condition is assumed for the remaining boundaries.

The pipe is located in a trench with 0.15 m (0.5 ft) sandy gravel as the bedding material, overlain by 0.9 m (3 ft) initial backfill that is mostly sandy soil, and 0.9 m (3 ft) final top backfill, from the native soil.

To study different scenarios, a sandy soil from UNSODA database with higher hydraulic conductivity was used as native soil in a separate scenario and two-phase fitting parameters; α_{gw} and n; are determined using RETC code. Three different conditions of concrete pipe materials were compared based on various unsaturated transport properties of concrete. The capillary pressure parameters are defined based on Van Genuchten two-phase parameters (α_{gw} and n) (Pour-Ghaz et al., 2016 and Kumar, 2010). For some of the materials used in simulations (Table D3), only two-phase parameters are available, and the scaling factors are needed to determine three-phase parameters α_{gn} , α_{nw} and α_{gw} .

The scaling factors were calculated by equation (D1).

$$\beta_{gn} = \frac{\sigma_{nw+\sigma_{gn}}}{\sigma_{gn}} = \frac{0.029+0.035}{0.029} = 2.2 \quad , \quad \beta_{nw} = \frac{\sigma_{nw+\sigma_{gn}}}{\sigma_{nw}} = \frac{0.029+0.035}{0.035} = 1.82 \qquad \text{(D1)}$$

Where σnw=0.035 Nm^{-1} and σgn=0.029 Nm^{-1} are the interfacial tension and surface tension for benzene respectively at 20 °C (Mercer & Cohen, 1990) and σref=0.0728 Nm^{-1} at 20 °C (The Engineering ToolBox, 2005), air and water being the reference fluids. The $\beta_{gn} = 2.2$ and

$\beta_{nw} = 1.82$ are in agreement with scaling factors from Van Genuchten regression analyses, (Parker et al., 1987).

The gasket materials are examined via two scenarios of good condition gaskets with their hydraulic conductivity same as concrete material, and damaged gaskets for which higher homogenized hydraulic conductivity due to the damage was assumed (Tables D2 and D3).

The diffusion parameters are defined as follows: reference diffusion coefficient for vapor-air mixtures (D_g^{awR}=2.13x10^{-5}), reference binary diffusivity of VOC in air (D_g^{acR} =7.7x10^{-6}), vapor-air diffusivity exponent (θ_{aw} =1.8), chemical diffusivity exponent (θ_{ca} =1.52).

The movement of organic pollutants in the subsurface is retarded by sorptive interaction. Chemical partitioning into the solid phase is defined by adsorption coefficient (Kd). Degree of organic chemicals adsorption (C_s^c) is mainly dependent on the quantity of organic carbon in the soil (foc). The soil organic carbons were specified in a range of 0.4-13.9 g per kg of soil (0.04-1.4 %) depending on the soil textures and depth within coastal plain regions of North Carolina (Deiss et al., 2017). Delle et al (2001) measured Kd for benzene transport for different soil textures and with different organic carbon fractions. Kd is estimated to be equal to 8.5×10^{-5} m^3/kg while koc is assigned as 0.085 m^3/kg (Delle site, 2001) and organic carbon fraction (foc) of 0.1% is applied (Deiss et al., 2017).

D.2. Simulation Process

The initial gravity-capillary equilibrium within the subsurface domain is first established in the simulation before contamination release. Figure displays the soil-water characteristic curves (SWCCs) for native soil, the trench material, and, water retention curve (WRC) for concrete pipe material. The initial water saturation and pressures are defined based on these diagrams. When water table level changes different initial water saturation and soil matric suction are defined based on new elevation of water table. In this case, the whole domain is analyzed for equilibrium one time without pipe but with including groundwater gradient, followed by a second time with the pipe is included in the domain.

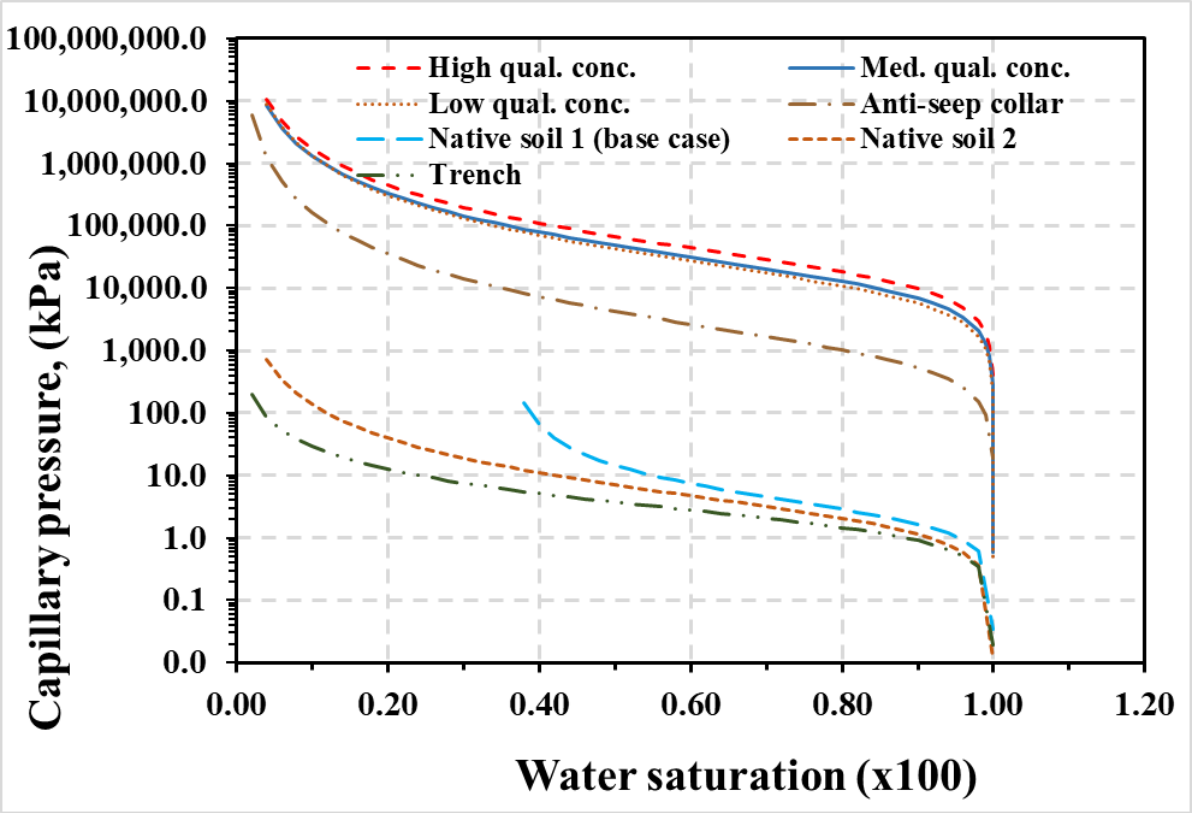

Figure D1: Water Retention Curves and SWCCs used in simulations.

Figure shows the water saturation in the domain after equilibrium at two water table levels of a. 3m (10 ft) and b. 2.1m (7 ft) from ground surface. Because of high capillary pressure of concrete, the pipe walls become completely saturated, with the trench around the pipe has lowest saturations in the domain. The half full flow inside the pipe was established.

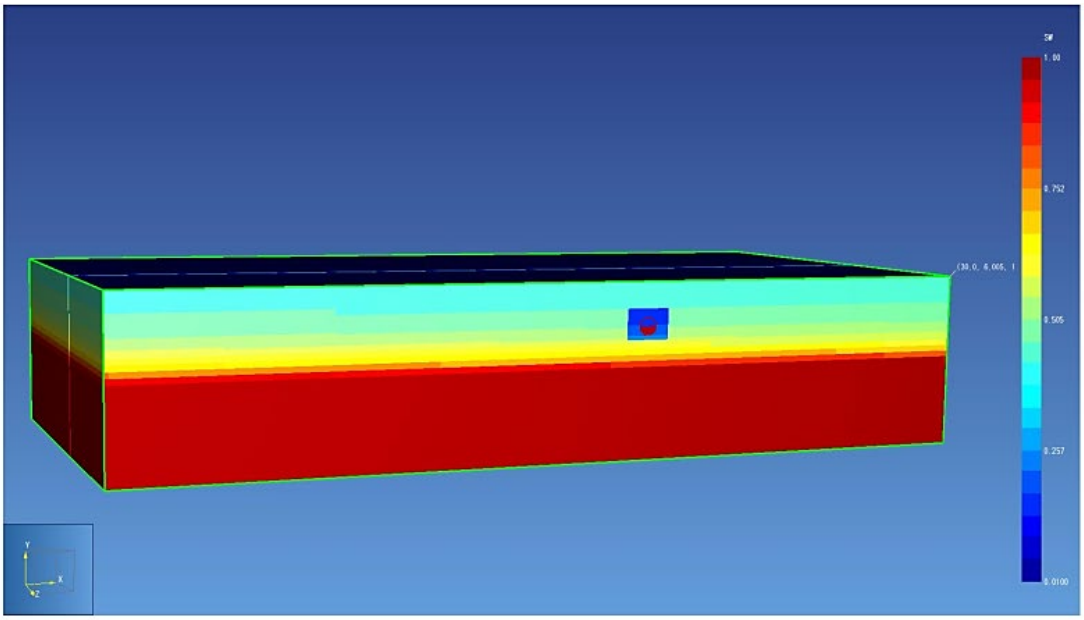

a. Water table level at 10ft from surface

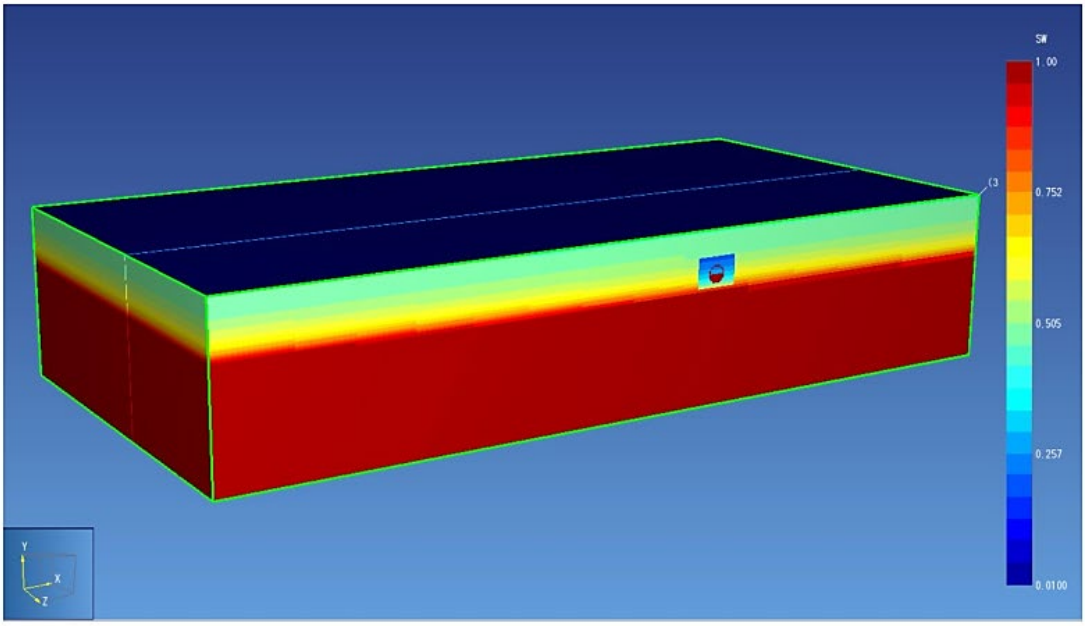

b.Water table level at 7ft from surface

Figure D2: Water Saturation after equilibrium within the depth of soil.

After establishing equilibrium, the results serve as initial conditions for following analyses in which contaminants are released in the domain and long-term redistribution of contaminant with time and the potential transport to subsurface concrete pipe are examined. The benzene concentrations are evaluated at location of MW4 which show good agreement with available data from groundwater specimens at this monitoring well. The contaminations in MW6 and MW8 at right side of pipe (East) were less than MCLs (Antea, 2016).

Table D1: Allowable benzene concentration.

Criteria	unit	Allowable for benzene	Reference
Acceptable ambient levels (AAL) (Concentration in air)	µg/l	1.2×10^{-4}	NC DEQ, 15A NCAC 02D.1104 toxic air pollutant guidelines,2018
Maximum allowable concentration in groundwater suitable for drinking	µg/l	1	NC DEQ, 15A NCAC 2L .0202 Groundwater quality standards, 2016
Maximum contaminant level (MCL) (concentration in drinking water)	µg/l	5	EPA, 2002
Maximum Soil Contaminant Concentration (MSCC)	mg/kg	0.0056	NC DEQ, 15A NCAC 02L .0411 Maximum soil contaminant concentrations, 2007

Table D2: Main Petrophysical Properties of soil and concrete materials.

Soil type	Rock density	K_V	K_h	Intrinsic K_V	Intrinsic K_h	Porosity
	kg/m3	cm/s	cm/s	m^2	m^2	
Native soil 1 (sandy clay)	2700	3.12×10^{-5}	6.24×10^{-5}	3.20×10^{-14}	6.40×10^{-14}	0.37
Final backfill (sandy clay)	2700	4.68×10^{-5}	9.36×10^{-5}	4.80×10^{-14}	9.60×10^{-14}	0.38
Native soil 2 (sand)	2700	1.00×10^{-3}	2.00×10^{-3}	1.025×10^{-12}	2.05×10^{-12}	0.34
Initial backfill	2700	7.5×10^{-2}	1.5×10^{-1}	7.70×10^{-11}	1.54×10^{-10}	0.34
Bedding material	2900	5×10^{-1}	1	5.13×10^{-10}	1.03×10^{-9}	0.32
High qual. pipe	2800	2.1×10^{-9}	2.1×10^{-9}	2.16×10^{-18}	2.16×10^{-18}	0.121
Med. qual. pipe	2800	3.90×10^{-9}	3.90×10^{-9}	4.00×10^{-18}	4.00×10^{-18}	0.125
Low qual. pipe	2800	5.85×10^{-9}	5.85×10^{-9}	6.00×10^{-18}	6.00×10^{-18}	0.131
Undamaged gasket	1500	3.90×10^{-9}	3.90×10^{-9}	4.00×10^{-18}	4.00×10^{-18}	0.1
Damaged gasket	1500	3.90×10^{-5}	3.90×10^{-5}	4.00×10^{-14}	4.00×10^{-14}	0.1
Flow	2700	10	10	1.00×10^{-8}	1.00×10^{-8}	0.999
Atm.	2700	1	1	1.00×10^{-9}	1.00×10^{-9}	0.999
Anti-seep collar	2800	1.00×10^{-8}	1.00×10^{-8}	1.026×10^{-17}	1.026×10^{-17}	0.33

Table D3: Capillary pressure and relative permeability of different soils and concretes.

Soil type	Sm	n	αgn (m^{-1})	αnw (m^{-1})	αgw (m^{-1})	Swr	Snr	Sgr	n	Reference
Native soil 1 (sandy clay)	0.36	1.86	10.8	6	3.2	0.38	0.07	0.01	3	CP (Parker, 1987) RP (Battistelli, 2008)
Final backfill sandy clay	0.36	1.86	10.8	6	3.2	0.38	0.07	0.01	3	
Native soil 2 (sand)	0	1.56	9.6	7.94	4.35	0.15	0.05	0.01	3	UNSODA, RETC
Initial backfill	0	1.84	10	11	5.2	0.15	0.05	0.01	3	CP (Parker, 1987) RP (Battistelli, 2008)
Bedding material	0	1.84	10	11	5.2	0.15	0.05	0.01	3	
High qual. pipe	0	1.51	1.14×10^{-3}	9.4×10^{-4}	5.16×10^{-4}	0.1	0.05	0.01	3	(Pour-Ghaz et al., 2009), (Kumar, 2010)
Med. qual. pipe	0	1.5	1.7×10^{-3}	1.3×10^{-3}	7.4×10^{-4}	0.1	0.05	0.01	3	
Low qual. pipe	0	1.48	2×10^{-3}	1.65×10^{-3}	9.04×10^{-4}	0.1	0.05	0.01	3	
Undamaged gasket	0	1.5	1.7×10^{-3}	1.3×10^{-3}	7.4×10^{-4}	0.1	0.05	0.01	3	
Damaged gasket	0	1.5	1.7×10^{-3}	1.3×10^{-3}	7.4×10^{-4}	0.1	0.05	0.01	3	
Flow	0	1.8	0.5	0.25	0.17	0.1	0.05	0.01	3	
Atm.	no capillary pressure					0.6	0.01	0	3	(Pruess, Battistelli, , 2002)
Anti-seep collar	0	1.45	0.022	0.0182	0.01	0.1	0.05	0.01	3	UNSODA, RETC

Appendix E: Saturated model

Table E1: Parameters used in the numerical model

Material	Parameter value				Reference
	$K_{xx}=k_{yy}$ (cm/s)	k_{zz} (cm/s)	n_e	ρ_b (kg/m^3)	
Sandy clay (native soils)	7.3×10^{-5}	3.6×10^{-5}	0.33	1700	Delta (2000)
Initial backfill	0.15	0.075	0.30	1800	Geotechdata (2013)
Final backfill (backfilled sandy clay)	9.3×10^{-5}	4.6×10^{-5}	0.34	1700	-
Bedding material	1	0.5	0.28	2000	Geotechdata (2013)
Clayey barrier	1×10^{-7}	1×10^{-7}	0.3	1800	Li et al. (2017)
Flowable fill	1×10^{-8}	1×10^{-8}	0.33	1900	Deng, and Tikalsky (2008)
Anti-seep collar	1×10^{-8}	1×10^{-8}	0.33	1900	Deng, and Tikalsky (2008)
Concrete pipe	3.8×10^{-9}	3.8×10^{-9}	0.15	2400	Smyl et al. (2016)
Gasket	3.8×10^{-9}	3.8×10^{-9}	0.1	1300	-
Flow inside the pipe	10	10	0.99	1000	-

Table E2: Transport parameters used in the model

Parameters	Value	Reference
Longitudinal Dispersion (m)	2.75	Neuman, (1990)
Horizontal/Long Dispersion	0.3	ASTM, (1994)
Vertical/Long Dispersion	0.05	ASTM, (1994)
Diffusion Coefficient of benzene in water (m^2/d)	8.5×10^{-5}	GSI Environmental (2014)
Partition Coefficient (K_d) (L/μg)	8.5×10^{-11}	Calculated
The first-order reaction rate of the dissolved (mobile) phase, K_1 (d^{-1})	1×10^{-5}	Borden et al. (1997)
The first-order reaction rate of the sorbed (immobile) phase, K_2 (d^{-1})	1×10^{-5}	Borden et al. (1997)